

Article

Statistical Properties of X-ray Flares in Gamma-ray Bursts

Yong-Rui Shi, Xiao-Kang Ding, Si-Yuan Zhu, Wan-Peng Sun and Fu-Wen Zhang * 

College of Science, Guilin University of Technology, Guilin 541004, China; shiyongrui1996@163.com (Y.-R.S.); teacherding@foxmail.com (X.-K.D.); glzhusiyuan@163.com (S.-Y.Z.); swp@glut.edu.cn (W.-P.S.)

* Correspondence: fwzhang@pmo.ac.cn

Abstract: X-ray flares are frequently detected in the X-ray afterglow light curves and are highly correlated with the prompt emission of gamma-ray bursts (GRBs). We compile a comprehensive sample of X-ray flares up to 2021 April, comprising 697 flares. We classify the total sample into four types: early flares ($t_p \leq 10^3$ s), late flares ($t_p > 10^3$ s), long gamma-ray burst (LGRB) flares and short gamma-ray burst (SGRB) flares, and analyze the distributions and relationships of the flare parameters. It is found that the early flares have a higher frequency, shorter duration, and more asymmetrical structure. In addition, the distributions of the morphological parameters of the SGRB flares are similar to those of the LGRB flares. We also find that the durations and rising (decay) times of the early flares are positively correlated with the peak times, but the late flares follow the different dependent relations. There is a strong anti-correlation between the peak luminosities ($L_{X,p}$) and the peak times of the flares, e.g., $L_{X,p} \propto t_{p,z}^{-1.45}$ for the LGRB flares, and $L_{X,p} \propto t_{p,z}^{-1.27}$ for the SGRB flares, respectively. Furthermore, the peak luminosity is highly dependent on the isotropic energy ($E_{X,iso}$) for the early LGRB flares, the best fit is $L_{X,p} \propto E_{X,iso}^{1.06}$ ($r = 0.89$). We also find a tight three-parameter correlation, $L_{X,p} \propto t_{p,z}^{-1.03} E_{X,iso}^{0.92}$ ($r = 0.96$). All the late flares fall into the 3σ confidence region defined by the early flares. In terms of the point of kinematic arguments, both the SGRB and LGRB flares support a common scheme of internal origin. The SGRB flares have similar properties to the LGRB flares, suggesting that both of them share a similar physical mechanism from the late-time activity of central engine.



Citation: Shi, Y.-R.; Ding, X.-K.; Zhu, S.-Y.; Sun, W.-P.; Zhang, F.-W.

Statistical Properties of X-ray Flares in Gamma-ray Bursts. *Universe* **2022**, *8*, 358. <https://doi.org/10.3390/universe8070358>

Received: 3 May 2022

Accepted: 21 June 2022

Published: 27 June 2022

Publisher's Note: MDPI stays neutral with regard to jurisdictional claims in published maps and institutional affiliations.



Copyright: © 2022 by the authors. Licensee MDPI, Basel, Switzerland. This article is an open access article distributed under the terms and conditions of the Creative Commons Attribution (CC BY) license (<https://creativecommons.org/licenses/by/4.0/>).

Keywords: gamma-ray burst; general-methods; data analysis

1. Introduction

Gamma-ray bursts (GRBs) are the most energetic and mysterious phenomena in the universe. Traditionally, GRBs are roughly classified into two subgroups based on their duration distribution: long gamma-ray bursts (LGRBs) with $T_{90} > 2$ s and short gamma-ray bursts (SGRBs) with $T_{90} < 2$ s [1,2]. It is generally accepted that LGRBs originate from the collapse of rapidly rotating massive stars [3,4], while SGRBs are associated with the coalescence of binary compact objects (double neutron stars or a neutron star and a black hole) [5–7].

Since the narrow-field instrument X-ray Telescope (XRT) on board Swift was operated with more rapid locating capability and higher sensitivity [6,8–13], the well-sampled GRBs with early afterglow detection and available redshift measurement were significantly accumulated [12,14–16]. Especially, a canonical X-ray afterglow light curve characterized by five components is revealed [17–19]: an initial steep decay (with a typical slope index around 3 or steeper), a shallow decay (the so-called plateau, with a typical slope index around 0.5), a normal decay (with a typical slope index around 1.2), a possible steep decay component following a jet break, as well as one or more X-ray flares. Flares can be detected in almost half of the early X-ray light curves [19,20], which show a steep rise and then steep decay characteristics. There is also a clustering phenomenon in the peak time of X-ray flares, most of which occur at the early time interval around 10^3 s [21]. Statistically, X-ray flares can appear in different types of GRBs [22,23], and even different environments. Meanwhile,

Ref. [24] reported the temporal behaviors and the spectral properties of the X-ray flares are similar to those of the prompt emission of GRBs. It is believed that the flares may share the same physical origin as the prompt emission pulse, indicating that both of them originate from the same central engine [8,11,12,17,19,25–29]. Ref. [30] found that flare lags evolve with time after collecting the multi-flare GRBs, which is consistent with the prompt emission pulses. The central engine of GRBs does not seem to shut down immediately after the prompt emission phase, the duration can be very long. Especially, the X-ray flares provide the important clues to the late-time activity of the central engine [31].

Ref. [8] reported two GRBs with strong X-ray flaring activity. The energy contained in the first flare of GRB 050502B is roughly consistent with the prompt emission phase detected in Swift/BAT, which puts the energy budget of the flare in doubt. From the kinematic view, Ref. [32] proposed a criterion to separate the internal and external origin of flares. Ref. [19] shaped the early X-ray light curves and explained that flares favor internal shock or similar energy dissipation at a later time, rather than the afterglow effect. Ref. [27] analyzed the rapid decay components of the flares and those of the prompt emissions, suggesting an erratic and unpredictable central engine. Each X-ray flare forms a unique and distinct central engine activity episode, and the central engine remains active after the termination of the prompt emission. Ref. [33] focused on seven extremely late X-ray flares (the peak time $t_p > 10^4$ s) to investigate the central engine of such flares based on the hypothesis of internal origin, a fast-rotating neutron star with strong bipolar magnetic fields may be responsible for such flares. Various models have been proposed to explain the flares, such as the fragmentation of a collapsing star [34], fragmentation of an accretion disk [35], and the magnetic reconnection process [20,36]. Another similar schemes can be referred to [11,28,37–41].

Previous studies have also found some correlations of the X-ray flares with continuously updated samples. Ref. [26] found that the width and the energy of the early flares (with a temporal boundary $< 10^3$ s) follow a power-law correlation and the 0.3–10 keV peak luminosity of the early flares decays with the peak time, i.e., $\omega \propto E^{-0.5}$ and $L_{X,p} \propto t_{p,z}^{-2.7}$, respectively. Ref. [36] fitted a hybrid sample of X-ray flares and re-found that the peak luminosity correlated with the peak time: $L_p \propto t_{p,z}^{-1.27}$. In addition, the power-law distributions of the energies, durations, peak fluxes, and waiting times of the X-ray flares are similar to those of solar flares, indicating that the physical origins of these two phenomena are similar, which can be explained by a fractal-diffusive, self-organized, criticality model [20,36]. Ref. [23] studied the possible SGRB X-ray flares in a small sample for the first time. They claimed that the SGRB flares show similar mechanisms to the long ones, despite the distributions of the SGRB flares being located at lower energies. However, due to the limited size of SGRB flares (only 8 SGRBs), the quantitative conclusion may require further investigation. In this work, we further analyze the characteristics and physical nature of the flares based on a large sample.

This paper is organized as follows. In Section 2, the sample selection and the data analysis are described. In Section 3, the distributions and correlations of X-ray flares with different classes are presented. In Section 4, we give the constraints on flares through the kinematic parameters. Conclusions and discussions are shown in Section 5. The cosmological parameters in a flat universe with $H_0 = 71 \text{ km s}^{-1} \text{ Mpc}^{-1}$, $\Omega_M = 0.27$, and $\Omega_\Lambda = 0.73$ is adopted throughout this paper.

2. Sample Selection and Data Analysis

The 0.3–10 keV flux data of X-ray light curves (LCs) are taken from the website of the UK Swift Science Data Centre at the University of Leicester <http://www.swift.ac.uk/xrtcurves/> (accessed date: 1 May 2021) [10,42]. We select all GRBs with X-ray flares observed from the Swift/XRT instrument for the last 15 years (up to April 2021). To extract the physical parameters of the flares, we adopt the following criteria: flare candidates can be obviously distinguished from the X-ray afterglow and generally have a complete structure, including significant rising and decaying phases. Then, we obtain 697 bright

X-ray flares, including 677 LGRB flares and 20 SGRB flares. Based on the peak time of the flares, there are also 636 early flares ($t_p < 10^3$ s) and 61 late flares ($t_p > 10^3$ s).

An X-ray afterglow LC contains one or more power-law segments and some flares, various LCs can be assembled from different components [36]. We adopt the fitting method used by [15] to fit the X-ray afterglow LCs. First, the global feature of the LCs is examined based on visual inspection. Then, the minimum number of basic components was introduced. Sometimes, it must add potential components by judging whether the chi-square value is close to 1. This fitting method is also similar to that of [15,33,36,43,44]. Usually a smooth broken power-law (SBPL) function,

$$F_1(t) = F_{01} \left[\left(\frac{t}{t_b} \right)^{\alpha_1 \omega} + \left(\frac{t}{t_b} \right)^{\alpha_2 \omega} \right]^{-\frac{1}{\omega}}, \quad (1)$$

and a single power-law function,

$$F_2(t) = F_{02} t^{-\alpha_3}, \quad (2)$$

were applied to fit the flares and underlying continuums [15,33,36,43], where α_1 , α_2 and α_3 are the temporal slopes, t_b is the break time, and ω represents the sharpness of the peak. The selection of ω does not significantly affect the value of t_b [43]. ω is usually fixed to 3 or 1 in the flare fitting. However, in some flares, ω can significantly affect the goodness of fitting, because the peaks of some flares are not sharp but rather smooth. Occasionally, the steep decay, the shallow decay and the jet break might appear in the LC, which can be jointly fitted by the above empirical formulas. The two examples of the best-fitting LCs are shown in Figure 1.

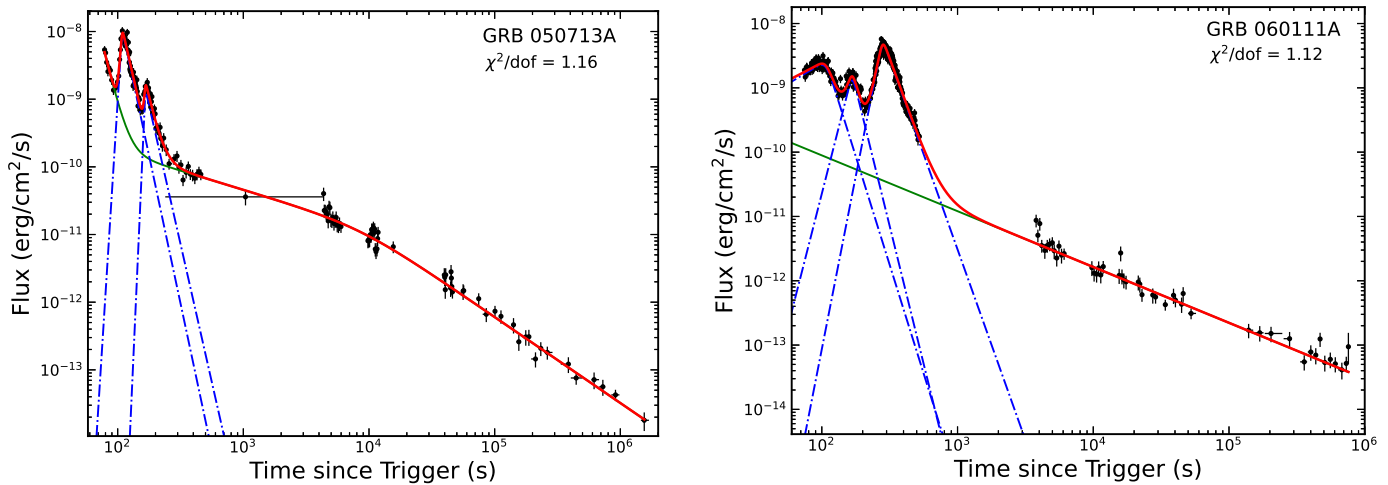


Figure 1. Best-fits for the X-ray LCs of GRB 050713A and GRB 060111A. The blue dot-dash lines show the best fit of individual flare, and the green lines show the underlying continuum component. The red lines show the best-fits of whole LCs of GRBs. GRB 050713A is a typical LC that two flares superimpose on the Nousek-Zhang power-law. In some cases, such as 060111A, the underlying continuum deviates from the Nousek-Zhang power-law with incomplete structure.

The other parameters of flares are derived as follows. The peak time of a flare can be transferred from the break time as [33]:

$$t_p = t_b \left(-\frac{\alpha_1}{\alpha_2} \right)^{\frac{1}{(\alpha_2 - \alpha_1)\omega}}, \quad (3)$$

and the peak flux of a flare at t_p is

$$F_{X,p} = F_{01} \left[\left(-\frac{\alpha_1}{\alpha_2} \right)^{\frac{\alpha_1}{\alpha_2 - \alpha_1}} + \left(-\frac{\alpha_1}{\alpha_2} \right)^{\frac{\alpha_2}{\alpha_2 - \alpha_1}} \right]^{-\frac{1}{\omega}}. \quad (4)$$

The duration (Δt) of a flare is defined as full width at half maximum (FWHM), which refer to [15,21,33]. The start time t_{start} (the end time t_{end}) is defined as the start point (the end point) at half peak. The rise time can be derived from $t_r = t_p - t_{start}$ and the decay time $t_d = t_{end} - t_p$. Each X-ray flare can be fitted with its corresponding SBPL function, as shown in the Equation (1). We also calculate t_d/t_r , relative variability of flux $\Delta F/F$ and relative temporal variability $\Delta t/t$, where ΔF is the increased flux of the flare at t_p , and F is the flux of the underlying continuum at t_p [16,21,25,26,32,33,45].

For the GRBs with measured redshift, we can calculate the flare parameters in the rest frame and explore the intrinsic properties of flares. The 0.3–10 keV isotropic energy ($E_{X,iso}$) of a flare can be calculated by the following formula [33,36,46]:

$$E_{X,iso} = \frac{4\pi D_L^2 S_X}{1+z}. \quad (5)$$

Here, the flare fluence (S_X) is calculated by integrating the corresponding SBPL function of the flare from the start time to the end time in the energy band of Swift/XRT [12,33,36]. Additionally, D_L is the luminosity distance of GRBs [47,48]:

$$D_L(z, \Omega_M, \Omega_\Lambda) = \frac{c(1+z)}{H_0} \int_0^z \frac{dz'}{\sqrt{\Omega_M(1+z')^3 + \Omega_\Lambda}}. \quad (6)$$

The peak luminosity of a flare can be derived from the formula $L_{X,p} = 4\pi D_L^2 F_{X,p}$. Cautiously, the k-correction is not considered in this paper like [33]. All the observed temporal parameters can be transferred to the rest frame by $T_z = T/(1+z)$.

The fitting and derived parameters of the flares are summarized in Tables 1 and 2, where the errors of these quantities are calculated by the error propagation formula. We take 10 percent of the central value as the error if the data have no error, or its error is greater than itself.

Table 1. The Main Physical quantities of Flares.

GRB	Type ^a	z ^b	Flare (Index)	ω	α_1	α_2	t_p (s)	$F_{X,p,-11}$ ^c (erg/cm ² /s)	$S_{X,-8}$ ^c (erg/cm ²)	Δt (s)	$\Delta F/F$	t_r (s)	t_d (s)	$\Delta t/t$	t_d/t_r
050406	Long		(1)	3	-3.22 ± 0.53	7.12 ± 0.57	213.17 ± 7.44	13.82 ± 1.49	0.88 ± 0.08	82.54	149.71	47.81	34.73	0.39	0.73
050502B	Long	5.2 ph	(1)	1	-9.54 ± 0.09	10.59 ± 0.09	720.54 ± 0.65	328.51 ± 3.47	49.36 ± 0.5	188.97	200.79	90.24	98.72	0.26	1.09
			(2)	3	-10.04 ± 0	1.84 ± 0.28	$29,898.12 \pm 161.76$	0.07 ± 0.02	0.92 ± 0.2	18,695.09	2.23	3624.95	15,070.15	0.63	4.16
			(3)	3	-2.87 ± 0.33	5.09 ± 0.27	$76,142.81 \pm 553.83$	0.1 ± 0.01	2.85 ± 0.22	36,398.71	9.31	19,346.01	17,052.7	0.48	0.88
050607	Long		(1)	3	-33.87 ± 15.17	7.93 ± 0.59	305.98 ± 3.5	91.75 ± 12.44	2.91 ± 0.28	41.84	17.05	10.93	30.9	0.14	2.83
050712	Long		(1)	3	-35.1 ± 14.18	50.34 ± 24.66	215.84 ± 2.38	35.04 ± 8.35	0.26 ± 0.05	9.55	1.66	5.28	4.27	0.04	0.81
			(2)	3	-11.18 ± 3.14	32.48 ± 9.02	264.52 ± 3.44	38.15 ± 6.31	0.81 ± 0.1	27.51	1.75	18.08	9.43	0.1	0.52
			(3)	3	-141.29 ± 83.12	14.38 ± 1.67	474.14 ± 2.28	36 ± 6.66	0.79 ± 0.11	29.41	8.36	4.88	24.53	0.06	5.03
			(4)	3	-16.49 ± 8.67	3.74 ± 1.43	950.68 ± 44.11	4.04 ± 1.02	0.86 ± 0.16	283.34	4.16	68.9	214.44	0.3	3.11
050713A	Long		(1)	3	-29.48 ± 2.96	8.73 ± 0.31	109.7 ± 0.47	906.43 ± 45.91	10.02 ± 0.41	14.53	16.8	4.28	10.25	0.13	2.39
			(2)	3	-41.67 ± 10.13	8.19 ± 0.52	167.79 ± 1.08	122.83 ± 10.61	1.97 ± 0.13	21.22	8.75	5.07	16.15	0.13	3.19
050714B	Long	2.4383	(1)	3	-9.31 ± 1.52	9.33 ± 1.13	386.3 ± 7.86	17.9 ± 1.67	1.06 ± 0.1	76.63	56.37	36.44	40.18	0.2	1.1
050716	Long		(1)	3	-35.09 ± 20.09	16.07 ± 5.54	171.63 ± 3.27	44.48 ± 11.52	0.48 ± 0.1	14.14	0.52	5.17	8.97	0.08	1.74
			(2)	3	-24.48 ± 9.69	9.07 ± 1.56	381.51 ± 6.61	20.45 ± 3.36	0.81 ± 0.1	52.15	1.1	17.07	35.08	0.14	2.06
050724	Short	0.258	(1)	3	-14.11 ± 0.96	9.01 ± 0.56	266.6 ± 1.53	56.47 ± 3.6	1.95 ± 0.12	44.93	3.18	18.3	26.63	0.17	1.45
			(2)	3	-2.06 ± 0.26	4.2 ± 0.33	$56,763.79 \pm 586.8$	0.18 ± 0.02	4.96 ± 0.4	35,000.6	26.19	18,734.69	16,265.92	0.62	0.87
050726	Long		(1)	3	-59.05 ± 5.9	22.79 ± 14.05	162.86 ± 5.07	16.53 ± 8.2	0.11 ± 0.05	8.87	0.66	3.04	5.83	0.05	1.92
			(2)	3	-14.98 ± 3.75	9.05 ± 1.61	266.51 ± 5.39	28.06 ± 3.37	0.94 ± 0.1	43.72	1.72	17.45	26.27	0.16	1.51
050730	Long	3.967	(1)	3	-55.16 ± 22.44	22.76 ± 5.36	229.9 ± 2.06	70.44 ± 13.25	0.69 ± 0.1	12.83	1.05	4.52	8.31	0.06	1.84
			(2)	3	-14 ± 1.34	11.49 ± 0.84	432.33 ± 3.5	105.11 ± 4.98	5.15 ± 0.23	63.46	2.25	28.55	34.91	0.15	1.22
			(3)	3	-43.31 ± 10.05	11.14 ± 1.67	681.61 ± 4.54	53.07 ± 5.84	2.72 ± 0.22	67.49	1.36	18.76	48.73	0.1	2.6
050802	Long		(1)	3	-5.18 ± 2.23	5.49 ± 1.91	439.4 ± 35.28	8.29 ± 1.21	0.98 ± 0.14	152.33	0.77	71	81.32	0.35	1.15
050803	Long	3.5 ph	(1)	3	-1.57 ± 0.71	29.37 ± 2.94	766.27 ± 44.39	4.54 ± 1.15	1.11 ± 0.25	322.93	1.84	278.53	44.4	0.42	0.16
			(2)	3	-9.61 ± 8.34	4.51 ± 3.65	1164.34 ± 126.09	3.41 ± 1.28	0.93 ± 0.26	355.09	1.55	122.39	232.7	0.3	1.9
050820A	Long	2.612	(1)	3	-69.29 ± 3.19	2.6 ± 0.35	233.79 ± 0.54	823.3 ± 30.28	46.89 ± 1.4	78.64	82.02	5.88	72.77	0.34	12.38
050822	Long	1.434	(1)	3	-15.53 ± 3.62	7.03 ± 0.71	236.31 ± 3.82	69.93 ± 7.05	2.41 ± 0.2	44.95	5.47	15.81	29.15	0.19	1.84
			(2)	3	-22.55 ± 1.77	7.99 ± 0.22	444.17 ± 1.94	186.19 ± 7.31	9.69 ± 0.31	68.16	140.57	21.72	46.44	0.15	2.14
050904	Long	6.29	(1)	3	-5.02 ± 0.33	19.75 ± 1.65	466.3 ± 2.92	93.42 ± 4.55	6.85 ± 0.26	95.66	3.18	66.16	29.5	0.21	0.45
			(2)	3	-16.71 ± 0.88	9.07 ± 1.02	6741.66 ± 14.77	6.68 ± 0.43	5.43 ± 0.31	1057.36	47.69	405.3	652.06	0.16	1.61
			(3)	3	-17.33 ± 2.41	4.13 ± 1.96	$13,862.36 \pm 135.09$	3.29 ± 0.47	9.33 ± 0.91	3765.46	99.23	948.46	2817	0.27	2.97
			(4)	3	-8.02 ± 4.52	5.13 ± 1.16	$21,456.72 \pm 367.59$	3.33 ± 0.59	16.47 ± 2.44	6427.98	241.17	2523.67	3904.31	0.3	1.55
050908	Long	3.344	(1)	3	-145.83 ± 0.03	7.2 ± 0.8	387.55 ± 0.89	19.9 ± 2.9	0.65 ± 0.09	44.55	26	4.44	40.12	0.11	9.04
050915A	Long	2.5273	(1)	3	-10 ± 3.74	7.64 ± 1.03	105.65 ± 3.04	45.58 ± 4.72	0.8 ± 0.07	22.69	9.27	9.76	12.93	0.21	1.32
			(2)	3	-63.47 ± 0.23	21.52 ± 2.15	525.43 ± 10.49	2.29 ± 0.89	0.05 ± 0.02	29.02	1.53	9.36	19.66	0.06	2.1

Table 1. *Cont.*

GRB	Type ^a	z ^b	Flare (Index)	ω	α_1	α_2	t_p (s)	$F_{X,p_r=11}$ ^c (erg/cm ² /s)	$S_{X,-8}$ ^c (erg/cm ²)	Δt (s)	$\Delta F/F$	t_r (s)	t_d (s)	$\Delta t/t$	t_d/t_r
050916	Long		(1)	3	-32.72 ± 3	14.68 ± 2.28	$19,599.25 \pm 221.17$	5.32 ± 1.59	7.17 ± 2.04	1756.27	84.34	634.73	1121.54	0.09	1.77
050922B	Long	4.5ph	(1)	3	-14.84 ± 3.63	5.12 ± 0.3	373.13 ± 3.4	134.85 ± 6.44	9.23 ± 0.25	89.88	478.38	27.52	62.37	0.24	2.27
			(2)	3	-289.66 ± 203.11	23.24 ± 5.38	498.23 ± 1.74	35.77 ± 7.44	0.49 ± 0.07	18.28	134.91	2.63	15.65	0.04	5.96
			(3)	3	-9.94 ± 0.7	9.38 ± 0.34	820.11 ± 6.39	179.71 ± 8	21.85 ± 0.96	157.32	752.98	73.41	83.91	0.19	1.14
051117A	Long		(1)	3	-1.69 ± 0.46	5.64 ± 0.84	155.92 ± 7.16	207.49 ± 19.26	15.1 ± 0.95	93.64	0.74	57.64	35.99	0.6	0.62
			(2)	3	-50.98 ± 27.47	5.57 ± 2.69	324.4 ± 5.16	64.72 ± 14.11	2.62 ± 0.4	54.34	0.47	9.04	45.29	0.17	5.01
			(3)	3	-3.84 ± 0.77	7.02 ± 1.15	447.8 ± 12.95	99.73 ± 13.23	12.27 ± 1.42	158.91	0.98	87.81	71.09	0.35	0.81
			(4)	3	-34.92 ± 11.19	17.2 ± 3.23	609.19 ± 5.51	53.18 ± 6.54	1.97 ± 0.19	48.15	0.7	18.16	29.99	0.08	1.65
			(5)	3	-20.35 ± 2.28	12.37 ± 3.57	945.34 ± 9.39	77.14 ± 6.72	6.73 ± 0.48	113.24	1.55	45.91	67.33	0.12	1.47
			(6)	3	-14.31 ± 3.92	30.73 ± 4.79	1109.67 ± 7.88	77.47 ± 8.24	6.04 ± 0.5	101.1	1.81	61.82	39.27	0.09	0.64
			(7)	3	-67.78 ± 4.95	7.92 ± 0.51	1318.83 ± 2.37	193.12 ± 6.91	22.3 ± 0.59	154.75	5.32	27.38	127.37	0.12	4.65
			(8)	3	-74.08 ± 35.22	12 ± 2.61	1543.3 ± 10.49	33.08 ± 6.11	3.14 ± 0.42	126.09	1.06	27.47	98.62	0.08	3.59
051210	Short		(1)	3	-342.91 ± 0	5.36 ± 1.83	121.97 ± 0.36	21.52 ± 6.91	0.28 ± 0.09	17.69	0.81	0.73	16.97	0.15	23.4
051227	Short		(1)	3	-6.71 ± 5.02	3.78 ± 0.37	116.41 ± 6.84	38.16 ± 5.41	1.33 ± 0.14	45.63	9.97	16.55	29.08	0.39	1.76
060105	Long		(1)	3	-2.98 ± 0	1.99 ± 0.1	$49,413.32 \pm 198.46$	0.11 ± 0.01	3.55 ± 0.25	40,832.9	2.39	14,031.99	26,800.91	0.83	1.91
060111A	Long	2.32	(1)	3	-1.26 ± 0.36	6.75 ± 1.25	100.04 ± 4.04	226.25 ± 21.66	11.6 ± 0.71	65.94	25.4	44.84	21.1	0.66	0.47
			(2)	3	-8.28 ± 2.12	8.56 ± 1.02	167.37 ± 3.31	129.9 ± 7.05	3.69 ± 0.2	36.73	22.8	17.56	19.17	0.22	1.09
			(3)	3	-10.77 ± 0.44	5.93 ± 0.09	283.73 ± 1.09	463.53 ± 7.71	24.6 ± 0.35	69.13	128.62	25.97	43.16	0.24	1.66
060115	Long	3.53	(1)	3	-8.67 ± 3.02	7.64 ± 1.29	409.45 ± 16	13.99 ± 2.15	1.01 ± 0.15	93.64	3.65	42.25	51.39	0.23	1.22
060124	Long	2.296	(1)	3	-26.53 ± 4.56	2.46 ± 0.26	369.12 ± 4.03	80.69 ± 7.68	8.67 ± 0.68	146.32	9.18	20.15	126.16	0.4	6.26
			(2)	3	-8.11 ± 0.16	26.77 ± 0.87	573.87 ± 0.95	1743.87 ± 35.98	104.79 ± 1.78	78.31	227.65	52.71	25.6	0.14	0.49
			(3)	3	-36.29 ± 1.3	16.61 ± 0.31	700.38 ± 0.9	1477.89 ± 30.95	63.32 ± 1.13	55.79	205.24	20.4	35.39	0.08	1.73
			(4)	3	-308.02 ± 100.07	2.91 ± 1.61	977.62 ± 2.9	67.93 ± 5.05	13.19 ± 0.81	270.89	10.46	6.98	263.9	0.28	37.78
060202	Long	0.783	(1)	3	-23.92 ± 5.95	4.89 ± 1.54	380.59 ± 5.91	66.48 ± 8.86	4.17 ± 0.38	83.24	1.02	19.65	63.59	0.22	3.24
			(2)	3	-14.66 ± 6.58	8.04 ± 4.19	532.62 ± 16.5	43.19 ± 9.78	3.15 ± 0.57	94.86	1.52	36.28	58.58	0.18	1.61
			(3)	3	-4.76 ± 1.23	8.03 ± 0.46	718.67 ± 12.47	83.92 ± 7.61	13.93 ± 1.08	214.45	5.97	117.31	97.14	0.3	0.83
060204B	Long	2.3393	(1)	3	-39.94 ± 6.82	11.91 ± 0.69	318.38 ± 1.39	94.31 ± 6.19	2.21 ± 0.11	30.76	10.72	9.21	21.55	0.1	2.34
060210	Long	3.91	(1)	3	-77.05 ± 27.7	6.6 ± 0.49	106.04 ± 0.6	273.12 ± 21.78	2.89 ± 0.16	14.3	3.3	2.06	12.24	0.13	5.94
			(2)	3	-11.56 ± 0.75	9.4 ± 0.32	199.06 ± 1.12	315.17 ± 8.74	8.67 ± 0.23	35.62	6.43	15.83	19.79	0.18	1.25
			(3)	3	-48.11 ± 5.1	9.55 ± 0.37	371.81 ± 1.1	152.59 ± 7.18	4.64 ± 0.17	40.25	5.24	9.73	30.52	0.11	3.14
060223A	Long	4.41	(1)	3	-9.81 ± 2.33	5.22 ± 2.77	1509.55 ± 69.59	2.61 ± 0.55	0.83 ± 0.14	413.93	8.04	151.89	262.05	0.27	1.73
060312	Long		(1)	3	-20.79 ± 10.77	19.2 ± 1.92	79.77 ± 2.27	51.76 ± 13.62	0.3 ± 0.08	7.39	1.28	3.51	3.87	0.09	1.1
			(2)	3	-12.94 ± 4	17.65 ± 7.5	98.94 ± 2.05	212.22 ± 18.6	1.99 ± 0.14	12.11	9.25	6.47	5.63	0.12	0.87
			(3)	3	-86.56 ± 32.71	9.2 ± 0.43	109.71 ± 0.49	301.27 ± 39.48	2.43 ± 0.25	10.84	17.19	1.82	9.02	0.1	4.95
			(4)	3	-35.72 ± 1.58	2.89 ± 1.1	530.1 ± 9.81	1.76 ± 0.61	0.22 ± 0.07	171.83	3.11	22.21	149.62	0.32	6.74

Table 1. *Cont.*

GRB	Type ^a	z ^b	Flare (Index)	ω	α_1	α_2	t_p (s)	$F_{X,p,-11}$ ^c (erg/cm ² /s)	$S_{X,-8}$ ^c (erg/cm ²)	Δt (s)	$\Delta F/F$	t_r (s)	t_d (s)	$\Delta t/t$	t_d/t_r
060313	Short	1.172	(1)	3	-6.44 ± 0.64	24.47 ± 2.45	100 ± 18.83	14.18 ± 6.73	0.18 ± 0.08	16.33	1.6	11.29	5.04	0.16	0.45
			(2)	3	-29.09 ± 2.91	4.36 ± 4.02	131.91 ± 7.11	15.41 ± 7.8	0.35 ± 0.15	30.4	2.08	5.99	24.41	0.23	4.07
			(3)	3	-48.04 ± 4.8	7.42 ± 3.98	184.8 ± 184.58	19.67 ± 2.87	0.36 ± 0.04	24.51	3.3	5.1	19.42	0.13	3.81
060319	Long	4.94	(1)	3	-54.43 ± 0.23	5.42 ± 1.56	251.57 ± 2.76	13.26 ± 4.35	0.42 ± 0.13	42.72	3.78	6.7	36.02	0.17	5.38
060413	Long		(1)	3	-15.25 ± 4.54	4.99 ± 0.77	641.89 ± 15.83	46.11 ± 7.09	5.48 ± 0.67	156.44	8.86	46.61	109.83	0.24	2.36
060418	Long	1.489	(1)	3	-50.88 ± 3.15	8.83 ± 0.16	129.05 ± 0.3	2074.94 ± 74.98	22.92 ± 0.69	14.67	11.62	3.29	11.39	0.11	3.47
060510B	Long	2.1	(1)	3	-15.97 ± 3.55	22.87 ± 5.44	197.2 ± 2.66	124.74 ± 14.86	1.85 ± 0.2	19.14	0.43	10.45	8.69	0.1	0.83
			(2)	3	-24.41 ± 2.68	24.88 ± 2.52	300.06 ± 1.54	245.08 ± 12.77	4.26 ± 0.22	22.48	0.98	11.1	11.38	0.07	1.03
060512	Long	5.11	(1)	3	-24.65 ± 9.11	7.61 ± 1.34	201.39 ± 3.54	35.98 ± 6.77	0.85 ± 0.13	31.09	3.66	9.29	21.81	0.15	2.35
060522	Long	3.221	(1)	3	-6.22 ± 4.74	9.68 ± 2.02	163.79 ± 9.18	22.07 ± 4.27	0.67 ± 0.11	38.97	4.07	21.11	17.87	0.24	0.85
060526	Long	2.1357	(1)	3	-53.83 ± 2.51	13.16 ± 1.08	251.13 ± 0.48	1503.18 ± 66.48	23.61 ± 0.82	20.69	362.39	5.64	15.05	0.08	2.67
			(2)	3	-18.96 ± 3.01	9.76 ± 0.17	310.42 ± 1.52	628.07 ± 31.42	21.38 ± 0.88	44.29	203.56	16.68	27.61	0.14	1.65
060604	Long	3.0749	(1)	3	-10.06 ± 0.82	6.19 ± 0.26	137.82 ± 1.07	371.83 ± 10.9	9.59 ± 0.24	33.54	250.4	13.18	20.37	0.24	1.55
			(2)	3	-114.53 ± 26.2	14.68 ± 1.21	169.35 ± 0.46	275.23 ± 21.04	2.21 ± 0.12	10.73	201.44	2.05	8.68	0.06	4.23
060607A	Long	3.425	(1)	3	-2.91 ± 2.56	11.65 ± 7.57	82.4 ± 5.69	181.26 ± 48.67	3.94 ± 0.61	28.2	3.37	19.13	9.07	0.34	0.47
			(2)	3	-82.13 ± 27.05	5.52 ± 0.32	96.51 ± 0.5	449.97 ± 52.02	5.04 ± 0.48	15.19	8.99	1.84	13.35	0.16	7.23
			(3)	3	-15.64 ± 5.51	10.65 ± 4.34	178.65 ± 5.03	65.92 ± 9.38	1.33 ± 0.16	26.1	1.73	10.97	15.13	0.15	1.38
			(4)	3	-11.59 ± 1.01	7.99 ± 0.23	260.12 ± 1.6	353.97 ± 9.74	13.95 ± 0.34	51.12	11.01	21.28	29.84	0.2	1.4
060707	Long	2.711	(1)	3	-402.95 ± 0	5.95 ± 1.36	186.74 ± 0.61	20.87 ± 5.68	0.37 ± 0.1	24.2	2.1	0.95	23.25	0.13	24.37
060714	Long	1.532	(1)	3	-7.04 ± 5.2	62.09 ± 32.85	114.56 ± 1.76	246.48 ± 75.01	2.59 ± 0.57	13.94	37.27	11.27	2.67	0.12	0.24
			(2)	3	-5.46 ± 0.86	15.2 ± 1.52	138.66 ± 1.45	543.76 ± 30.62	12.35 ± 0.48	29.47	90.81	18.79	10.68	0.21	0.57
			(3)	3	-29.54 ± 3.78	13.77 ± 0.46	174.62 ± 0.63	409.66 ± 17.64	5.32 ± 0.18	16.93	77.13	6.2	10.72	0.1	1.73
060719	Long	0.54	(1)	3	-14.76 ± 10.08	9.71 ± 3.05	206.46 ± 10.59	10.88 ± 2.89	0.27 ± 0.06	32.64	4.43	13.49	19.15	0.16	1.42
060729	Long	1.9229	(1)	3	-44.67 ± 4.47	7.17 ± 5.15	446.74 ± 234.41	5.48 ± 0.87	0.25 ± 0.03	61.88	1.01	13.14	48.75	0.14	3.71
060804	Long	1.314	(1)	3	-44.3 ± 13.05	3.05 ± 0.06	129.77 ± 1.18	571.55 ± 29.52	16.27 ± 0.57	38.86	1.23	4.54	34.32	0.3	7.56
060904A	Long	2.1357	(1)	3	-8.92 ± 0.85	10.51 ± 0.71	319.51 ± 3.46	54.64 ± 2.81	2.57 ± 0.13	60.81	6.01	30.57	30.24	0.19	0.99
			(2)	3	-88.24 ± 29.57	9.5 ± 0.92	675.74 ± 3.97	15.49 ± 1.85	0.75 ± 0.07	64.75	5.19	10.98	53.77	0.1	4.9
060904B	Long	3.2	(1)	3	-27.14 ± 2.54	6.41 ± 0.64	155.26 ± 1.26	1060.64 ± 204.72	21.27 ± 3.8	26.52	95.25	6.88	19.64	0.17	2.85
			(2)	3	-22.7 ± 10.83	6.38 ± 2.41	176.03 ± 2.35	1434.06 ± 606.99	34.54 ± 12.48	31.73	140.46	8.97	22.76	0.18	2.54
060926	Long	0.703	(1)	3	-32.82 ± 3.28	2.43 ± 0.82	404.61 ± 214.05	2.93 ± 0.36	0.34 ± 0.03	157.48	1.65	18.73	138.75	0.39	7.41
060929	Long	2.1357	(1)	3	-7.44 ± 0.42	9.66 ± 0.16	538.48 ± 2.49	236.03 ± 4.66	21.36 ± 0.39	116.97	669.98	60.23	56.75	0.22	0.94
061121	Long	1.314	(1)	3	-23.34 ± 3.73	38.7 ± 6.39	74.93 ± 0.47	6045.83 ± 610.34	21.81 ± 1.92	4.67	2.19	2.68	1.99	0.06	0.74
			(2)	3	-40.94 ± 16.38	14.54 ± 1.38	118.47 ± 1.06	381.19 ± 54.23	2.88 ± 0.31	9.88	0.91	3.23	6.65	0.08	2.06

Table 1. *Cont.*

GRB	Type ^a	z ^b	Flare (Index)	ω	α_1	α_2	t_p (s)	$F_{X,p,-11}$ ^c (erg/cm ² /s)	$S_{X,-8}$ ^c (erg/cm ²)	Δt (s)	$\Delta F/F$	t_r (s)	t_d (s)	$\Delta t/t$	t_d/t_r
061202	Long	2.2543	(1)	3	-11.57 ± 1.69	5.09 ± 0.17	140.26 ± 1.3	391.52 ± 15.12	11.03 ± 0.31	36.84	1475.37	12.51	24.33	0.26	1.94
			(2)	3	-181.33 ± 0.04	2 ± 0.2	239.43 ± 3.68	16.22 ± 2.64	1.18 ± 0.19	102.52	48.73	2.83	99.69	0.43	35.19
070103	Long	2.6208	(1)	3	-2.42 ± 1.56	2.42 ± 1.1	790.91 ± 193.46	0.91 ± 0.23	0.43 ± 0.11	618.61	1.08	251.1	367.51	0.78	1.46
070107	Long		(1)	3	-90.28 ± 0.01	30.8 ± 0.04	321.39 ± 0.47	140.98 ± 10.34	1.34 ± 0.1	12.39	7.06	4.03	8.36	0.04	2.07
			(2)	3	-26.1 ± 0.06	94.45 ± 0.02	359.29 ± 0.65	128.89 ± 11.27	1.48 ± 0.13	15.06	7.1	10.5	4.56	0.04	0.43
			(3)	3	-9.02 ± 0.48	10.57 ± 0.63	381.83 ± 1.07	136.8 ± 5.3	7.63 ± 0.28	72.07	7.94	36.18	35.88	0.19	0.99
			(4)	3	-28.94 ± 0.24	18.42 ± 0.66	445.29 ± 1.14	63.01 ± 6.57	1.77 ± 0.18	36.4	4.18	15.19	21.21	0.08	1.4
			(5)	3	-36.39 ± 0	15.64 ± 0	1354.07 ± 0	9.57 ± 1.46	0.82 ± 0.13	112.02	1.66	39.83	72.19	0.08	1.81
			(6)	3	-6.68 ± 1.82	4.52 ± 0.69	$87,733.69 \pm 1004.11$	0.11 ± 0.01	2.52 ± 0.29	30,612.35	1.28	12,109.67	18,502.68	0.35	1.53
070129	Long	2.3384	(1)	3	-18.47 ± 4.98	25.15 ± 18.5	210.54 ± 4.08	65.79 ± 10.12	0.92 ± 0.12	18.09	1.06	9.75	8.34	0.09	0.85
			(2)	3	-32.37 ± 20.42	9.64 ± 4.77	238.41 ± 3.99	77.99 ± 18.78	1.7 ± 0.27	28.57	1.79	8.48	20.09	0.12	2.37
			(3)	3	-21.29 ± 1.79	14.37 ± 3.59	307.47 ± 2.24	696.48 ± 47.19	17.77 ± 1.02	33.07	33.03	14.01	19.07	0.11	1.36
			(4)	3	-13.18 ± 2.35	32.39 ± 1.96	366.67 ± 1.6	1054.42 ± 56.21	27.94 ± 1.08	34.43	82.31	21.78	12.65	0.09	0.58
			(5)	3	-23.77 ± 2.2	9.94 ± 0.61	444.4 ± 1.71	374.91 ± 13.44	16.56 ± 0.44	57.66	50.09	19.96	37.69	0.13	1.89
			(6)	3	-37.3 ± 8.86	13.79 ± 4.97	550.52 ± 5.16	117.21 ± 16.18	4.4 ± 0.44	49.1	28.09	16.3	32.8	0.09	2.01
			(7)	3	-304.87 ± 0.22	12.67 ± 4.35	578.86 ± 0.95	88.52 ± 13.97	2.37 ± 0.34	36.49	24.25	3.28	33.21	0.06	10.12
			(8)	3	-52.78 ± 15.12	15.08 ± 1.36	664.24 ± 2.59	68.14 ± 7.12	2.59 ± 0.2	49.85	26.7	14.72	35.13	0.08	2.39
			(9)	3	-47.8 ± 2.98	16.8 ± 6.2	901.92 ± 12.48	3.69 ± 1.22	0.18 ± 0.06	64.75	2.99	21.12	43.63	0.07	2.07
070306	Long	1.4959	(1)	3	-34.05 ± 6.43	7.77 ± 0.31	181.17 ± 0.98	299.03 ± 18.62	5.68 ± 0.26	25.12	1.1	6.47	18.65	0.14	2.88
070318	Long	0.836	(1)	3	-7.35 ± 0.79	4.69 ± 0.27	284.45 ± 4.6	76.91 ± 3.76	5.52 ± 0.24	93.39	3.19	36.31	57.08	0.33	1.57
070330	Long		(1)	3	-6.23 ± 1.24	4.03 ± 0.41	211.67 ± 8.84	22.01 ± 2.64	1.38 ± 0.15	81.76	136.61	31.43	50.33	0.39	1.6
070419B	Long	1.9591	(1)	3	-11 ± 0.94	4.98 ± 0.2	231.86 ± 2.02	467.33 ± 16.94	22.5 ± 0.65	62.96	1.7	21.59	41.36	0.27	1.92
070518	Long		(1)	3	-3.55 ± 0.8	13.47 ± 10.51	109.33 ± 2.9	71.87 ± 34.38	1.75 ± 0.71	31.57	50.62	21.36	10.21	0.29	0.48
			(2)	3	-5.95 ± 0.59	4.34 ± 0.45	140.26 ± 6.18	43.51 ± 11.42	1.76 ± 0.45	52.58	37.29	21.26	31.32	0.37	1.47
			(3)	3	-15.93 ± 3.59	10.9 ± 1.02	188.05 ± 2.22	83.05 ± 5.91	1.72 ± 0.11	26.88	89.7	11.33	15.56	0.14	1.37
070520B	Long		(1)	1	-16.09 ± 0.93	6.07 ± 0.15	194.13 ± 1.5	229.68 ± 8.8	9.99 ± 0.22	55.26	5.81	20.36	34.89	0.28	1.71
070621	Long		(1)	3	-25.5 ± 6.97	19.89 ± 4.86	146.62 ± 1.84	103.89 ± 12.49	0.97 ± 0.11	12.12	1.08	5.45	6.67	0.08	1.22
			(2)	3	-16.59 ± 8.35	7 ± 0.86	192.68 ± 4.4	33.96 ± 4.73	0.93 ± 0.1	35.92	1.27	12.26	23.66	0.19	1.93
070704	Long		(1)	1	-25.76 ± 0.99	5.86 ± 0.11	316.34 ± 1.19	526.61 ± 16.53	31.58 ± 0.59	76.88	50.73	24.61	52.27	0.24	2.12
070721B	Long	3.626	(1)	3	-126.52 ± 0.02	14.01 ± 7.56	266.19 ± 1.41	116.27 ± 48.21	1.49 ± 0.57	17.21	4.73	3.01	14.2	0.06	4.72
			(2)	3	-87.61 ± 65.34	63.68 ± 15.69	310.31 ± 3.83	248.15 ± 126.45	1.48 ± 0.72	7.74	9.6	3.45	4.29	0.02	1.25
			(3)	3	-58.49 ± 24.07	25.75 ± 4.72	346.32 ± 2.4	87.32 ± 14.32	1.17 ± 0.15	17.47	3.32	6.34	11.13	0.05	1.75
070724A	Short	0.457	(1)	3	-9.74 ± 2.66	20.37 ± 5.3	108.88 ± 2.18	75.11 ± 12.12	0.85 ± 0.11	14.66	2.29	8.83	5.83	0.13	0.66
			(2)	3	-7.8 ± 2.64	26.8 ± 1.33	221.85 ± 3.8	80.36 ± 34.19	1.91 ± 0.76	31.04	47.43	21.07	9.97	0.14	0.47

Table 1. *Cont.*

GRB	Type ^a	z ^b	Flare (Index)	ω	α_1	α_2	t_p (s)	$F_{X,p,-11}$ ^c (erg/cm ² /s)	$S_{X,-8}$ ^c (erg/cm ²)	Δt (s)	$\Delta F/F$	t_r (s)	t_d (s)	$\Delta t/t$	t_d/t_r
071021	Long	2.452	(1)	3	-15.17 ± 2.59	16.94 ± 2.56	219.02 ± 2.8	169.92 ± 15.87	3.31 ± 0.3	25.21	2.38	12.69	12.52	0.12	0.99
			(2)	3	-12.66 ± 1.78	10.79 ± 0.98	6214.18 ± 20.07	2.84 ± 0.23	2.17 ± 0.17	988.68	18.14	449.34	539.34	0.16	1.2
071031	Long	2.692	(1)	3	-1.18 ± 0.28	7.97 ± 1.05	145.78 ± 4.37	714.94 ± 52.02	52.78 ± 2.45	95.07	73.03	68.02	27.05	0.65	0.4
			(2)	3	-31.87 ± 9.32	6.19 ± 0.94	199.85 ± 1.7	240.85 ± 33.22	6.11 ± 0.64	33.71	34.66	7.88	25.83	0.17	3.28
			(3)	3	-30.51 ± 8.6	8.42 ± 0.94	258.62 ± 1.81	133.23 ± 14.84	3.52 ± 0.29	34.8	25.37	9.9	24.9	0.13	2.52
			(4)	3	-9.04 ± 0.94	3.74 ± 0.1	449.96 ± 4.06	93.98 ± 3.04	11.45 ± 0.28	159.89	32.67	51.31	108.58	0.36	2.12
071112C	Long	0.823	(1)	3	-10.27 ± 4.97	3.87 ± 0.64	645.79 ± 30.74	15.37 ± 2.95	2.51 ± 0.38	214.8	1.58	66.51	148.3	0.33	2.23
071118	Long		(1)	3	-57.31 ± 5.73	4.95 ± 1.97	210.87 ± 5.12	18.86 ± 5.07	0.54 ± 0.13	38.52	0.59	5.48	33.04	0.18	6.02
			(2)	3	-175.08 ± 0.02	2.66 ± 0.57	368.13 ± 1.47	17.48 ± 4.12	1.44 ± 0.33	114.85	1.94	4.29	110.56	0.31	25.75
			(3)	3	-12.99 ± 4.29	6.92 ± 1.14	603.09 ± 15.74	34.92 ± 4.56	3.32 ± 0.36	123.8	7.62	46.4	77.4	0.21	1.67
071122	Long	1.14	(1)	3	-153.8 ± 0.03	13.61 ± 6.41	405.36 ± 2.42	12.05 ± 7.4	0.23 ± 0.14	26	2.45	3.94	22.06	0.06	5.6
080210	Long	2.641	(1)	3	-22.5 ± 3.84	12.66 ± 1.36	191.03 ± 2.01	166.05 ± 16.98	2.77 ± 0.25	21.68	16.9	8.54	13.14	0.11	1.54
080212	Long		(1)	3	-27.22 ± 4.76	6.38 ± 3.83	191.55 ± 3.34	107.3 ± 16.06	2.66 ± 0.25	32.82	5.25	8.48	24.34	0.17	2.87
			(2)	3	-20.12 ± 3.63	6.58 ± 0.89	238.65 ± 1.79	360.86 ± 37.57	11.98 ± 0.99	43.61	46.89	13.26	30.36	0.18	2.29
			(3)	3	-11.46 ± 1.61	9.3 ± 0.76	296.61 ± 2.56	342.17 ± 18.01	14.16 ± 0.69	53.6	78.32	23.8	29.8	0.18	1.25
080310	Long	2.42	(1)	3	-34.6 ± 5.5	2.92 ± 0.14	147.71 ± 1	253.85 ± 20.22	8.88 ± 0.6	47.59	6.52	6.33	41.25	0.32	6.51
			(2)	3	-29.51 ± 7.67	6.45 ± 4.1	193.05 ± 3.15	257.5 ± 53.52	6.25 ± 0.88	32.12	13.3	8.01	24.11	0.17	3.01
			(3)	3	-7.71 ± 2.46	6.98 ± 2.43	231.07 ± 8.27	282.41 ± 81.99	12.78 ± 3.64	58.56	22.88	26.51	32.05	0.25	1.21
			(4)	3	-101.83 ± 71.92	18.25 ± 7.72	281.11 ± 2.28	141.91 ± 37.36	1.64 ± 0.3	15.34	18.29	3.57	11.76	0.05	3.29
			(5)	3	-4.12 ± 0.75	11.93 ± 0.48	361.65 ± 3.57	382.05 ± 17.67	29.31 ± 0.92	99.46	84.22	63.29	36.17	0.28	0.57
			(6)	3	-48.74 ± 6.25	15.68 ± 6.34	507.53 ± 3.22	136.99 ± 13.53	3.97 ± 0.24	37.97	53.78	11.87	26.1	0.07	2.2
			(7)	3	-39.65 ± 6.34	11.92 ± 0.25	564.13 ± 1.1	335.06 ± 23.95	13.94 ± 0.82	54.58	151.45	16.4	38.18	0.1	2.33
080319D	Long		(1)	3	-2.62 ± 0.26	9.81 ± 7.81	188.75 ± 17.41	32.06 ± 13.74	1.8 ± 0.65	72.8	17.83	48.24	24.56	0.39	0.51
			(2)	3	-6.87 ± 1.99	7.98 ± 1.62	330.39 ± 11.02	66.3 ± 6.66	4.22 ± 0.4	82.23	60.15	40.55	41.68	0.25	1.03
			(3)	3	-13.81 ± 8.49	14.87 ± 4.22	466.54 ± 15.59	24.6 ± 5.08	1.14 ± 0.23	60.08	30.17	29.79	30.29	0.13	1.02
080320	Long		(1)	3	-17.88 ± 6.83	15.84 ± 6.14	212.2 ± 5.69	25.36 ± 5.7	0.46 ± 0.1	23.36	4.8	10.9	12.46	0.11	1.14
			(2)	3	-20.04 ± 6.37	7.81 ± 0.94	313.24 ± 5.44	40 ± 5.43	1.55 ± 0.17	50.76	9.81	16.86	33.91	0.16	2.01
			(3)	3	-114.28 ± 0.07	9.68 ± 2.73	749.35 ± 4.22	8.14 ± 2.5	0.41 ± 0.12	67.77	3.56	9.87	57.89	0.09	5.86
080325	Long	1.78	(1)	3	-5.88 ± 3.22	18.8 ± 5.55	167.03 ± 3.82	340.7 ± 69.39	8.25 ± 1.19	31.49	153.66	20.85	10.63	0.19	0.51
			(2)	3	-7.44 ± 1.55	4.32 ± 0.38	218.48 ± 3.75	410.81 ± 14.84	23.71 ± 0.56	75.25	212.72	28.04	47.2	0.34	1.68
			(3)	3	-48.28 ± 29.47	5.43 ± 1.51	296.68 ± 4.44	62.1 ± 14.43	2.37 ± 0.41	51.27	37.64	8.68	42.6	0.17	4.91
			(4)	3	-30.83 ± 13.22	21.5 ± 5.25	344.19 ± 4.39	61.11 ± 8.68	1.18 ± 0.14	25.04	39.98	10.84	14.2	0.07	1.31
080506	Long		(1)	3	-14.49 ± 1.82	8.01 ± 0.61	476.39 ± 4.77	86.3 ± 4.72	5.67 ± 0.26	85.42	48.22	32.77	52.65	0.18	1.61
			(2)	3	-2.59 ± 1.64	4.11 ± 0.63	841.56 ± 87.14	6.26 ± 1.04	2.28 ± 0.31	470.17	13.75	236.88	233.28	0.56	0.98

Table 1. *Cont.*

GRB	Type ^a	z ^b	Flare (Index)	ω	α_1	α_2	t_p (s)	$F_{X,p,-11}$ ^c (erg/cm ² /s)	$S_{X,-8}$ ^c (erg/cm ²)	Δt (s)	$\Delta F/F$	t_r (s)	t_d (s)	$\Delta t/t$	t_d/t_r	
080607	Long	3.036	(1)	3	-215.09 ± 73.82	6.16 ± 0.2	120.49 ± 0.36	1616.32 ± 135.79	18.35 ± 1.32	15.58	4.51	1.03	14.55	0.13	14.1	
				(2)	3	-11.9 ± 1.71	11.78 ± 1.09	140.66 ± 1.82	997.91 ± 84.26	16.94 ± 1.43	21.95	4.65	10.51	11.44	0.16	1.09
080802	Long	1.505	(1)	3	-17.71 ± 4.98	8.86 ± 0.74	93.37 ± 1.28	155.36 ± 14.71	1.73 ± 0.13	14.54	13.73	5.39	9.15	0.16	1.7	
				(2)	3	-7.52 ± 0.95	3.55 ± 0.12	119.28 ± 1.69	308.51 ± 12.32	11.03 ± 0.34	46.84	721.54	15.77	31.08	0.39	1.97
080810	Long	3.35	(1)	3	-7.94 ± 0.59	9.11 ± 0.39	104.85 ± 0.92	617.24 ± 23.29	10.84 ± 0.39	22.71	12.18	11.24	11.47	0.22	1.02	
				(2)	3	-29.73 ± 5.02	7.39 ± 0.48	208.38 ± 1.42	141.53 ± 10.84	3.34 ± 0.2	31.17	4.71	8.36	22.81	0.15	2.73
080906	Long	2.1ph	(1)	3	-21.33 ± 4.3	5.52 ± 0.33	174.59 ± 1.72	104.59 ± 8	2.83 ± 0.16	35.72	1.63	9.6	26.11	0.2	2.72	
				(2)	3	-14.4 ± 4.67	2.22 ± 0.34	590.39 ± 17.07	11.49 ± 1.37	2.44 ± 0.21	286.23	1.92	52.59	233.64	0.48	4.44
080928	Long	1.692	(1)	3	-8.88 ± 0.58	7.32 ± 0.15	208.51 ± 1.26	1349.64 ± 32.57	50.33 ± 1.15	48.31	36.05	21.28	27.03	0.23	1.27	
				(2)	3	-25.78 ± 2.35	18.26 ± 0.92	356.44 ± 1.34	227.86 ± 9.18	5.41 ± 0.2	30.77	9.23	13.34	17.42	0.09	1.31
081008	Long	1.9685	(1)	3	-51.25 ± 4.67	9.88 ± 0.31	297.5 ± 0.74	240.04 ± 9.76	5.59 ± 0.18	30.88	10.6	7.36	23.52	0.1	3.2	
				(2)	3	-316.19 ± 0.01	7.4 ± 0.42	953.65 ± 0.81	59.32 ± 4.63	4.34 ± 0.33	100.44	36.25	5.76	94.68	0.11	16.45
081210	Long	2.0631	(1)	3	-21.6 ± 3.07	14.47 ± 3.24	138.19 ± 1.26	266.52 ± 20.2	3.03 ± 0.19	14.72	13.97	6.22	8.5	0.11	1.37	
				(2)	3	-7.14 ± 6.21	14.98 ± 9.25	164.62 ± 7.51	61.08 ± 31.82	1.42 ± 0.62	30.03	4.72	17.92	12.12	0.18	0.68
				(3)	3	-4.15 ± 2.92	7.26 ± 2.13	212.5 ± 13.38	65.46 ± 8.44	3.62 ± 0.31	71.33	8.52	39.09	32.24	0.34	0.82
				(4)	3	-14.48 ± 6.08	2.6 ± 0.21	312.67 ± 6.77	34.92 ± 5.94	3.41 ± 0.45	131.06	8.84	26.9	104.16	0.42	3.87
				(5)	3	-17.91 ± 8.66	22.83 ± 7.74	393.02 ± 8.21	21.65 ± 3.78	0.6 ± 0.1	35.93	7.58	18.96	16.97	0.09	0.89
090111	Long	1.4485	(1)	3	-5.9 ± 0.59	4.52 ± 0.54	482.61 ± 35.52	6.53 ± 1.34	0.89 ± 0.18	177.17	19.2	73.13	104.04	0.37	1.42	
090407	Long		(1)	3	-8.7 ± 0.63	10.38 ± 0.95	139.24 ± 1.19	274.26 ± 9.79	5.73 ± 0.19	27	209.69	13.62	13.38	0.19	0.98	
			(2)	3	-2.34 ± 0.4	11.41 ± 4.48	252.09 ± 5.15	120.14 ± 10.59	9.16 ± 0.42	99.08	114.34	69.48	29.6	0.39	0.43	
			(3)	3	-35.14 ± 19.23	6.3 ± 0.49	300.49 ± 2.62	77.13 ± 22.15	2.83 ± 0.68	48.82	78.31	10.94	37.88	0.16	3.46	
090417B	Long	0.345	(1)	3	-1.2 ± 0.24	4.86 ± 0.16	514 ± 14.62	187.47 ± 9.71	56.86 ± 1.98	388.73	6.03	242.24	146.49	0.76	0.6	
			(2)	3	-32.15 ± 3.09	4.61 ± 0.5	1388.4 ± 6.8	157.4 ± 7.95	35.08 ± 1.26	298.56	5.33	57.68	240.88	0.22	4.18	
			(3)	3	-54.2 ± 9.37	13.24 ± 5.55	1539.09 ± 9.2	164.84 ± 20	15.76 ± 1.22	125.98	5.72	34.31	91.67	0.08	2.67	
			(4)	3	-33.28 ± 10.72	20.14 ± 4.17	1679.07 ± 11.19	135.73 ± 24.41	12.85 ± 2.04	122.84	4.85	50.4	72.44	0.07	1.44	
090423	Long	8.26	(1)	3	-13.01 ± 1.91	6.02 ± 0.56	165.21 ± 3.81	45.54 ± 5.94	1.3 ± 0.15	37.17	81.09	13.05	24.12	0.22	1.85	
090429A	Long		(1)	3	-5.01 ± 0.5	9.26 ± 0.93	68.28 ± 9.96	98.62 ± 10.78	1.42 ± 0.14	18.59	21.13	10.5	8.09	0.27	0.77	
			(2)	3	-13.43 ± 1.34	21.22 ± 2.12	84.25 ± 2.78	89.89 ± 57.87	0.65 ± 0.41	9.29	22.4	5.21	4.09	0.11	0.79	
			(3)	3	-6.42 ± 0.64	17.33 ± 14.35	100.64 ± 3.77	102.17 ± 51.22	1.45 ± 0.64	18.48	28.92	11.76	6.72	0.18	0.57	
			(4)	3	-2.76 ± 0.28	19.38 ± 7.37	130.25 ± 3.35	95.66 ± 16.58	2.93 ± 0.41	40.11	32.59	30.59	9.52	0.31	0.31	
090516	Long		(5)	3	-14.39 ± 3.56	5.56 ± 0.35	169.21 ± 1.97	111.47 ± 7.23	3.3 ± 0.15	38.83	45.83	12.57	26.27	0.23	2.09	
			(1)	3	-55.52 ± 4.99	21.08 ± 0.88	274.82 ± 0.6	991.44 ± 49.04	12.23 ± 0.5	16.1	2.63	5.46	10.64	0.06	1.95	
			(2)	3	-58.69 ± 31.42	6.77 ± 0.92	400.56 ± 4.61	38.93 ± 5.95	1.6 ± 0.17	55.18	1.05	9.61	45.56	0.14	4.74	

Table 1. *Cont.*

GRB	Type ^a	z ^b	Flare (Index)	ω	α_1	α_2	t_p (s)	$F_{X,p,-11}$ ^c (erg/cm ² /s)	$S_{X,-8}$ ^c (erg/cm ²)	Δt (s)	$\Delta F/F$	t_r (s)	t_d (s)	$\Delta t/t$	t_d/t_r
090607	Short		(1)	3	-3.71 ± 1.74	8.35 ± 2.72	136.68 ± 9.74	41.1 ± 9.8	1.46 ± 0.28	45.85	1.67	27	18.85	0.34	0.7
090621A	None		(1)	3	-12.98 ± 3.59	20.34 ± 19.71	242.4 ± 5.13	1296.5 ± 544.07	27.81 ± 10.44	27.75	157.68	15.49	12.26	0.11	0.79
			(2)	3	-20.39 ± 14.33	22.23 ± 6.44	268.66 ± 4.36	2024.85 ± 396.65	36.47 ± 6.88	23.29	266.38	11.72	11.57	0.09	0.99
			(3)	3	-19.04 ± 14.32	10.84 ± 1.3	302.11 ± 4.18	363.92 ± 157.94	11.28 ± 4.47	40.29	52.36	15.85	24.43	0.13	1.54
090709A	Long		(1)	3	-7.61 ± 1.16	8.44 ± 2.56	278.53 ± 7.46	77.86 ± 5.38	3.86 ± 0.25	64.09	1.2	31.27	32.82	0.23	1.05
			(2)	3	-12.1 ± 2.86	2.38 ± 0.48	409.61 ± 8.13	99.58 ± 9.26	14.34 ± 0.87	193.18	1.86	41.05	152.13	0.47	3.71
090715B	Long	3	(1)	3	-9.51 ± 1.04	14.37 ± 1.44	77.18 ± 0.87	1035.2 ± 66.97	9.79 ± 0.57	12.23	4.42	6.69	5.54	0.16	0.83
			(2)	3	-25.19 ± 8.42	5.87 ± 2.54	108.01 ± 2.01	176.49 ± 25.26	2.69 ± 0.23	20.15	1.13	5.16	14.99	0.19	2.9
			(3)	3	-66.17 ± 21.48	27.73 ± 7.8	158.02 ± 0.97	261.06 ± 40.89	1.46 ± 0.17	7.27	2.66	2.59	4.68	0.05	1.81
			(4)	3	-49.64 ± 22.36	93.49 ± 54.6	180.22 ± 1.27	191.62 ± 46.17	0.74 ± 0.14	5.02	2.29	3.01	2.02	0.03	0.67
			(5)	3	-4.29 ± 0.97	17.76 ± 2.95	193.81 ± 2.48	368.27 ± 31.93	12.85 ± 0.74	45.47	4.8	31.63	13.83	0.23	0.44
			(6)	3	-123.76 ± 30.12	19.98 ± 6.45	249.81 ± 1.07	760.6 ± 133.72	6.96 ± 0.94	12.14	13.5	2.67	9.47	0.05	3.54
			(7)	3	-8.46 ± 0.67	19.66 ± 0.68	285.43 ± 1.62	1122.68 ± 95.47	36.64 ± 2.87	42.34	23.43	26.12	16.21	0.15	0.62
090727	Long		(1)	3	-5.18 ± 0.55	3.37 ± 0.69	279.39 ± 10.24	137.77 ± 8.24	13.77 ± 0.68	130.29	166.47	49.03	81.27	0.47	1.66
090807	Long		(1)	3	-40.53 ± 3.75	7.38 ± 0.13	186.07 ± 0.49	453.86 ± 14.38	8.8 ± 0.21	25.74	5.99	5.87	19.87	0.14	3.39
			(2)	3	-49.07 ± 13.23	7.58 ± 1.46	6105.17 ± 18.43	0.79 ± 0.15	0.47 ± 0.07	792.2	3.78	164.93	627.27	0.13	3.8
090809	Long	2.737	(1)	3	-8.45 ± 0.72	5.74 ± 0.46	4839.16 ± 18.18	3.33 ± 0.21	3.4 ± 0.2	1323.86	8.78	535.99	787.87	0.27	1.47
			(2)	3	-5.73 ± 2.6	5.98 ± 2.61	$19,863.25 \pm 504.22$	0.23 ± 0.11	1.14 ± 0.52	6279.96	2.93	2936.48	3343.48	0.32	1.14
090812	Long	2.452	(1)	3	-8.5 ± 0.66	4.03 ± 0.17	133.87 ± 1.38	354.43 ± 12.02	12.48 ± 0.34	46.09	2.45	15.77	30.32	0.34	1.92
			(2)	3	-26.96 ± 3.72	6.91 ± 0.31	260.27 ± 1.32	180.12 ± 9.26	5.75 ± 0.22	42.09	3.44	11.42	30.67	0.16	2.68
090831C	Long		(1)	3	-23.29 ± 7.95	6.13 ± 1.02	176.05 ± 3.45	32.14 ± 6.25	0.79 ± 0.12	32.46	8.1	8.86	23.6	0.18	2.66
			(2)	3	-5.52 ± 2.72	19.88 ± 1.99	512.79 ± 44.73	5.36 ± 2.89	0.41 ± 0.2	98.72	3.72	67.1	31.61	0.19	0.47
090904A	Long		(1)	3	-30.92 ± 2.09	10.22 ± 0.22	305.15 ± 0.73	519.96 ± 15.05	14.12 ± 0.32	35.58	9.96	11.11	24.47	0.12	2.2
090904B	Long		(1)	3	-85.26 ± 0.02	1.56 ± 0.23	249.16 ± 2.3	15.59 ± 2.87	1.63 ± 0.29	146.69	1.17	5.76	140.93	0.59	24.47
			(2)	3	-25.45 ± 2.55	4.95 ± 4.18	653.92 ± 102.93	3.91 ± 3.45	0.41 ± 0.33	139.48	0.82	32.1	107.38	0.21	3.34
090929B	Long		(1)	3	-7.12 ± 0.89	5.68 ± 1.44	109.87 ± 3.02	197.83 ± 11.65	4.96 ± 0.26	32.49	3.58	13.89	18.61	0.3	1.34
			(2)	3	-22.82 ± 3.35	3.26 ± 0.31	151.7 ± 1.16	445.12 ± 29.81	15.66 ± 0.78	47.3	10.99	8.81	38.49	0.31	4.37
091026	Long		(1)	3	-29.28 ± 13.1	4.86 ± 0.79	174.28 ± 3.29	36.05 ± 5.96	0.99 ± 0.12	36.52	1.32	7.7	28.82	0.21	3.74
			(2)	3	-18.88 ± 4.78	5.93 ± 0.4	347.38 ± 3.87	77.98 ± 5.51	4.14 ± 0.2	69.79	19.21	20.69	49.1	0.2	2.37
			(3)	3	-7.72 ± 1.97	3.22 ± 0.88	849.88 ± 37.44	19.38 ± 2.44	5.24 ± 0.49	355.39	18.99	112.29	243.1	0.42	2.16
091029	Long	2.752	(1)	3	-13.61 ± 8.47	5.94 ± 1.29	310.73 ± 12.72	8.73 ± 2.2	0.46 ± 0.09	69.37	3.48	23.76	45.61	0.22	1.92
091104	Long		(1)	3	-164.44 ± 148.76	9.62 ± 1.54	203.79 ± 1.55	44.18 ± 8.66	0.58 ± 0.08	17.66	0.76	2.01	15.66	0.09	7.8
091130B	Long		(1)	3	-5.26 ± 0.34	3.33 ± 0.08	103.09 ± 1.36	952.45 ± 25.35	35.17 ± 0.82	48.16	1345.1	17.94	30.22	0.47	1.68
091221	Long		(1)	3	-19.84 ± 2.43	6.12 ± 0.28	106.29 ± 0.78	217.97 ± 12.33	3.41 ± 0.15	20.57	8.48	6.06	14.51	0.19	2.4

Table 1. *Cont.*

GRB	Type ^a	z ^b	Flare (Index)	ω	α_1	α_2	t_p (s)	$F_{X,p,-11}$ ^c (erg/cm ² /s)	$S_{X,-8}$ ^c (erg/cm ²)	Δt (s)	$\Delta F/F$	t_r (s)	t_d (s)	$\Delta t/t$	t_d/t_r
100117A	Short	0.92	(1)	3	-47.12 ± 4.71	54.5 ± 5.45	139.3 ± 4.39	42.79 ± 4.38	0.17 ± 0.02	5.08	1.01	2.64	2.44	0.04	0.93
			(2)	3	-15.61 ± 7.87	61.25 ± 60.2	184.76 ± 2.65	41.09 ± 17.24	0.39 ± 0.12	12.57	1.37	8.88	3.69	0.07	0.42
			(3)	3	-8.82 ± 6.58	25.66 ± 25.06	226.77 ± 9.02	25.5 ± 9.7	0.58 ± 0.15	29.74	1.1	19.46	10.28	0.13	0.53
100302A	Long	4.813	(1)	3	-3.67 ± 1.26	11.29 ± 2.47	134.81 ± 4.01	175.81 ± 22.51	5.49 ± 0.49	40.48	419.83	26	14.47	0.3	0.56
			(2)	3	-12.69 ± 5	9.47 ± 1.78	187.07 ± 4.26	70.38 ± 6.9	1.74 ± 0.15	32	189	13.82	18.18	0.17	1.32
			(3)	3	-48.38 ± 7.1	12.5 ± 0.79	252.78 ± 0.81	231.66 ± 13.37	3.92 ± 0.17	22.29	693.04	6.23	16.06	0.09	2.58
			(4)	3	-62.75 ± 14.15	5.09 ± 0.16	313.07 ± 1.47	98.34 ± 5.46	4 ± 0.16	55.04	317.64	7.54	47.5	0.18	6.3
100413A	Long		(1)	3	-11.08 ± 2.55	37.34 ± 11.94	222.21 ± 2.63	234.68 ± 40.55	3.99 ± 0.53	22.2	1.29	15.1	7.09	0.1	0.47
			(2)	3	-33.26 ± 14.52	45.72 ± 20.12	277.74 ± 3.57	117.8 ± 27.47	1.2 ± 0.25	13.22	1.12	7.21	6.01	0.05	0.83
100526A	Long		(1)	3	-21.28 ± 2.23	5.94 ± 0.15	187.19 ± 0.89	247.39 ± 9.7	6.81 ± 0.2	36.27	2.44	10.17	26.11	0.19	2.57
100614A	Long		(1)	3	-123.46 ± 57.37	7.91 ± 1.56	161.99 ± 1.01	172.29 ± 22.95	2.21 ± 0.22	17.39	0.94	2.09	15.31	0.11	7.34
			(2)	3	-44.8 ± 24.31	12.66 ± 2.84	203.56 ± 2.12	84.38 ± 17.22	1.17 ± 0.17	18.18	0.77	5.32	12.87	0.09	2.42
			(3)	3	-18.52 ± 7.69	5.34 ± 0.65	301.73 ± 5.62	34.26 ± 4.66	1.71 ± 0.17	65.97	0.77	18.63	47.34	0.22	2.54
			(4)	3	-33.68 ± 25.3	13.12 ± 5.73	997.97 ± 27.95	4.92 ± 1.99	0.36 ± 0.12	95.31	1.56	32.32	62.99	0.1	1.95
100619A	Long		(1)	3	-4.95 ± 0.44	10.94 ± 0.21	88.42 ± 0.79	4818.23 ± 239.68	84.17 ± 3.67	22.6	193.28	13.47	9.14	0.26	0.68
			(2)	3	-46.73 ± 1.81	9.71 ± 0.13	947.15 ± 1.11	316.95 ± 5.95	24.43 ± 0.36	101.96	87.14	25.27	76.69	0.11	3.03
100704A	Long		(1)	3	-3.08 ± 0.3	5.41 ± 1.1	110.39 ± 3	342.09 ± 15.05	13.14 ± 0.4	49.53	15.42	26.47	23.07	0.45	0.87
			(2)	3	-11.92 ± 0.48	8.22 ± 0.1	176.5 ± 0.62	3757.4 ± 79.68	97.58 ± 1.92	33.69	236.43	14.05	19.64	0.19	1.4
100725B	Long		(1)	3	-13.68 ± 4.53	11.15 ± 2.5	90.5 ± 1.83	894.37 ± 62.96	9.43 ± 0.58	13.65	202.95	6.12	7.53	0.15	1.23
			(2)	3	-9.88 ± 1.69	5.04 ± 0.18	129.35 ± 1.75	1023.57 ± 66.31	28.39 ± 1.55	36.19	270.76	13.03	23.16	0.28	1.78
			(3)	3	-16.43 ± 2.57	9.76 ± 0.83	161.14 ± 1.4	1460.2 ± 72.9	27.33 ± 1.1	24.31	424.49	9.68	14.63	0.15	1.51
			(4)	3	-28.38 ± 1.73	18.62 ± 0.47	215.33 ± 0.54	2986.2 ± 95.09	40.61 ± 1.18	17.63	983.19	7.44	10.19	0.08	1.37
			(5)	3	-72.95 ± 5.86	21.13 ± 0.63	271.7 ± 0.39	876.12 ± 37.42	9.72 ± 0.34	14.55	318.75	4.36	10.19	0.05	2.34
100727A	Long		(1)	3	-10.61 ± 1.15	7.93 ± 0.28	246.44 ± 2.12	123.48 ± 4.81	4.81 ± 0.17	50.49	44.62	21.61	28.88	0.2	1.34
100728A	Long	1.567	(1)	3	-58.22 ± 5.82	22.51 ± 19.37	72.12 ± 1.29	614.98 ± 232.92	1.88 ± 0.6	3.98	0.75	1.36	2.62	0.06	1.92
			(2)	3	-3.02 ± 1.09	10.14 ± 3.67	90.96 ± 3.17	1182.71 ± 166.97	29.08 ± 2.61	31.85	1.84	20.71	11.15	0.35	0.54
			(3)	3	-14.49 ± 3.64	7.63 ± 0.5	122.93 ± 1.36	1576.77 ± 116.52	27.54 ± 1.61	22.74	3.32	8.54	14.2	0.18	1.66
			(4)	3	-8.2 ± 1.01	10.2 ± 2.31	223.3 ± 3.61	579.83 ± 23.76	20.19 ± 0.7	45	2.23	22.95	22.05	0.2	0.96
			(5)	3	-33.89 ± 12.88	21.88 ± 5.42	267.28 ± 2.57	343.84 ± 48.7	4.9 ± 0.59	18.48	1.59	7.78	10.7	0.07	1.37
			(6)	3	-31.84 ± 3.08	15.53 ± 0.66	317.57 ± 0.91	1067.25 ± 41.32	22.74 ± 0.71	27.72	5.87	10.39	17.34	0.09	1.67
			(7)	3	-223.1 ± 29.55	29.96 ± 1.43	388.64 ± 0.34	966.26 ± 51.43	8.75 ± 0.36	12.05	6.52	2.4	9.65	0.03	4.02
			(8)	3	-54.82 ± 10.41	37.59 ± 6.06	462.43 ± 1.99	226.23 ± 20.27	3.33 ± 0.26	19.06	1.82	8.27	10.79	0.04	1.3
			(9)	3	-25.67 ± 0.94	22.44 ± 0.69	570.59 ± 1.02	1010.82 ± 20.26	34.4 ± 0.66	44.02	10.08	20.63	23.39	0.08	1.13
			(10)	3	-60.78 ± 8.56	11 ± 0.46	699.55 ± 1.87	240.63 ± 12.21	11.62 ± 0.43	64.06	2.95	14.81	49.25	0.09	3.33

Table 1. *Cont.*

GRB	Type ^a	z ^b	Flare (Index)	ω	α_1	α_2	t_p (s)	$F_{X,p_r=11}^*$ (erg/cm ² /s)	$S_{X_r=8}^*$ (erg/cm ²)	Δt (s)	$\Delta F/F$	t_r (s)	t_d (s)	$\Delta t/t$	t_d/t_r	
100802A	Long		(1)	3	-72.44 ± 40.19	10.46 ± 3.85	308.4 ± 3.35	64.75 ± 14.19	1.37 ± 0.21	28.29	1.35	5.75	22.54	0.09	3.92	
			(2)	1	-7.15 ± 0.32	7.15 ± 0.14	490.39 ± 5.13	424.03 ± 5.57	61.19 ± 0.8	181.66	14.96	82.52	99.15	0.37	1.2	
100805A	Long		(1)	3	-19.69 ± 13.54	3.25 ± 0.36	631.54 ± 17.05	32.58 ± 5.01	4.95 ± 0.47	203.83	22.05	41.12	162.7	0.32	3.96	
			(1)	3	-12.43 ± 2.14	7.12 ± 0.62	91.35 ± 1.73	105.89 ± 9.88	1.52 ± 0.13	18.72	37.2	7.23	11.49	0.2	1.59	
100816A	Short	0.8049	(1)	3	-14.75 ± 5.39	4.36 ± 0.71	137.41 ± 3.98	41.43 ± 6.9	1.17 ± 0.15	37.42	2.85	10.51	26.9	0.27	2.56	
			(2)	3	-88.74 ± 8.87	4.77 ± 2.61	280.63 ± 28.87	5.08 ± 0.66	0.19 ± 0.02	50.26	1.04	5.18	45.08	0.18	8.7	
100901A	Long	1.408	(1)	3	-4.01 ± 1.49	7.33 ± 1.38	214.86 ± 4.14	86.28 ± 8.08	4.88 ± 0.33	73.1	10.21	40.52	32.58	0.34	0.8	
			(2)	3	-112.25 ± 0.02	6.1 ± 1.9	249.96 ± 1.31	56.52 ± 10.53	1.44 ± 0.25	34.56	7.38	3.65	30.91	0.14	8.47	
			(3)	3	-33.47 ± 0.29	4.72 ± 0.86	311.64 ± 2.37	58.54 ± 7.9	2.85 ± 0.35	65.21	8.82	12.49	52.72	0.21	4.22	
			(4)	3	-20.1 ± 1.46	5.59 ± 0.21	396.57 ± 1.67	210.38 ± 8.04	13.03 ± 0.39	81.71	37.08	22.78	58.93	0.21	2.59	
			(5)	3	-2.69 ± 0.26	2.19 ± 0.08	$26,639.75 \pm 232.37$	0.84 ± 0.05	13.68 ± 0.72	21,340.49	2.27	7976.28	13,364.21	0.8	1.68	
100902A	Long		(1)	3	-37.04 ± 0.67	16.95 ± 0.15	404.23 ± 0.42	5676.73 ± 105.83	137.55 ± 2.36	31.55	138.88	11.54	20.01	0.08	1.73	
100905A	Long		(1)	3	-17.73 ± 2.04	10.12 ± 1.67	316.15 ± 3.6	52.28 ± 4.12	1.82 ± 0.12	45.26	45.58	17.78	27.48	0.14	1.55	
			(2)	3	-57.4 ± 22.17	12.5 ± 1.48	398.6 ± 3	43.97 ± 7.3	1.12 ± 0.14	33.54	46.95	8.6	24.94	0.08	2.9	
100906A	Long	1.727	(1)	3	-9.8 ± 0.32	12.42 ± 0.19	119.33 ± 0.46	9412.02 ± 253.54	145.19 ± 3.78	19.94	30.45	10.32	9.62	0.17	0.93	
101219B	Long	0.55	(1)	3	-6.47 ± 1.45	5.14 ± 0.55	356.25 ± 11.52	26.22 ± 2.19	2.35 ± 0.18	116.38	0.86	49.26	67.12	0.33	1.36	
110102A	Long		(1)	3	-93.24 ± 5.91	7.44 ± 0.2	203.78 ± 0.3	2091.05 ± 70.43	37.15 ± 1.06	23.99	20.42	3.32	20.67	0.12	6.22	
			(2)	3	-16.7 ± 1.14	14.21 ± 0.37	269.78 ± 0.99	1930.38 ± 52.35	48.5 ± 1.25	32.51	80.35	14.92	17.59	0.12	1.18	
110119A	Long		(1)	3	-12.82 ± 1.01	14.88 ± 1.5	127.99 ± 0.91	394.68 ± 16.51	5.22 ± 0.21	17.1	2.87	8.67	8.42	0.13	0.97	
			(2)	3	-8.9 ± 1.16	17.43 ± 3.69	203.79 ± 1.98	527.13 ± 63.18	12.54 ± 1.29	30.81	9.28	18.16	12.64	0.15	0.7	
			(3)	3	-37.49 ± 11.23	41.69 ± 12.84	235.84 ± 1.48	302.74 ± 37.45	2.58 ± 0.31	11.01	7.02	5.63	5.38	0.05	0.96	
			(4)	3	-6.11 ± 5.11	29.7 ± 2.76	260 ± 4.23	194.95 ± 29.75	6.18 ± 0.52	41.55	5.44	30.23	11.32	0.16	0.37	
			(5)	3	-128.79 ± 58.19	21.78 ± 4.88	385.81 ± 1.91	28.37 ± 5.74	0.37 ± 0.06	17.36	2.1	3.93	13.43	0.05	3.42	
			(6)	3	-18.86 ± 4.5	3.07 ± 0.64	626.32 ± 12.83	24.58 ± 2.96	3.92 ± 0.34	213.96	7.87	42.61	171.35	0.34	4.02	
110205A	Long	2.22	(1)	3	-142.88 ± 100.45	14.36 ± 2.82	470.75 ± 3.16	49.33 ± 10.14	1.07 ± 0.16	29.18	0.44	4.8	24.38	0.06	5.07	
			(2)	3	-94.67 ± 15.78	18.14 ± 1.11	610.02 ± 1.35	131.83 ± 8.91	3.39 ± 0.17	34.03	2.22	8.23	25.81	0.06	3.14	
110407A	Long		(1)	3	-4.05 ± 2.29	2.45 ± 0.1	163.44 ± 7.98	159.99 ± 9.54	12.71 ± 0.45	104.05	170.76	36.19	67.87	0.64	1.88	
			(2)	3	-17.79 ± 2.17	3.6 ± 0.15	454.47 ± 3.63	70.21 ± 3.23	7.23 ± 0.24	137.19	156.73	31.32	105.87	0.3	3.38	
			(3)	3	-9.08 ± 6.46	16.23 ± 4.3	4987.77 ± 67.73	0.14 ± 0.06	0.08 ± 0.03	768.29	1.72	441.44	326.84	0.15	0.74	
110414A	Long		(1)	3	-10 ± 2.48	7.76 ± 0.29	144.41 ± 1.99	340.79 ± 20.19	8.08 ± 0.43	30.72	225.51	13.31	17.42	0.21	1.31	
			(2)	3	-6.21 ± 2.09	4.84 ± 0.68	365.19 ± 17.72	15.21 ± 1.98	1.48 ± 0.18	125.88	8.95	52.58	73.3	0.34	1.39	
110520A	Long		(1)	3	-8.6 ± 2.42	5.3 ± 0.76	232.68 ± 9.13	40.38 ± 5.77	2.06 ± 0.26	66.47	3.83	25.81	40.66	0.29	1.58	
110610A	Long		(1)	3	-122.29 ± 1.4	3.1 ± 0.98	632.73 ± 12.47	6.98 ± 1.86	0.86 ± 0.22	170.57	1.92	9.7	160.87	0.27	16.58	
110709A	Long		(1)	3	-82.14 ± 56.13	11.1 ± 1.92	90.74 ± 0.91	129.09 ± 27.33	0.75 ± 0.11	7.73	1.34	1.51	6.21	0.09	4.11	
			(2)	3	-26.61 ± 2.66	2.44 ± 0.55	215.93 ± 9.64	13.55 ± 3.1	0.86 ± 0.18	86.07	0.33	11.77	74.3	0.4	6.31	

Table 1. *Cont.*

GRB	Type ^a	z ^b	Flare (Index)	ω	α_1	α_2	t_p (s)	$F_{X,p,-11}$ ^c (erg/cm ² /s)	$S_{X,-8}$ ^c (erg/cm ²)	Δt (s)	$\Delta F/F$	t_r (s)	t_d (s)	$\Delta t/t$	t_d/t_r
110709B	Long		(1)	3	-33.15 ± 15.23	6.62 ± 1.16	154.62 ± 2.55	44.08 ± 7.85	0.81 ± 0.11	24.49	0.93	5.83	18.66	0.16	3.2
			(2)	3	-11.53 ± 0.2	17.2 ± 1.04	654.99 ± 1.75	808.73 ± 15.9	53.93 ± 0.93	86.24	23.99	47.27	38.97	0.13	0.82
			(3)	3	-9.46 ± 0.73	42.55 ± 3.34	848.89 ± 1.91	498.9 ± 16.21	34.54 ± 0.72	90.78	17.87	65.55	25.23	0.11	0.38
			(4)	3	-55.18 ± 8.36	12.11 ± 0.34	936.49 ± 1.76	207.83 ± 8.56	12.84 ± 0.36	81.59	8.07	20.97	60.62	0.09	2.89
			(5)	3	-104.14 ± 13.15	21.8 ± 1.12	1302.37 ± 2.09	84.63 ± 4.71	3.95 ± 0.17	61.68	4.42	15.68	46	0.05	2.93
110731A	Long	2.83	(1)	3	-3.44 ± 0.91	14.69 ± 3.04	75.09 ± 1.99	206.31 ± 31.1	3.41 ± 0.39	21.51	0.96	14.94	6.57	0.29	0.44
110801A	Long	1.858	(1)	3	-9.01 ± 0.94	7.76 ± 0.58	212.65 ± 2.69	111.55 ± 5.31	4.08 ± 0.19	47.4	2.93	21.25	26.15	0.22	1.23
			(2)	3	-36.63 ± 0.87	8.32 ± 0.08	358.28 ± 0.46	1643.47 ± 29.05	57.54 ± 0.88	46.26	98.66	11.93	34.33	0.13	2.88
110820A	Long		(1)	3	-9.97 ± 0.25	18.8 ± 0.55	258.31 ± 0.77	1023.47 ± 26.39	28.02 ± 0.65	35.45	462.11	20.75	14.71	0.14	0.71
110915A	Long		(1)	3	-64.17 ± 25.95	4.19 ± 0.38	155.54 ± 1.53	72.77 ± 7.44	1.75 ± 0.13	32.73	1.84	3.82	28.92	0.21	7.58
			(2)	3	-23.15 ± 10.33	9.93 ± 3.13	327.93 ± 7.48	22.73 ± 4.49	0.75 ± 0.11	42.98	0.96	15.04	27.94	0.13	1.86
			(3)	3	-13.33 ± 8.24	33.14 ± 20.26	496.52 ± 13.23	11.05 ± 3.51	0.39 ± 0.09	45.91	0.58	29.13	16.78	0.09	0.58
110921A	Long		(1)	3	-7.05 ± 2.08	6.26 ± 1.19	236.56 ± 10.95	20.12 ± 3.06	1.03 ± 0.15	66.38	4.32	29.62	36.76	0.28	1.24
			(2)	3	-258.17 ± 0	7.93 ± 1.27	495.01 ± 0.85	17.79 ± 3.35	0.64 ± 0.12	49.38	6.82	3.49	45.88	0.1	13.14
111016A	Long		(1)	3	-60.29 ± 5.68	13.68 ± 2.75	415.83 ± 1.3	250.58 ± 16.81	6.13 ± 0.28	32.27	17.38	8.47	23.8	0.08	2.81
			(2)	3	-23.64 ± 4.04	8.94 ± 1.42	482.55 ± 3.14	276.93 ± 23.28	14.27 ± 0.9	67.43	32.42	22.24	45.18	0.14	2.03
			(3)	3	-11.33 ± 1.32	14.05 ± 0.59	611.99 ± 3.07	329.2 ± 11.64	22.78 ± 0.74	89.47	61.11	46.2	43.26	0.15	0.94
			(4)	3	-48.49 ± 5.16	3.93 ± 0.18	792.2 ± 2.55	136.25 ± 4.49	18.45 ± 0.44	183.76	34.81	24.59	159.17	0.23	6.47
111103B	Long		(1)	3	-22.35 ± 1.24	3.99 ± 0.16	117.29 ± 0.55	1096.14 ± 51.19	25.33 ± 1	30.84	19.48	6.65	24.2	0.26	3.64
			(2)	3	-47.37 ± 27.86	2.31 ± 0.37	214.29 ± 4.15	117.03 ± 16.47	7.16 ± 0.77	84.3	3.03	7.48	76.82	0.39	10.27
			(3)	3	-94.46 ± 65.3	12.19 ± 5.19	347.91 ± 3.59	75.35 ± 21.18	1.51 ± 0.31	26.68	2.6	5.1	21.59	0.08	4.24
111107A	Long	2.893	(1)	3	-4.86 ± 1.72	7.98 ± 1.89	324.1 ± 18.48	8.79 ± 1.92	0.65 ± 0.13	95.93	5.56	52.06	43.87	0.3	0.84
111123A	Long	3.1516	(1)	3	-15.37 ± 2.92	4.79 ± 0.53	281.41 ± 3.15	137.82 ± 11.24	7.37 ± 0.45	70.45	1.02	20.48	49.97	0.25	2.44
			(2)	3	-85.65 ± 49.66	9.14 ± 5.16	449.02 ± 4.69	48.46 ± 10.61	1.61 ± 0.23	44.71	1.66	7.53	37.18	0.1	4.94
			(3)	3	-2.57 ± 0.81	11.17 ± 1.51	518.55 ± 12.06	78.94 ± 15.97	11.79 ± 1.99	193.8	4.25	133.07	60.73	0.37	0.46
111129A	Long	1.0796	(1)	3	-15.91 ± 1.59	25.44 ± 2.54	263.91 ± 30.1	7.96 ± 0.86	0.15 ± 0.02	24.47	1.76	13.81	10.66	0.09	0.77
			(2)	3	-11.07 ± 1.11	9.2 ± 7.69	416.15 ± 41.08	3.71 ± 1.66	0.22 ± 0.1	76.82	1.05	34.36	42.46	0.18	1.24
111215A	Long	2.06ph	(1)	3	-14.5 ± 1.94	11.99 ± 1.27	650.56 ± 6.88	70.09 ± 4.22	4.97 ± 0.28	91.78	0.95	41.47	50.31	0.14	1.21
			(2)	3	-31.35 ± 2.38	3.57 ± 0.09	974.75 ± 3.22	160.62 ± 4.1	31.48 ± 0.6	264.5	3.24	43.45	221.05	0.27	5.09
111225A	Long	0.297	(1)	3	-13.23 ± 3.2	3.51 ± 0.18	234.36 ± 3.83	56.49 ± 4.49	3.33 ± 0.19	78.03	1.18	20.34	57.69	0.33	2.84
120102A	Long		(1)	3	-15.08 ± 9.22	9.46 ± 2.06	115.03 ± 4.3	121.12 ± 36.81	1.71 ± 0.47	18.31	4.26	7.43	10.88	0.16	1.46
			(2)	3	-27.5 ± 4.71	4.39 ± 0.78	1090.76 ± 12.75	83.36 ± 8.76	15.75 ± 1.25	252.56	13.5	51.67	200.89	0.23	3.89
120116A	Long		(1)	3	-13.33 ± 6.51	8.1 ± 1.93	113.37 ± 4.13	23.38 ± 4.61	0.38 ± 0.06	20.86	1.37	8.3	12.56	0.18	1.51
			(1)	3	-0.86 ± 0.22	4.21 ± 0.74	$20,676.5 \pm 517.22$	0.1 ± 0.02	1.59 ± 0.19	19,351.14	2.41	12,076.86	7274.28	0.94	0.6

Table 1. *Cont.*

GRB	Type ^a	z ^b	Flare (Index)	ω	α_1	α_2	t_p (s)	$F_{X,p,-11}$ ^c (erg/cm ² /s)	$S_{X,-8}$ ^c (erg/cm ²)	Δt (s)	$\Delta F/F$	t_r (s)	t_d (s)	$\Delta t/t$	t_d/t_r
120308A	Long		(1)	3	-24.25 ± 3.43	5.19 ± 0.39	123.8 ± 0.83	434.07 ± 26.37	8.41 ± 0.37	25.7	5.08	6.25	19.45	0.21	3.11
			(2)	3	-2.51 ± 0.73	10.98 ± 1.81	204.64 ± 5.7	95.54 ± 13.35	5.74 ± 0.61	77.98	4.07	53.55	24.43	0.38	0.46
120324A	Long		(1)	3	-31.9 ± 5.59	5.02 ± 0.16	104.48 ± 0.66	418.48 ± 22.48	6.56 ± 0.25	20.94	3	4.29	16.65	0.2	3.88
			(2)	3	-16.53 ± 3.39	11.37 ± 1.21	118.86 ± 1.7	132.24 ± 16.66	1.66 ± 0.19	16.32	13.96	6.9	9.42	0.14	1.36
120514A	Long		(2)	3	-5.32 ± 2.97	7.26 ± 2.29	526.46 ± 45.24	6.37 ± 2	0.77 ± 0.22	155.75	3.52	79.91	75.83	0.3	0.95
			(1)	3	-6.62 ± 1.96	13.94 ± 2.83	100.07 ± 2.53	565.16 ± 55.92	8.57 ± 0.62	19.63	132.5	11.69	7.94	0.2	0.68
			(3)	3	-16.62 ± 1.37	8.96 ± 0.21	142.89 ± 0.64	886.41 ± 26.45	15.42 ± 0.38	22.63	247.28	8.65	13.98	0.16	1.62
120701A	Long		(3)	3	-68.44 ± 0.68	4.1 ± 0.86	611.41 ± 4.57	9.07 ± 2.04	0.87 ± 0.19	130.21	5.15	14.3	115.91	0.21	8.11
			(1)	3	-5.11 ± 3.09	7.77 ± 4.1	334.05 ± 31.94	6.54 ± 2.21	0.49 ± 0.15	97.57	1.96	51.79	45.78	0.29	0.88
			(1)	3	-15.36 ± 3.71	6.99 ± 0.77	532.05 ± 11.98	15.02 ± 2.09	1.17 ± 0.14	102.02	24.64	35.93	66.09	0.19	1.84
120805A	Long	3.1	(1)	3	-11.47 ± 4.01	4.58 ± 3.78	186.2 ± 11.66	35.51 ± 9.17	1.43 ± 0.26	52.9	2.15	17.08	35.82	0.28	2.1
120922A	Long	3.1 pH	(1)	3	-55.34 ± 9.73	12.3 ± 1.8	318.97 ± 1.46	177.95 ± 15.39	3.7 ± 0.23	27.43	1.44	7.1	20.33	0.09	2.86
			(2)	3	-104.59 ± 62.96	17.14 ± 16	372.17 ± 3.55	69.32 ± 21.3	1.11 ± 0.22	21.2	0.96	4.69	16.5	0.06	3.52
			(3)	3	-23.22 ± 12.17	19.21 ± 3.12	412.96 ± 4.51	100.06 ± 21.53	2.81 ± 0.57	36.3	1.98	16.64	19.66	0.09	1.18
121024A	Long	2.298	(1)	3	-17.61 ± 3.4	10 ± 1.92	207.34 ± 3.25	62 ± 6.52	1.43 ± 0.13	29.98	2.78	11.75	18.23	0.14	1.55
			(2)	3	-42.12 ± 18.25	10.93 ± 2.03	269.7 ± 2.74	38.29 ± 6.6	0.79 ± 0.1	27.31	2.7	7.62	19.69	0.1	2.59
121027A	Long	1.773	(1)	3	-18.8 ± 2.38	4.69 ± 0.17	253.58 ± 1.89	143.38 ± 7.28	6.61 ± 0.26	61.02	3.64	15.89	45.12	0.24	2.84
121028A	Long		(1)	3	-13.53 ± 3.77	7.65 ± 1.19	832.05 ± 21.96	7.04 ± 1.42	0.85 ± 0.16	157.74	10.14	60.86	96.88	0.19	1.59
121031A	Long		(1)	3	-5.65 ± 2.01	2.96 ± 0.17	59.62 ± 1.94	411.39 ± 25.42	9.25 ± 0.39	29.45	19.1	10.06	19.39	0.49	1.93
			(2)	3	-187.88 ± 18.79	6.22 ± 1.23	74.93 ± 0.51	179.94 ± 26.02	1.27 ± 0.17	9.7	9.29	0.72	8.98	0.13	12.54
			(3)	3	-40.74 ± 33.94	3.23 ± 0.54	189.88 ± 5.06	22.57 ± 4.85	0.9 ± 0.14	54.35	1.79	7.02	47.33	0.29	6.74
121108A	Long		(1)	3	-32.06 ± 2.51	13.07 ± 0.44	138.88 ± 0.4	577.96 ± 22.58	5.99 ± 0.19	13.52	55.65	4.68	8.85	0.1	1.89
121123A	Long		(1)	3	-13.48 ± 0.56	4.28 ± 0.13	249.13 ± 1.06	910.76 ± 22.48	48.83 ± 0.96	70.65	9.56	20.49	50.16	0.28	2.45
			(2)	3	-3.34 ± 0.38	7.62 ± 0.43	457.67 ± 6.16	175.81 ± 8.96	22.98 ± 0.94	168.81	3.21	98.99	69.82	0.37	0.71
121125A	Long		(1)	3	-65.24 ± 29.48	11.91 ± 1.68	92.28 ± 0.74	137.9 ± 22.18	0.81 ± 0.1	7.81	1.09	1.82	5.99	0.08	3.3
121128A	Long	2.2	(1)	3	-15.58 ± 4.25	9.98 ± 1.27	96.51 ± 1.67	131.88 ± 13.92	1.49 ± 0.14	14.68	1.52	6.02	8.66	0.15	1.44
121211A	Long	1.023	(1)	3	-3.57 ± 1.17	7.98 ± 1.18	94.67 ± 3.34	422.1 ± 46.94	10.79 ± 0.91	33.04	31.05	19.35	13.69	0.35	0.71
			(2)	3	-8.27 ± 0.49	3.79 ± 0.08	165.61 ± 1.22	1238.51 ± 29.7	56.79 ± 1.11	60.06	135.26	20.14	39.92	0.36	1.98
121212A	Long		(1)	3	-10.67 ± 2.9	7.3 ± 0.79	236.7 ± 5.99	47.81 ± 5.31	1.87 ± 0.19	50.8	18.11	20.98	29.83	0.21	1.42
			(2)	3	-20.49 ± 9.64	7.08 ± 0.83	561.35 ± 11.01	16.56 ± 2.63	1.22 ± 0.15	96.71	11.71	30.29	66.42	0.17	2.19
121217A	Long		(1)	3	-5.41 ± 0.11	8.99 ± 0.11	751.22 ± 2.14	435.2 ± 5.79	67 ± 0.81	198.94	112.02	109.15	89.78	0.26	0.82
121229A	None		(1)	3	-12.26 ± 0.49	7.52 ± 0.2	445 ± 1.91	182.78 ± 4.12	12.47 ± 0.25	88.61	78.56	35.23	53.38	0.2	1.52
130131A	Long		(1)	3	-17.57 ± 3.88	23.13 ± 4.09	192.6 ± 2.31	90.06 ± 9.66	1.23 ± 0.12	17.67	27.98	9.42	8.25	0.09	0.88
			(2)	3	-10.22 ± 0.44	11.69 ± 0.31	282.04 ± 1.22	281.83 ± 6.56	10.37 ± 0.23	47.59	132.06	23.82	23.76	0.17	1

Table 1. *Cont.*

GRB	Type ^a	z ^b	Flare (Index)	ω	α_1	α_2	t_p (s)	$F_{X,p,-11}$ ^c (erg/cm ² /s)	$S_{X,-8}$ ^c (erg/cm ²)	Δt (s)	$\Delta F/F$	t_r (s)	t_d (s)	$\Delta t/t$	t_d/t_r
130211A	Long		(1)	3	-6.19 ± 0.43	8.67 ± 0.38	215.05 ± 2.14	103.16 ± 4.02	4.32 ± 0.15	54.06	11.39	28.26	25.79	0.25	0.91
130427B	Long	2.78	(1)	3	-13.04 ± 2.71	13.85 ± 2.21	130.35 ± 2.16	83.05 ± 8.16	1.15 ± 0.11	17.9	2.23	8.82	9.08	0.14	1.03
130514A	Long	3.6 ph	(1)	3	-5.98 ± 0.36	4.39 ± 0.35	110.21 ± 1.68	1545.41 ± 56.72	48.73 ± 1.62	40.97	53.28	16.61	24.35	0.37	1.47
			(2)	3	-2.76 ± 0.36	8.93 ± 0.89	238.91 ± 3.51	881.98 ± 42.78	62.94 ± 2.03	92.35	61.64	59.08	33.26	0.39	0.56
			(3)	3	-8.16 ± 1.53	15.85 ± 1.15	374.94 ± 3.88	332.04 ± 20.71	15.88 ± 0.79	61.93	35.08	36.32	25.61	0.17	0.71
130528A	Long		(1)	3	-383.93 ± 0	6.83 ± 1.33	614.85 ± 0.42	113.77 ± 8.95	5.74 ± 0.43	69.51	52.04	3.2	66.31	0.11	20.72
			(2)	3	-8.46 ± 0.91	12.03 ± 2.16	780.12 ± 11.24	60.52 ± 7.79	6.69 ± 0.81	142.82	32.59	76.25	66.57	0.18	0.87
			(3)	3	-182.76 ± 35.61	6.1 ± 0.27	1021.06 ± 2.34	173.89 ± 6.38	17.12 ± 0.48	134.9	107.64	10.02	124.89	0.13	12.47
			(4)	3	-120.52 ± 24.11	7.59 ± 0.88	1303.01 ± 3.68	91.96 ± 6.33	9.88 ± 0.52	145.72	63.29	17.24	128.49	0.11	7.45
130606A	Long	5.913	(1)	3	-25.48 ± 6.9	2.38 ± 0.19	87.32 ± 1.41	198.92 ± 24.55	5.25 ± 0.54	35.99	3.8	4.95	31.04	0.41	6.27
			(2)	3	-5.33 ± 0.84	42.78 ± 8.28	163.63 ± 1.23	224.49 ± 20.61	4.5 ± 0.31	26.48	7.72	21.02	5.46	0.16	0.26
			(3)	3	-28.46 ± 3.44	18.88 ± 2.67	221.06 ± 1.33	267.5 ± 17.67	3.7 ± 0.21	17.93	12.2	7.6	10.33	0.08	1.36
			(4)	3	-56.12 ± 8.88	7.54 ± 0.45	257.8 ± 0.87	360.46 ± 19.39	8.81 ± 0.34	32.66	18.99	6.27	26.39	0.13	4.21
			(5)	3	-14.09 ± 1.99	17.64 ± 1.22	409.57 ± 2.86	154.75 ± 7.03	5.74 ± 0.24	47.96	12.58	25.02	22.94	0.12	0.92
130609B	Long		(1)	3	-2.83 ± 0.68	12.73 ± 2	87.81 ± 2.24	380.32 ± 50.96	8.69 ± 0.91	29.7	2.44	20.67	9.03	0.34	0.44
			(2)	3	-12.03 ± 0.28	7.79 ± 0.34	178.3 ± 0.84	3853.57 ± 101.08	103.93 ± 2.48	35.02	38.28	14.23	20.79	0.2	1.46
			(3)	3	-18.61 ± 2.06	8.03 ± 0.16	274.02 ± 1.39	1385.79 ± 53.52	47.44 ± 1.47	44.69	17.95	15.52	29.17	0.16	1.88
130615A	Long		(1)	3	-14.29 ± 1.61	5.98 ± 0.94	221.55 ± 2.29	381.73 ± 28.64	14.14 ± 0.83	48.45	3.96	16.31	32.14	0.22	1.97
			(2)	3	-23.52 ± 7.26	7.13 ± 2.7	285.27 ± 4.01	190.74 ± 35.21	6.8 ± 0.92	46.86	4.28	13.82	33.04	0.16	2.39
			(3)	3	-4.26 ± 1.4	7.27 ± 0.66	362.75 ± 8.8	163.59 ± 33.18	15.2 ± 2.82	120.02	7.63	65.34	54.68	0.33	0.84
130722A	Long		(1)	3	-4.62 ± 0.3	13.82 ± 2.54	268.07 ± 2.56	230.43 ± 12.12	11.59 ± 0.41	65.26	3.05	42.12	23.14	0.24	0.55
			(2)	3	-17.44 ± 4.68	13.48 ± 1.16	342.48 ± 3.56	150.38 ± 9.75	4.84 ± 0.28	41.69	2.67	18.48	23.2	0.12	1.26
130803A	Long		(1)	3	-29.39 ± 11.12	6.27 ± 1.8	506.06 ± 9.38	20.31 ± 5.03	1.32 ± 0.26	86.2	8.75	21.18	65.01	0.17	3.07
131004A	Short	0.717	(1)	3	-9.01 ± 3.18	2.75 ± 0.5	475.4 ± 21.63	10.56 ± 1.7	1.7 ± 0.21	213.79	4.73	57.69	156.1	0.45	2.71
			(2)	3	-74.19 ± 7.42	8.61 ± 3.07	771.41 ± 102.22	10.4 ± 1.04	0.64 ± 0.63	82.94	7.15	14.67	68.27	0.11	4.65
131018A	Long		(1)	3	-11.87 ± 2.85	11.45 ± 1.5	191.14 ± 3.56	91.2 ± 8.56	2.14 ± 0.2	30.33	1.51	14.38	15.94	0.16	1.11
131030A	Long	1.295	(1)	3	-1.41 ± 0.11	6.15 ± 0.07	114.68 ± 1.4	6560.96 ± 241.66	374.14 ± 11.25	73.35	40.22	47.79	25.56	0.64	0.53
131103A	Long	0.599	(1)	3	-3.6 ± 0.9	9.66 ± 0.89	84.31 ± 2.31	165.96 ± 18.89	3.48 ± 0.32	27.13	36.28	16.77	10.36	0.32	0.62
			(2)	3	-130.59 ± 0.01	10.1 ± 3.52	407.38 ± 2.74	20.61 ± 7.78	0.53 ± 0.19	34.79	3.93	4.78	30	0.09	6.27
			(3)	3	-118.9 ± 6.84	6.79 ± 0.31	682.05 ± 0.78	476.72 ± 15.4	29.69 ± 0.81	84.64	99.11	9.31	75.32	0.12	8.09
131117A	Long	4.042	(1)	3	-22.49 ± 3.96	10.17 ± 0.78	95.09 ± 0.89	119.91 ± 10.17	1.14 ± 0.08	12.4	19.33	4.44	7.96	0.13	1.79
131127A	Long		(1)	3	-9.33 ± 2.25	2.63 ± 0.4	770.68 ± 25.27	5.28 ± 0.66	1.42 ± 0.14	356.9	5.87	92.03	264.87	0.46	2.88
140108A	Long		(1)	3	-9.33 ± 0.36	10.88 ± 0.27	87.72 ± 0.44	2417.56 ± 78.08	30.01 ± 0.95	16.05	65.97	8.05	7.99	0.18	0.99
			(2)	3	-40.44 ± 8.27	5.36 ± 0.29	219.06 ± 1.54	110.56 ± 8.1	3.26 ± 0.18	39.53	4.69	7.38	32.15	0.18	4.36

Table 1. *Cont.*

GRB	Type ^a	z ^b	Flare (Index)	ω	α_1	α_2	t_p (s)	$F_{X,p,-11}$ ^c (erg/cm ² /s)	$S_{X,-8}$ ^c (erg/cm ²)	Δt (s)	$\Delta F/F$	t_r (s)	t_d (s)	$\Delta t/t$	t_d/t_r	
140114A	Long	3	(1)	3	-1.41 ± 0.08	6.34 ± 0.14	191.52 ± 1.88	1403.39 ± 34.18	132.44 ± 2.47	121.43	2799.59	79.83	41.6	0.63	0.52	
				(2)	3	-55.86 ± 4.45	7.46 ± 0.1	319.73 ± 0.58	530.49 ± 13.59	16.23 ± 0.31	40.91	1196.83	7.82	33.09	0.13	4.23
140206A	Long	2.73	(1)	3	-14.59 ± 1.13	6.28 ± 0.12	59.76 ± 0.44	5215.26 ± 240.58	50.05 ± 2.03	12.54	31.98	4.29	8.26	0.21	1.93	
				(2)	3	-13.54 ± 0.39	7.56 ± 0.11	221.92 ± 0.74	1256.46 ± 26.55	40.92 ± 0.78	42.37	16.77	16.26	26.11	0.19	1.61
140301A	Long	1.416	(1)	3	-15.93 ± 3.06	3.95 ± 0.11	85.91 ± 0.8	235.92 ± 13.5	4.4 ± 0.18	24.74	139.29	6.32	18.42	0.29	2.91	
				(2)	3	-35.32 ± 6.01	7.56 ± 0.57	574.32 ± 4.08	25.43 ± 2.11	1.55 ± 0.1	80.61	33.86	20.06	60.55	0.14	3.02
140304A	Long	5.283	(1)	3	-3.55 ± 0.67	2.92 ± 0.52	340.36 ± 22.34	37.37 ± 3.55	5.81 ± 0.52	202.32	18.24	80.44	121.88	0.59	1.52	
				(2)	3	-14.6 ± 6.62	3.06 ± 0.3	815.04 ± 22.67	16.49 ± 2.5	3.66 ± 0.4	296.26	17.1	67.48	228.78	0.36	3.39
140323A	Long		(1)	3	-36.66 ± 12.58	8.97 ± 8.51	108.32 ± 2.15	932.9 ± 219.54	9.34 ± 1.3	13.21	1.48	3.55	9.66	0.12	2.72	
				(2)	3	-50.2 ± 32.37	8.56 ± 2.89	119.22 ± 1.11	939.78 ± 389.64	9.86 ± 3.38	13.94	2.94	3.09	10.86	0.12	3.52
140413A	Long		(1)	3	-12.11 ± 0.85	5.74 ± 1.01	2484.32 ± 25.99	106.49 ± 3.77	48.28 ± 1.06	591.92	20.94	209.14	382.78	0.24	1.83	
				(2)	3	-37 ± 7.11	22.28 ± 4.42	2848.77 ± 13.79	60.04 ± 6.25	8.7 ± 0.77	187.9	14.08	77.1	110.8	0.07	1.44
				(3)	3	-58.21 ± 18.39	38.88 ± 11.53	3231.11 ± 17.08	27.82 ± 3.75	2.73 ± 0.31	127.3	7.67	54.75	72.55	0.04	1.33
				(4)	3	-28.02 ± 6.11	7.12 ± 0.79	3641.97 ± 18.36	35.22 ± 5.15	15.21 ± 1.85	569.58	11.33	154.17	415.41	0.16	2.69
140419A	Long	3.956	(1)	3	-28.68 ± 6.37	8.05 ± 0.71	196.44 ± 1.62	137.04 ± 12.28	2.9 ± 0.19	27.84	1	7.96	19.88	0.14	2.5	
140430A	Long	1.6	(1)	3	-51.55 ± 11.84	14.48 ± 6.07	154.8 ± 1.32	549.65 ± 94.34	5.04 ± 0.63	12.04	2.87	3.52	8.52	0.08	2.42	
				(2)	3	-74.29 ± 18.13	15.49 ± 1	171.6 ± 0.5	1233.26 ± 111.62	10.71 ± 0.72	11.48	11.63	2.89	8.58	0.07	2.97
				(3)	3	-46.45 ± 3.96	11.98 ± 0.24	217.3 ± 0.46	882.89 ± 34.38	13.41 ± 0.42	19.99	30.81	5.58	14.41	0.09	2.58
140506A	Long	0.889	(1)	3	-11.59 ± 0.29	8.07 ± 0.14	120.51 ± 0.51	5617.07 ± 142.85	101.89 ± 2.46	23.53	60.35	9.83	13.7	0.2	1.39	
				(2)	3	-17.2 ± 1.23	5.74 ± 0.46	238.89 ± 1.44	609.51 ± 23.38	23.47 ± 0.66	50.58	12.26	15.38	35.2	0.21	2.29
				(3)	3	-17.2 ± 1.15	9.77 ± 0.26	345.78 ± 1.36	1382.67 ± 49.79	54.45 ± 1.74	51.18	39.05	20.04	31.15	0.15	1.55
140512A	Long	0.725	(1)	3	-8.78 ± 0.42	9.96 ± 0.34	128.68 ± 0.88	2174.97 ± 77.65	42.68 ± 1.49	25.37	13.12	12.57	12.8	0.2	1.02	
				(2)	3	-63.69 ± 47.03	17.02 ± 5.6	229 ± 2.88	78.54 ± 23.42	0.89 ± 0.2	14.9	0.71	4.27	10.62	0.07	2.49
140515A	Long	6.32	(1)	3	-3.6 ± 0.3	1.7 ± 0.09	2974.58 ± 20.52	2.22 ± 0.24	4.36 ± 0.45	2607.61	36.13	761.74	1845.87	0.88	2.42	
140709A	Long		(1)	3	-68.46 ± 6.9	7.48 ± 0.51	139.93 ± 0.37	745.09 ± 34.54	9.56 ± 0.34	17.22	12.47	2.92	14.3	0.12	4.91	
				(2)	3	-14.54 ± 1.09	16.72 ± 0.77	184.97 ± 0.8	1055.03 ± 38.05	17.86 ± 0.62	21.88	50.07	11.11	10.77	0.12	0.97
140709B	Long		(1)	3	-3.99 ± 0.54	4.19 ± 0.11	115.04 ± 2.22	226.84 ± 7.68	9.14 ± 0.3	52.16	120.01	23.56	28.61	0.45	1.21	
				(2)	3	-24.42 ± 12.61	8.31 ± 2.46	545.6 ± 14.11	6.24 ± 1.64	0.38 ± 0.08	79.34	3.69	24.89	54.45	0.15	2.19
				(3)	3	-21.49 ± 12.21	12.87 ± 4.67	898.27 ± 26.75	3.7 ± 1.03	0.29 ± 0.07	102.77	2.32	41.49	61.28	0.11	1.48
140710A	Long	0.558	(1)	3	-14.43 ± 4.37	5.75 ± 1.11	383.65 ± 10.41	16.71 ± 3.2	1.1 ± 0.18	85.88	9.82	28.24	57.64	0.22	2.04	
140713A	Long		(1)	3	-18.81 ± 3.03	5.69 ± 0.4	669.62 ± 7.64	62.13 ± 5.52	6.55 ± 0.47	138.8	13.23	40.33	98.47	0.21	2.44	

Table 1. *Cont.*

GRB	Type ^a	z ^b	Flare (Index)	ω	α_1	α_2	t_p (s)	$F_{X,p,-11}$ ^c (erg/cm ² /s)	$S_{X,-8}$ ^c (erg/cm ²)	Δt (s)	$\Delta F/F$	t_r (s)	t_d (s)	$\Delta t/t$	t_d/t_r
140817A	Long		(1)	3	-29.74 ± 3.49	6.12 ± 2.9	189.99 ± 2.05	381.9 ± 53.49	9.47 ± 0.91	32.9	13.96	7.92	24.98	0.17	3.15
			(2)	3	-21.98 ± 5.54	14.27 ± 3.29	216.64 ± 2.25	563.03 ± 69.37	10.02 ± 1.07	23.09	23.09	9.64	13.45	0.11	1.4
			(3)	3	-6.77 ± 0.78	5.29 ± 0.22	290.14 ± 3.28	319.43 ± 33.43	22.5 ± 2.28	91.38	16.93	38.54	52.84	0.31	1.37
			(4)	3	-43.32 ± 6.93	5.9 ± 0.34	509.51 ± 2.45	97 ± 5.66	6.06 ± 0.26	83.63	8.43	15.96	67.67	0.16	4.24
			(5)	3	-96.81 ± 9.68	9.55 ± 1.52	741.23 ± 11.26	52.66 ± 10.88	2.73 ± 0.52	69.61	6.36	11.18	58.43	0.09	5.23
140907A	Long	1.21	(1)	3	-15.54 ± 14.14	3.12 ± 0.79	179.27 ± 10.12	16.23 ± 5.23	0.77 ± 0.18	63.13	1.56	14.1	49.03	0.35	3.48
141005A	Long		(1)	3	-13.31 ± 7.91	9.37 ± 2.72	436.47 ± 23.82	5.11 ± 1.36	0.29 ± 0.07	73.63	3.82	31.14	42.49	0.17	1.36
141020A	Long		(1)	3	-5.73 ± 2.31	6.43 ± 1.66	418.55 ± 25.13	10.42 ± 2	1.02 ± 0.19	127.2	5.88	61.15	66.06	0.3	1.08
141031A	Long		(1)	3	-7.88 ± 2.43	2.77 ± 0.3	449.51 ± 19.33	29.42 ± 4.1	4.66 ± 0.52	209.43	6.18	60.2	149.23	0.47	2.48
			(2)	3	-10.71 ± 1.09	110.81 ± 25.54	804.16 ± 2.31	152.1 ± 12.46	7.23 ± 0.44	63.35	63.4	52.56	10.79	0.08	0.21
			(3)	3	-33.31 ± 1.61	17.2 ± 0.49	886.95 ± 1.52	559.27 ± 11.87	30.71 ± 0.54	71.38	261.47	27.44	43.95	0.08	1.6
			(4)	3	-42.25 ± 4.26	14.4 ± 0.55	1098.87 ± 2.54	160.97 ± 6.25	11.23 ± 0.33	91.29	96.65	29.25	62.04	0.08	2.12
141109A	Long	2.993	(1)	3	-140.5 ± 23.03	9.47 ± 0.32	310.1 ± 0.57	388.57 ± 16.37	7.98 ± 0.25	27.8	2.17	3.48	24.32	0.09	6.99
			(2)	3	-6971.18 ± 0	22.07 ± 5.85	455.1 ± 0.08	46.84 ± 9.86	0.5 ± 0.1	14.71	0.61	0.17	14.54	0.03	86.7
141130A	Long		(1)	1	-5.03 ± 0.29	6.87 ± 0.23	274.85 ± 5.34	100.11 ± 3.14	9.79 ± 0.24	122.91	15.48	58.36	64.55	0.45	1.11
141221A	Long	1.452	(1)	3	-4.72 ± 1.04	4.93 ± 0.75	340.74 ± 16.46	51.33 ± 5.7	5.19 ± 0.57	130.85	10.05	60.08	70.77	0.38	1.18
150206A	Long	2.087	(1)	3	-6.11 ± 0.4	13.07 ± 0.29	2329.41 ± 10.6	572.79 ± 13.62	217.31 ± 4.11	491.17	14.9	292.86	198.31	0.21	0.68
150222A	Long		(1)	3	-10.43 ± 1.07	9.51 ± 0.82	180.34 ± 2.19	80.12 ± 4.52	2.08 ± 0.11	33.58	6.68	15.52	18.07	0.19	1.16
			(2)	3	-71.86 ± 14.99	8.06 ± 0.53	283.52 ± 1.71	97.7 ± 8.13	2.36 ± 0.15	32.41	12.52	5.6	26.81	0.11	4.79
150323C	Long		(1)	3	-5.19 ± 0.56	28.47 ± 4.34	190.69 ± 1.21	264.08 ± 19.51	6.95 ± 0.38	34.55	342.41	25.64	8.9	0.18	0.35
			(2)	3	-5.96 ± 0.63	7.9 ± 0.21	251.88 ± 2.3	275.49 ± 7.32	14.41 ± 0.34	67.59	413.56	34.6	32.99	0.27	0.95
			(3)	3	-61.35 ± 25.12	9.5 ± 0.97	401.32 ± 3.08	21.55 ± 2.85	0.67 ± 0.06	41.25	41.36	8.69	32.56	0.1	3.75
			(4)	3	-481.19 ± 0	13.28 ± 2.27	589.31 ± 0.61	8.83 ± 1.99	0.22 ± 0.05	34.28	20.77	2.28	32	0.06	14.06
150615A	Long		(1)	3	-3.96 ± 2.52	4.31 ± 2.01	8256.84 ± 369.28	0.18 ± 0.12	0.52 ± 0.33	3702.61	1.31	1695.46	2007.15	0.45	1.18
150616A	Long		(1)	3	-18.51 ± 0.98	6.56 ± 0.26	1770.24 ± 6.87	115.77 ± 3.2	29.36 ± 0.63	332.61	18.68	104.87	227.74	0.19	2.17
			(2)	3	-35.52 ± 11.47	3.47 ± 0.13	2554.42 ± 28.76	37.93 ± 3.4	19.52 ± 1.31	696.94	8.76	103.85	593.1	0.27	5.71
150626A	Long		(1)	3	-36.44 ± 7.46	13.23 ± 1.45	108.97 ± 0.73	341.38 ± 31.8	2.63 ± 0.19	10.08	1	3.31	6.76	0.09	2.04
150626B	Long		(1)	3	-2.64 ± 0.4	3.87 ± 0.55	$20,525.75 \pm 872.82$	0.96 ± 0.07	8.71 ± 0.6	11,718.51	3.35	5736.1	5982.41	0.57	1.04
150711A	Long		(1)	3	-13.65 ± 2.39	9.69 ± 0.96	173.52 ± 2.47	76.05 ± 6.02	1.66 ± 0.12	28.38	2.54	12.05	16.32	0.16	1.35
150722A	Long		(1)	3	-14.53 ± 2.05	3.56 ± 0.24	5045.65 ± 73.46	2.99 ± 0.24	3.64 ± 0.23	1617.45	13.06	406.67	1210.79	0.32	2.98
150724A	Long		(1)	3	-32.4 ± 4.23	4.44 ± 0.32	150.27 ± 0.9	256.42 ± 13.62	6.38 ± 0.25	33.34	4.7	6.25	27.09	0.22	4.33
			(2)	3	-27.12 ± 1.3	14.77 ± 0.92	231.67 ± 0.75	1140.18 ± 42.2	19.48 ± 0.62	22.2	62.87	8.68	13.52	0.1	1.56
			(3)	3	-24.77 ± 3.62	7.49 ± 0.19	289.26 ± 1	352.52 ± 14.75	12.11 ± 0.36	45.14	34.12	13.33	31.81	0.16	2.39
			(4)	3	-21.48 ± 6.58	3.88 ± 0.78	1108.34 ± 24.67	5.54 ± 0.8	1.25 ± 0.13	301.05	12.56	65.15	235.91	0.27	3.62

Table 1. *Cont.*

GRB	Type ^a	z ^b	Flare (Index)	ω	α_1	α_2	t_p (s)	$F_{X,p,-11}$ ^c (erg/cm ² /s)	$S_{X,-8}$ ^c (erg/cm ²)	Δt (s)	$\Delta F/F$	t_r (s)	t_d (s)	$\Delta t/t$	t_d/t_r
150821A	Long	0.755	(1)	3	-6.66 ± 0.88	6.03 ± 0.59	611.28 ± 10.81	70.32 ± 2.88	9.75 ± 0.38	179.59	2.01	80.4	99.19	0.29	1.23
			(2)	3	-0.59 ± 0.16	17.86 ± 2.8	1124.84 ± 23.89	25.77 ± 2.01	18.2 ± 1.14	901.11	2.28	781.59	119.52	0.8	0.15
			(3)	3	-64.53 ± 3.04	10.16 ± 3.13	1548.96 ± 15.41	7.81 ± 1.98	0.88 ± 0.2	149.16	1.18	31.8	117.37	0.1	3.69
150910A	Long	1.359	(1)	3	-13.52 ± 5.47	5.16 ± 0.96	331.96 ± 10.59	22.65 ± 3.69	1.42 ± 0.18	81.99	0.48	26.25	55.74	0.25	2.12
151001A	Long		(1)	3	-16.9 ± 4.95	4.95 ± 0.56	607.51 ± 12.82	15.34 ± 2.12	1.68 ± 0.18	144.34	5.79	40.84	103.49	0.24	2.53
151001B	Long		(1)	3	-114.41 ± 0.84	8.06 ± 3.47	1293.33 ± 10.11	2.13 ± 1.17	0.22 ± 0.11	137.7	2.2	17.64	120.07	0.11	6.81
151006A	Long		(1)	3	-7.26 ± 2.46	5.67 ± 0.7	68.75 ± 2.59	330.54 ± 34.41	5.14 ± 0.49	20.17	0.82	8.56	11.61	0.29	1.36
151027A	Long	0.81	(1)	3	-6.38 ± 0.26	8.09 ± 0.18	125.84 ± 0.87	3686.97 ± 122.87	91.98 ± 2.95	32.24	88.67	16.33	15.91	0.26	0.97
			(2)	3	-4 ± 0.49	6.15 ± 0.31	311.44 ± 5.41	116.82 ± 4.6	10.43 ± 0.35	115.27	2.92	60.25	55.02	0.37	0.91
151111A	Long	3.5 ph	(1)	3	-5.26 ± 0.94	4.7 ± 0.42	132.63 ± 4.18	92.57 ± 6.44	3.56 ± 0.24	49.88	1.12	21.74	28.14	0.38	1.29
151118A	Long		(1)	3	-8.8 ± 3.22	3.87 ± 0.44	151.01 ± 6.88	91.08 ± 16.79	3.67 ± 0.57	52.88	9.26	17.47	35.4	0.35	2.03
151210A	Long		(1)	3	-18.37 ± 1.11	13.07 ± 0.39	533.82 ± 2.38	135.24 ± 4.81	6.74 ± 0.22	64.63	205.23	27.81	36.82	0.12	1.32
160104A	Long		(1)	3	-95.23 ± 0.02	4.37 ± 0.69	228.25 ± 3.01	16.95 ± 3.32	0.55 ± 0.1	44.22	11.76	4.04	40.17	0.19	9.93
			(2)	3	-15.7 ± 7.97	3.03 ± 0.28	707.26 ± 26.54	4.36 ± 0.69	0.83 ± 0.09	254.55	21.81	55.5	199.06	0.36	3.59
160117B	None		(1)	3	-43.52 ± 6.29	4.47 ± 0.09	80.52 ± 0.38	441.34 ± 17.83	5.51 ± 0.16	16.84	5.86	2.66	14.19	0.21	5.34
			(2)	3	-107.23 ± 0.11	2.59 ± 0.43	509.59 ± 2.98	3.49 ± 0.72	0.42 ± 0.09	167.32	2.16	8.97	158.35	0.33	17.65
160119A	Long		(1)	3	-52.32 ± 7.82	31.5 ± 4.8	1125.7 ± 4.42	78.8 ± 6.9	3.19 ± 0.24	52.42	86.43	21.63	30.79	0.05	1.42
			(2)	3	-20.76 ± 4.84	16.53 ± 1.44	1307.71 ± 10.71	40.12 ± 2.39	4.07 ± 0.22	131.34	44.61	59.21	72.13	0.1	1.22
160123A	Long		(1)	3	-48.4 ± 3.14	3.12 ± 0.65	630.76 ± 7.16	2.39 ± 0.6	0.32 ± 0.08	182.49	6.06	20.48	162.01	0.29	7.91
160127A	Long		(1)	3	-9.65 ± 2.4	3.75 ± 0.38	104.63 ± 2.88	42.16 ± 4.25	1.17 ± 0.09	36.35	4.08	11.36	24.99	0.35	2.2
160227A	Long	2.38	(1)	3	-39.01 ± 1.77	7.27 ± 0.11	201.95 ± 0.37	1072.01 ± 29.88	23.03 ± 0.54	28.53	19.84	6.58	21.94	0.14	3.33
			(2)	3	-62.47 ± 5.85	3.53 ± 0.05	393.47 ± 1.02	217.17 ± 5.07	15.59 ± 0.28	98.14	43.36	10.18	87.96	0.25	8.64
160325A	Long		(1)	3	-42.83 ± 10.14	10.58 ± 1	166.86 ± 1.06	143.89 ± 14.25	1.88 ± 0.14	17.23	1.68	4.68	12.54	0.1	2.68
160410A	Short	1.717	(1)	3	-10.93 ± 7.26	13.34 ± 8.62	312.02 ± 19.37	8.12 ± 2.52	0.3 ± 0.09	47.65	1.16	24.45	23.2	0.15	0.95
160425A	Long	0.555	(1)	3	-13.08 ± 4.63	87.42 ± 54.26	224.26 ± 2.01	61.59 ± 14.81	0.74 ± 0.13	15.83	5.78	12.33	3.5	0.07	0.28
			(2)	3	-65.22 ± 3.16	16.82 ± 2.02	271.66 ± 0.59	4248.9 ± 239.22	57.2 ± 2.51	17.7	476.3	4.99	12.72	0.07	2.55
			(3)	3	-13.18 ± 0.38	13.43 ± 0.15	311.58 ± 1.02	3254.76 ± 180.44	108.84 ± 6.03	43.24	414.1	21	22.24	0.14	1.06
160506A	Long		(1)	3	-30.85 ± 7.92	5.12 ± 0.37	378.73 ± 3.71	58.73 ± 4.96	3.31 ± 0.2	75.14	1.29	15.91	59.23	0.2	3.72
160804A	Long	0.736	(1)	3	-48.01 ± 8.48	12.26 ± 0.86	422.11 ± 1.68	177.91 ± 12.48	5.11 ± 0.27	37.84	0.82	10.51	27.33	0.09	2.6
160824A	Long		(1)	3	-65.82 ± 14.19	12.08 ± 7.22	92.16 ± 1.16	1284.38 ± 706.43	7.46 ± 3.65	7.7	5.12	1.8	5.9	0.08	3.28
			(2)	3	-46.16 ± 31.62	19.23 ± 6.19	109.58 ± 1.28	582.25 ± 168.15	3.25 ± 0.74	7.27	4.72	2.57	4.71	0.07	1.84
			(3)	3	-128.8 ± 45.19	12.53 ± 0.83	120.35 ± 0.41	849.47 ± 90.57	5.4 ± 0.43	8.53	9.95	1.37	7.16	0.07	5.22
160905A	Long		(1)	3	-2.66 ± 1.87	29.25 ± 2.93	84.53 ± 2.67	183.28 ± 124.05	3.41 ± 2.14	24.53	0.43	20.09	4.43	0.29	0.22
			(2)	3	-9 ± 0.9	10.3 ± 2.08	100.48 ± 3.16	235.13 ± 28.04	3.5 ± 0.41	19.24	0.61	9.58	9.66	0.19	1.01

Table 1. *Cont.*

GRB	Type ^a	z ^b	Flare (Index)	ω	α_1	α_2	t_p (s)	$F_{X,p,-11}^c$ (erg/cm ² /s)	$S_{X,-8}^c$ (erg/cm ²)	Δt (s)	$\Delta F/F$	t_r (s)	t_d (s)	$\Delta t/t$	t_d/t_r
160912A	Long		(1)	3	-5.87 ± 0.62	10.79 ± 0.4	177.22 ± 1.71	868.41 ± 40.13	27.82 ± 1.1	41.43	4.64	23.57	17.86	0.23	0.76
			(2)	3	-19.09 ± 4.6	5.49 ± 0.71	1633.53 ± 26.26	10.77 ± 1.33	2.83 ± 0.27	346.55	4.46	98	248.55	0.21	2.54
161001A	Short		(1)	3	-8.42 ± 2.19	4.55 ± 0.74	127.17 ± 4.63	40.99 ± 4.95	1.27 ± 0.13	40.43	1.66	14.74	25.69	0.32	1.74
161004A	Short		(1)	3	-4.51 ± 0.6	6.75 ± 0.35	322.83 ± 7.02	73.56 ± 5.17	6.12 ± 0.39	107.5	21.5	56.23	51.27	0.33	0.91
161007A	Long		(1)	3	-7.12 ± 1.5	9.49 ± 1.38	221.1 ± 5.91	156.92 ± 17.08	6.02 ± 0.6	49.56	0.99	25.68	23.88	0.22	0.93
161011A	Long		(1)	3	-11.58 ± 3.48	4.32 ± 0.68	27,828.79 ± 165.67	0.41 ± 0.08	2.56 ± 0.41	8215.41	1.6	2563.03	5652.37	0.3	2.21
161017A	Long	2.013	(1)	3	-31.92 ± 15.55	30.49 ± 14.54	89.27 ± 1.53	117.82 ± 25.22	0.48 ± 0.1	5.29	0.7	2.56	2.72	0.06	1.06
			(2)	3	-8.1 ± 2.05	2.95 ± 1.55	148.49 ± 7.08	273.42 ± 66.7	13.52 ± 2.6	65.23	2.73	19.25	45.98	0.44	2.39
			(3)	3	-47.38 ± 22.27	9.49 ± 7.81	195.73 ± 3.38	357.15 ± 105.87	5.76 ± 1.15	21.37	4.74	5.19	16.18	0.11	3.12
			(4)	3	-4.03 ± 0.77	8.57 ± 1.64	236.32 ± 6.36	735.8 ± 175.75	42.66 ± 9.3	74.92	11.86	43.58	31.34	0.32	0.72
			(5)	3	-126.52 ± 64	3.75 ± 1.07	326.53 ± 2.4	158.76 ± 25.88	8.29 ± 1.14	71.98	3.57	4.71	67.27	0.22	14.27
			(6)	3	-15.76 ± 4.03	14.89 ± 6.98	390.31 ± 6.9	238.06 ± 40.29	8.67 ± 1.44	47.12	6.44	22.42	24.7	0.12	1.1
			(7)	3	-9.53 ± 5.36	18.91 ± 2.35	459.49 ± 7.73	201.63 ± 32.58	10.05 ± 1.27	64.56	6.46	38.28	26.28	0.14	0.69
161022A	Long		(1)	3	-3.25 ± 0.74	10.22 ± 2.18	663.08 ± 25.09	4.7 ± 0.77	0.8 ± 0.11	221.65	7.1	142.2	79.45	0.33	0.56
161108A	Long	1.159	(1)	3	-8.34 ± 1.4	14.09 ± 1.79	113.78 ± 1.75	477.98 ± 41.36	7.22 ± 0.54	19.53	0.98	11	8.53	0.17	0.78
161113A	Long		(1)	3	-120.11 ± 47.34	13.56 ± 1.52	62.67 ± 0.28	969.66 ± 123.38	3.05 ± 0.29	4.2	1.61	0.74	3.46	0.07	4.66
161117A	Long	1.549	(1)	3	-9.57 ± 0.31	7.9 ± 0.14	116.98 ± 0.57	5303.61 ± 130.78	102.86 ± 2.45	25.12	11.31	11.12	14.01	0.21	1.26
161117B	Long		(1)	3	-7.23 ± 2.61	9.61 ± 8.79	81.81 ± 5.53	247.58 ± 42.67	3.47 ± 0.49	18.09	33.61	9.37	8.71	0.22	0.93
			(2)	3	-24.14 ± 4.51	13.92 ± 2.03	101.29 ± 0.76	1405.54 ± 99.43	11.41 ± 0.65	10.54	209.47	4.21	6.34	0.1	1.51
			(3)	3	-35.97 ± 6.79	66.78 ± 32.63	127.3 ± 0.63	2027.14 ± 360.52	7.69 ± 1.12	4.92	333.83	2.93	1.99	0.04	0.68
			(4)	3	-28.98 ± 13.16	51.77 ± 15.13	136.12 ± 1.04	2397.56 ± 339.14	12.26 ± 1.33	6.63	406.55	3.89	2.74	0.05	0.7
			(5)	3	-10.22 ± 2.4	19.76 ± 0.95	154.52 ± 1.31	2455.39 ± 149.56	38.84 ± 1.82	20.49	440.06	12.08	8.4	0.13	0.7
			(6)	3	-75.79 ± 25.76	10.01 ± 0.45	185.24 ± 0.83	219.89 ± 20.91	2.88 ± 0.2	17.46	42.66	3.36	14.1	0.09	4.2
161219B	Long	0.1475	(1)	3	-15.53 ± 1.95	4.58 ± 0.19	383.2 ± 2.95	99.52 ± 4.37	7.47 ± 0.24	98.98	7.18	27.92	71.06	0.26	2.55
170111A	Long		(1)	3	-5.85 ± 1.58	5.13 ± 1.05	458.65 ± 22.96	31.63 ± 3.86	3.82 ± 0.45	156.59	18.04	68.39	88.2	0.34	1.29
170113A	Long	1.968	(1)	3	-5.97 ± 0.31	8.08 ± 0.22	93.71 ± 0.74	804.98 ± 29.33	15.47 ± 0.53	24.84	35.91	12.81	12.03	0.27	0.94
170206B	Long		(1)	3	-5.54 ± 0.6	5.81 ± 0.25	127.16 ± 2.08	81.45 ± 3.69	2.61 ± 0.12	41.48	89.69	19.38	22.11	0.33	1.14
170208B	Long		(1)	1	-26.1 ± 1.33	5.49 ± 0.05	104.64 ± 0.45	3437.39 ± 114.97	70.83 ± 1.41	26.47	23.28	8.23	18.25	0.25	2.22
170405A	Long	3.51	(1)	3	-20.05 ± 2.47	8.53 ± 0.43	161.3 ± 1.05	586.57 ± 31.22	11.06 ± 0.47	24.63	3.2	8.53	16.1	0.15	1.89
170519A	Long	0.818	(1)	3	-80.49 ± 3.21	7.66 ± 0.07	193.39 ± 0.23	2968.91 ± 67.14	50.03 ± 0.98	22.68	100.4	3.53	19.15	0.12	5.43
170531B	Long	2.366	(1)	3	-15.58 ± 0.54	6.37 ± 0.11	163.5 ± 0.52	552.26 ± 11.48	14.03 ± 0.25	33.23	593.44	11.13	22.11	0.2	1.99
			(2)	3	-25.98 ± 1.1	14.09 ± 0.32	572.18 ± 1.22	210.27 ± 5.3	9.29 ± 0.21	57.42	320.8	22.38	35.04	0.1	1.57
			(3)	3	-175.34 ± 84.32	14.65 ± 5.01	368.37 ± 1.6	416.68 ± 58.35	6.73 ± 0.62	21.74	8.21	3.18	18.56	0.06	5.84
170604A	Long	1.329	(1)	3	-37.83 ± 21.76	37.74 ± 26.61	268.69 ± 4.92	63.87 ± 16.41	0.65 ± 0.17	13.13	0.71	6.48	6.65	0.05	1.03
			(2)	3	-20.3 ± 1.67	5.3 ± 1.2	339.07 ± 3.26	623.28 ± 43.66	34.24 ± 1.62	72.56	10.81	19.54	53.02	0.21	2.71
			(3)	3	-175.34 ± 84.32	14.65 ± 5.01	368.37 ± 1.6	416.68 ± 58.35	6.73 ± 0.62	21.74	8.21	3.18	18.56	0.06	5.84

Table 1. *Cont.*

GRB	Type ^a	z ^b	Flare (Index)	ω	α_1	α_2	t_p (s)	$F_{X,p,-11}$ ^c (erg/cm ² /s)	$S_{X,-8}$ ^c (erg/cm ²)	Δt (s)	$\Delta F/F$	t_r (s)	t_d (s)	$\Delta t/t$	t_d/t_r
170607A	Long		(1)	3	-10.02 ± 1.93	15.44 ± 2.79	108.72 ± 1.94	435.26 ± 48.77	5.46 ± 0.54	16.21	0.95	8.94	7.28	0.15	0.81
170626A	Long		(1)	3	-8.96 ± 0.82	5.62 ± 0.86	86.55 ± 1.49	967.28 ± 54.71	17.42 ± 0.83	23.41	4.93	9.2	14.22	0.27	1.55
			(2)	3	-12.45 ± 1.5	8.07 ± 0.27	137.97 ± 1.02	1346.6 ± 50.76	27.14 ± 0.88	26.17	7.45	10.66	15.51	0.19	1.46
			(3)	3	-20.89 ± 3.16	5.34 ± 0.24	264.72 ± 1.86	162.74 ± 8.82	6.89 ± 0.27	55.94	1.37	14.91	41.03	0.21	2.75
170705A	Long	2.01	(1)	3	-7.36 ± 0.18	4.68 ± 0.06	197.61 ± 0.86	752.15 ± 12.82	37.5 ± 0.59	64.88	36.27	25.2	39.68	0.33	1.57
170710A	Long		(1)	3	-3.64 ± 0.44	7.25 ± 0.19	140.34 ± 1.87	342.53 ± 14.06	13.4 ± 0.45	50.51	235.55	28.59	21.92	0.36	0.77
170810A	Long		(1)	3	-55.68 ± 22.6	11.45 ± 4.23	97.27 ± 1.06	324.97 ± 65.9	2.17 ± 0.31	8.82	0.97	2.19	6.64	0.09	3.03
			(2)	3	-41.5 ± 30.12	14.65 ± 3.27	115.89 ± 1.5	186.06 ± 46.44	1.36 ± 0.25	9.57	0.77	3.12	6.45	0.08	2.07
			(3)	3	-71.09 ± 11.02	16.27 ± 1.62	153.83 ± 0.46	391.97 ± 30.2	2.98 ± 0.17	10.03	2.93	2.66	7.38	0.07	2.78
			(4)	3	-46.17 ± 19.38	22.97 ± 5.4	184.61 ± 1.73	109.54 ± 17.84	0.92 ± 0.12	10.94	1.2	4.17	6.77	0.06	1.62
			(5)	3	-63.16 ± 11.27	34.25 ± 3.62	216.61 ± 0.73	213.77 ± 18.29	1.46 ± 0.11	8.89	3.28	3.53	5.36	0.04	1.52
			(6)	3	-28 ± 8.72	14.59 ± 2.63	340.94 ± 4.41	31.67 ± 4.53	0.79 ± 0.09	32.52	1.2	12.49	20.03	0.1	1.6
			(7)	3	-30.22 ± 13.93	12.79 ± 3.04	776.3 ± 13.96	21.74 ± 4.8	1.31 ± 0.23	78.31	2.7	27.5	50.81	0.1	1.85
170822A	Long		(1)	3	-9 ± 7.69	7.17 ± 4.37	213.34 ± 28.84	24.8 ± 9.43	0.95 ± 0.34	49.73	1.87	21.63	28.11	0.23	1.3
			(2)	3	-8.81 ± 3.8	190.72 ± 0.17	1427.58 ± 6.38	15.14 ± 5.57	1.38 ± 0.48	123.09	1.74	110.31	12.78	0.09	0.12
			(3)	3	-6.53 ± 4.2	4.59 ± 2.19	1995.17 ± 200.96	8.4 ± 1.92	4.5 ± 0.88	695.68	1.04	279.31	416.37	0.35	1.49
170906A	Long		(1)	3	-3.28 ± 0.43	5.57 ± 0.08	89.63 ± 1.5	5082.51 ± 216.16	151.22 ± 5.52	38.39	95.4	20.4	17.99	0.43	0.88
171120A	Long		(1)	3	-11.06 ± 5.76	8.15 ± 5.36	186.83 ± 11.61	26.9 ± 6.17	0.77 ± 0.15	37.01	1	15.78	21.23	0.2	1.35
			(2)	3	-4.97 ± 0.98	5.15 ± 0.31	372.03 ± 10.14	100.94 ± 5.73	10.62 ± 0.6	136.18	14.13	62.65	73.53	0.37	1.17
180205A	Long	1.409	(1)	3	-28.91 ± 8.58	7.13 ± 0.62	175.41 ± 1.92	110.3 ± 13.87	2.27 ± 0.22	27.15	5.47	7.24	19.91	0.15	2.75
180316A	Long		(1)	3	-18.9 ± 11.48	4.71 ± 0.47	243.78 ± 9.69	16.51 ± 4.61	0.73 ± 0.17	58.37	0.78	15.2	43.17	0.24	2.84
			(2)	3	-12.54 ± 5.62	5.11 ± 0.83	337.61 ± 7.19	41.43 ± 8.54	2.72 ± 0.46	86.1	2.4	28.31	57.79	0.26	2.04
			(3)	3	-36.49 ± 5.86	27.07 ± 3.32	481.79 ± 2.56	72.49 ± 5.71	1.6 ± 0.11	28.58	5.23	12.7	15.88	0.06	1.25
180325A	Long	2.248	(1)	3	-30.13 ± 3.64	6.53 ± 0.21	80.85 ± 0.73	1865.09 ± 118.79	18.66 ± 0.98	13.25	19.03	3.29	9.96	0.16	3.02
180329B	Long	1.998	(1)	1	-43.8 ± 4.35	5.01 ± 0.28	150.12 ± 1.05	730.15 ± 55.58	19.34 ± 0.87	34.54	73.01	8.53	26.02	0.23	3.05
			(2)	3	-11.35 ± 4	7.78 ± 1.96	201.87 ± 5.77	182.91 ± 23.77	5.73 ± 0.64	40.66	39.27	16.86	23.8	0.2	1.41
			(3)	3	-43.1 ± 14.75	13.2 ± 2.05	223.21 ± 1.32	239.7 ± 28.76	3.58 ± 0.3	19.59	58.87	5.96	13.63	0.09	2.29
180411A	Long		(1)	3	-53.37 ± 27.84	5.06 ± 1.59	90.34 ± 1.34	609.42 ± 108.3	7.38 ± 0.93	16.35	2.21	2.47	13.87	0.18	5.61
			(2)	3	-31.3 ± 3.13	17.36 ± 15.31	112.41 ± 3.34	181.5 ± 66.16	1.29 ± 0.41	9.22	4.73	3.65	5.57	0.08	1.53
			(3)	3	-40.85 ± 28.07	4.06 ± 0.3	147.48 ± 2.77	198.91 ± 47.9	5 ± 0.96	33.99	12.67	5.21	28.79	0.23	5.53
180425A	Long		(1)	3	-17.28 ± 1.73	2.94 ± 0.44	320.46 ± 18.16	8.05 ± 1.9	0.7 ± 0.15	116.16	1.28	23.52	92.64	0.36	3.94
180510A	Long		(1)	3	-14.7 ± 2.88	15.24 ± 2.06	95.95 ± 1.57	169.81 ± 18.79	1.55 ± 0.17	11.83	2.58	5.8	6.03	0.12	1.04
			(2)	3	-66.28 ± 9.47	5.52 ± 0.25	216.66 ± 0.77	204.6 ± 10.11	5.31 ± 0.2	35.07	6.88	4.91	30.15	0.16	6.14
180514A	Long		(1)	3	-7.25 ± 2.3	29.22 ± 10.97	80.77 ± 1.77	421.16 ± 132.11	3.72 ± 0.98	11.55	3.41	8.11	3.44	0.14	0.42

Table 1. *Cont.*

GRB	Type ^a	z ^b	Flare (Index)	ω	α_1	α_2	t_p (s)	$F_{X,p,-11}$ ^c (erg/cm ² /s)	$S_{X,-8}$ ^c (erg/cm ²)	Δt (s)	$\Delta F/F$	t_r (s)	t_d (s)	$\Delta t/t$	t_d/t_r
180620B	Long	1.1175	(1)	3	-40.17 ± 15.37	5.22 ± 0.39	101.68 ± 1.17	747.52 ± 80.71	10.48 ± 0.8	18.8	0.67	3.46	15.34	0.18	4.43
180623A	Long		(1)	3	-41.16 ± 12.5	50.81 ± 13.33	112.36 ± 0.83	422.4 ± 66.41	1.48 ± 0.22	4.54	1.41	2.4	2.14	0.04	0.89
180624A	Long	2.855	(1)	3	-26.86 ± 0.92	6.28 ± 0.12	180.12 ± 0.39	1084.05 ± 28.77	25.71 ± 0.58	31.37	52.05	8.08	23.29	0.17	2.88
			(2)	3	-23.87 ± 1.21	4.13 ± 0.07	338.95 ± 1.02	480.33 ± 12.55	30.66 ± 0.65	85.25	362.04	18.14	67.11	0.25	3.7
			(3)	3	-75.89 ± 14.4	14.94 ± 1.17	375 ± 1.23	453.74 ± 39.23	8.8 ± 0.59	25.64	495.8	6.26	19.38	0.07	3.1
			(4)	3	-52.16 ± 10.73	25.26 ± 2.7	461.67 ± 1.84	169.86 ± 13.34	3.22 ± 0.2	24.61	342.66	9.29	15.32	0.05	1.65
180706A	Long		(1)	3	-14.46 ± 1.15	5.46 ± 0.1	109.41 ± 0.58	418.08 ± 12.74	8.09 ± 0.19	25.37	13.49	8.12	17.25	0.23	2.12
180720B	Long		(1)	3	-3.91 ± 0.52	3.63 ± 0.1	99.41 ± 2.19	6760.81 ± 240.97	258.07 ± 8.94	49.49	3.99	21.15	28.35	0.5	1.34
180809B	Long		(1)	3	-18.89 ± 11.49	14.95 ± 6.8	64.78 ± 1.89	1053.43 ± 157.24	5.84 ± 0.75	7.18	0.9	3.22	3.96	0.11	1.23
			(2)	3	-19.74 ± 1.74	8.26 ± 0.27	221.91 ± 1.31	2108.33 ± 118.56	56.2 ± 2.75	34.82	3.89	11.95	22.87	0.16	1.91
180812A	Long		(1)	3	-5.26 ± 2.22	5.85 ± 1.76	194.36 ± 15.54	11.56 ± 2.44	0.58 ± 0.12	64.64	3.25	30.74	33.9	0.33	1.1
180818B	Long		(1)	3	-11.51 ± 1.43	7.29 ± 0.36	274.69 ± 2.93	115.46 ± 5.61	5.09 ± 0.22	57.23	2.14	22.98	34.25	0.21	1.49
180821A	Long		(1)	3	-78.51 ± 47.11	25.82 ± 16.12	273.47 ± 2.54	26.03 ± 8.27	0.25 ± 0.06	12.45	1.71	3.97	8.47	0.05	2.13
			(2)	3	-15.43 ± 9.27	7.51 ± 1.12	315.89 ± 8.06	18.11 ± 3.18	0.8 ± 0.11	57.64	1.93	20.95	36.68	0.18	1.75
180904A	Long		(1)	3	-51.01 ± 21.28	9.92 ± 1.11	475.28 ± 5.25	31.52 ± 5.03	1.17 ± 0.14	49.24	75.06	11.79	37.45	0.1	3.18
180930A	Long		(1)	3	-23.58 ± 15.17	20.79 ± 9.27	219.69 ± 5.88	15.96 ± 3.79	0.23 ± 0.05	18.37	1.11	8.62	9.75	0.08	1.13
			(2)	3	-16.44 ± 5.63	23.06 ± 7.23	616.86 ± 12.31	15.22 ± 3.11	0.69 ± 0.13	58.71	3.37	31.87	26.84	0.1	0.84
181013A	Long		(1)	3	-6.18 ± 2.24	2.95 ± 0.36	460.2 ± 27.72	8.99 ± 1.39	1.51 ± 0.19	221.08	6.02	72.79	148.29	0.48	2.04
181020A	Long	2.938	(1)	3	-6.79 ± 0.16	11.58 ± 0.73	249.87 ± 1.35	1165.49 ± 28.47	47.16 ± 0.98	52.32	7.56	29.3	23.02	0.21	0.79
			(2)	3	-7.68 ± 0.92	12.21 ± 0.46	370.97 ± 2.71	345.38 ± 10.38	18.96 ± 0.46	70.97	3.06	39.09	31.88	0.19	0.82
181228A	Long		(1)	3	-3 ± 0.78	9.7 ± 1.56	106.35 ± 3.31	79.29 ± 9.37	2.33 ± 0.21	37.98	3.12	24.43	13.55	0.36	0.55
			(2)	3	-6.86 ± 0.26	9.48 ± 0.25	328.05 ± 1.64	353.85 ± 7.58	20.53 ± 0.4	74.96	14.16	39.26	35.7	0.23	0.91
190103B	Long		(1)	3	-10.42 ± 0.87	15.53 ± 2.05	170.78 ± 1.52	225.92 ± 11.97	4.35 ± 0.2	24.88	3.93	13.59	11.29	0.15	0.83
			(2)	3	-7.45 ± 2.62	10.83 ± 1.63	249.04 ± 6.81	54.44 ± 5.75	2.16 ± 0.2	51.17	1.33	27.36	23.81	0.21	0.87
190106A	Long	1.859	(1)	3	-24.22 ± 10.74	40.28 ± 26.84	77.44 ± 1.32	912.33 ± 203.42	3.27 ± 0.59	4.65	0.61	2.67	1.98	0.06	0.74
			(2)	3	-131.41 ± 68.91	26.78 ± 4.82	98.57 ± 0.45	938.98 ± 187.09	2.68 ± 0.39	3.77	0.88	0.95	2.82	0.04	2.98
190109A	Long		(1)	3	-55.85 ± 29.7	5.07 ± 3.16	203.76 ± 3.34	74.47 ± 17.01	2.02 ± 0.32	36.59	0.93	5.38	31.21	0.18	5.8
			(2)	3	-7.95 ± 1.08	5.32 ± 0.37	270.74 ± 3.47	183.63 ± 18.1	11.23 ± 1.03	79.5	4.8	31.82	47.68	0.29	1.5
190204A	Long		(1)	3	-29.85 ± 12.93	7.69 ± 1.31	207.59 ± 3.2	74.87 ± 12.52	1.71 ± 0.21	30.08	0.45	8.24	21.85	0.14	2.65
190519A	Long		(1)	3	-14.42 ± 6.02	6.87 ± 1.29	112.12 ± 3.36	52.78 ± 8.85	0.9 ± 0.12	22.25	1.13	7.98	14.28	0.2	1.79
190604B	Long		(1)	3	-16.61 ± 1.85	8.92 ± 1.79	156.64 ± 1.71	2741.36 ± 179.76	52.45 ± 2.67	24.89	4.72	9.49	15.4	0.16	1.62
			(2)	3	-7.36 ± 1.11	10.21 ± 0.19	221.18 ± 1.78	3159.42 ± 118.84	114.98 ± 3.81	47.03	27.28	24.75	22.28	0.21	0.9

Table 1. *Cont.*

GRB	Type ^a	z ^b	Flare (Index)	ω	α_1	α_2	t_p (s)	$F_{X,p,-11}$ ^c (erg/cm ² /s)	$S_{X,-8}$ ^c (erg/cm ²)	Δt (s)	$\Delta F/F$	t_r (s)	t_d (s)	$\Delta t/t$	t_d/t_r
190613A	Long		(1)	3	-12.24 ± 7.84	7.74 ± 2.76	139.54 ± 5.68	93.42 ± 16.29	1.97 ± 0.27	27.32	5.29	11	16.32	0.2	1.48
			(2)	3	-7.43 ± 5.32	7.79 ± 0.96	205.76 ± 8.82	33.42 ± 4.75	1.29 ± 0.18	49.97	3.66	23.85	26.12	0.24	1.1
190613B	Long		(1)	3	-23.19 ± 6.92	36.83 ± 27.8	93.11 ± 1.43	257.42 ± 49.51	1.18 ± 0.18	5.95	21.22	3.37	2.58	0.06	0.76
			(2)	1	-7.65 ± 0.69	10.09 ± 0.45	132.33 ± 2.54	1246.23 ± 56.24	39.25 ± 1.41	39.6	123.43	19.4	20.2	0.3	1.04
190718A	Long		(3)	3	-12.25 ± 2.06	4.01 ± 0.18	248.52 ± 2.87	111.62 ± 6.23	6.45 ± 0.27	76.2	15.36	22.26	53.94	0.31	2.42
			(1)	3	-22.26 ± 1.52	33.08 ± 6.51	717.55 ± 3	200.73 ± 8.63	7.63 ± 0.26	49.2	26.63	27.33	21.87	0.07	0.8
190926A	Long		(2)	3	-194.85 ± 32.95	18 ± 1.84	756.59 ± 0.93	373.13 ± 24.92	10.22 ± 0.51	36.75	49.9	5.76	30.99	0.05	5.38
			(3)	3	-159.98 ± 70.59	45.09 ± 33.93	824.44 ± 3.38	106.92 ± 27.71	1.66 ± 0.29	20.4	14.52	6.09	14.31	0.02	2.35
191031C	Long		(4)	3	-40.82 ± 9.61	26.1 ± 0.86	868.1 ± 2.15	323.98 ± 28.05	12.51 ± 0.96	50.07	44.49	21.07	28.99	0.06	1.38
			(1)	3	-17.4 ± 1.12	9.08 ± 0.47	246.49 ± 1.3	571.84 ± 24.81	16.72 ± 0.63	38.05	3.01	14.36	23.69	0.15	1.65
191101A	Long		(2)	3	-29.75 ± 1.72	7.16 ± 0.23	359.31 ± 0.92	714.99 ± 24.05	29.77 ± 0.8	54.99	7.48	14.5	40.49	0.15	2.79
			(3)	3	-27.76 ± 4.12	4.02 ± 0.46	545.67 ± 3.78	153.09 ± 9.59	15.53 ± 0.68	136.04	3.49	26.11	109.93	0.25	4.21
191123A	Long		(4)	3	-9.45 ± 3.7	16.64 ± 5.11	748.25 ± 17.04	46.97 ± 7.91	4.05 ± 0.56	111.49	2.11	63.85	47.64	0.15	0.75
			(1)	3	-20.92 ± 4.95	3.01 ± 0.35	312.45 ± 4.91	30.94 ± 2.9	2.45 ± 0.17	106.6	2.64	19.72	86.89	0.34	4.41
200122A	Long	1.148	(2)	3	-26.24 ± 7.94	3.91 ± 0.91	826.75 ± 16.93	48.23 ± 7.89	7.68 ± 0.96	213.47	11.73	41.56	171.91	0.26	4.14
			(3)	3	-29.19 ± 1.62	7.77 ± 1.71	1361.26 ± 6.62	343.52 ± 18.08	51.36 ± 1.67	196.99	109.79	54.84	142.15	0.14	2.59
191221B	Long		(4)	3	-18.14 ± 3.6	10.95 ± 1.28	1576.19 ± 11.05	273.69 ± 35.99	44.9 ± 5.34	213	93.49	85.73	127.27	0.14	1.48
			(5)	3	-56.86 ± 9.22	11.26 ± 1.08	1801.82 ± 4.62	173.62 ± 14.43	21.61 ± 1.38	164.73	62.83	40	124.73	0.09	3.12
191101A	Long		(6)	3	-88.34 ± 28.7	7.08 ± 0.75	2077.32 ± 9.41	48.88 ± 5.29	9.33 ± 0.78	257.71	18.77	35.72	221.99	0.12	6.21
			(1)	3	-13.46 ± 1.29	11.19 ± 4.37	121.26 ± 1.74	2310.5 ± 164.31	32.82 ± 2.09	18.39	11.95	8.3	10.09	0.15	1.22
191123A	Long		(2)	3	-19.7 ± 10.92	6.52 ± 0.38	140.97 ± 1.14	1206.15 ± 413.37	23.96 ± 7.2	26.09	14.81	7.97	18.12	0.19	2.27
			(1)	1	-10 ± 3.51	3.58 ± 0.89	76.21 ± 5.89	126.48 ± 30.48	3.66 ± 0.44	36.97	70.42	12.64	24.33	0.49	1.92
200122A	Long		(2)	3	-75.1 ± 22.08	20.95 ± 6.81	112.94 ± 0.58	257.18 ± 39.82	1.18 ± 0.13	6.03	149.2	1.77	4.26	0.05	2.4
			(3)	3	-14.72 ± 3.51	7.39 ± 0.8	130.62 ± 1.51	259.17 ± 23.23	4.87 ± 0.35	24.51	152.65	9.01	15.49	0.19	1.72
191221B	Long		(4)	3	-20.89 ± 8.26	31.75 ± 9.42	168.23 ± 2.25	83.42 ± 13.78	0.78 ± 0.11	12.17	50.45	6.8	5.37	0.07	0.79
			(5)	3	-19.31 ± 1.65	7.84 ± 0.29	276.86 ± 1.48	180.97 ± 7.41	6.27 ± 0.21	45.32	115.29	15.32	30	0.16	1.96
191221B	Long		(1)	3	-5.86 ± 0.74	2.85 ± 0.29	960.59 ± 24.68	31.37 ± 1.65	11.5 ± 0.47	481.2	0.81	158.78	322.42	0.5	2.03
			(1)	3	-17.7 ± 1.61	9.61 ± 5.14	112.29 ± 1.88	455.21 ± 56.23	5.81 ± 0.55	16.61	9.17	6.38	10.23	0.15	1.6
200122A	Long		(2)	3	-15.54 ± 6.95	9.03 ± 3.72	134.76 ± 3.18	551.07 ± 118.84	9.25 ± 1.66	21.81	13.31	8.58	13.23	0.16	1.54
			(3)	3	-181.99 ± 119.48	36.67 ± 22.32	143.7 ± 0.69	309.82 ± 86.42	0.94 ± 0.17	3.99	7.91	1	2.99	0.03	2.98
200122A	Long		(4)	3	-409.87 ± 130.24	7.31 ± 0.53	156.39 ± 0.31	1412.2 ± 139.68	16.87 ± 1.52	16.46	38.59	0.76	15.69	0.11	20.59
			(5)	3	-38.09 ± 4.92	55.15 ± 13.72	175.73 ± 0.69	4859.02 ± 402.42	26.79 ± 1.92	7.14	145.02	3.96	3.18	0.04	0.8
200122A	Long		(6)	3	-19.64 ± 3.53	14.52 ± 0.58	195.9 ± 1.07	5618.79 ± 211	94.1 ± 3.02	21.69	181.22	9.49	12.2	0.11	1.29
			(7)	3	-3677.53 ± 0	31.27 ± 2.35	221.89 ± 0.02	2474.72 ± 181.93	9.21 ± 0.67	5.13	86.94	0.14	4.99	0.02	36.91

Table 1. *Cont.*

GRB	Type ^a	z ^b	Flare (Index)	ω	α_1	α_2	t_p (s)	$F_{X,p,-11}$ ^c (erg/cm ² /s)	$S_{X,-8}$ ^c (erg/cm ²)	Δt (s)	$\Delta F/F$	t_r (s)	t_d (s)	$\Delta t/t$	t_d/t_r
200227A	Long		(1)	3	-33.04 ± 4.46	5.87 ± 0.22	325.69 ± 1.66	184.33 ± 8.58	7.87 ± 0.27	56.82	12.19	12.62	44.2	0.17	3.5
			(2)	3	-13.94 ± 4.82	7.12 ± 1.03	715.5 ± 18.51	23.07 ± 3.34	2.49 ± 0.3	140.34	3.73	51.85	88.49	0.2	1.71
			(1)	3	-33.38 ± 18.33	11.5 ± 2.75	198.36 ± 3.48	75.4 ± 16.73	1.2 ± 0.2	20.79	0.38	6.64	14.14	0.1	2.13
			(1)	3	-15.67 ± 2.19	5.79 ± 0.35	182.38 ± 2.05	126.5 ± 8.8	3.82 ± 0.22	39.56	7.13	12.59	26.97	0.22	2.14
			(1)	3	-20.02 ± 5.89	12.45 ± 2.37	1042.48 ± 20.02	15.26 ± 2.35	1.47 ± 0.2	125.29	3.87	51.24	74.05	0.12	1.45
			(1)	3	-53.56 ± 28.61	4.09 ± 0.44	117.59 ± 1.82	51.88 ± 7.39	0.99 ± 0.11	25.89	1.51	3.35	22.55	0.22	6.74
200509A			(1)	3	-11.31 ± 0.66	4.26 ± 0.62	353.1 ± 3.97	232.67 ± 11.94	18.78 ± 0.72	106.01	98.91	33.18	72.84	0.3	2.2
			(2)	3	-38.63 ± 8.95	5.59 ± 3.25	443.01 ± 5.32	204.71 ± 35.66	11.93 ± 1.39	77.91	113.81	15.34	62.57	0.18	4.08
			(3)	3	-11.81 ± 2.23	5.89 ± 1.22	529.11 ± 7.45	305.68 ± 54.62	29.29 ± 4.64	125	203.45	45.18	79.82	0.24	1.77
			(4)	3	-155.9 ± 22.01	11.05 ± 0.57	596.61 ± 0.83	493.63 ± 21.69	16.78 ± 0.56	45.91	366.04	5.97	39.94	0.08	6.68
			(5)	3	-254.34 ± 41.53	21.05 ± 2.38	753.06 ± 0.85	320.37 ± 21.08	7.31 ± 0.36	30.68	285.22	4.5	26.18	0.04	5.83
			(6)	3	-126.36 ± 6.04	21.07 ± 0.27	819.34 ± 0.47	2164.34 ± 50.43	62.01 ± 1.17	38	2043.48	8.53	29.46	0.05	3.45
200519A	Long		(1)	3	-10 ± 2.66	4.86 ± 2.61	50.93 ± 2.74	1397.59 ± 368.5	15.57 ± 3.44	14.55	5.05	5.12	9.43	0.29	1.84
			(2)	3	-17.58 ± 6.07	5.4 ± 3.29	75.6 ± 2.02	1564.24 ± 311.64	19.75 ± 2.6	16.62	6.7	4.85	11.78	0.22	2.43
			(3)	3	-10 ± 5.41	5.05 ± 0.62	100.48 ± 2.07	1235.55 ± 394.13	26.47 ± 7.55	27.96	5.99	10.03	17.93	0.28	1.79
200528A	Long		(1)	3	-14.74 ± 1.37	7.04 ± 0.88	95.43 ± 0.94	3351.57 ± 162.31	47.48 ± 1.74	18.47	5.75	6.64	11.83	0.19	1.78
			(2)	3	-7.39 ± 2.38	7.33 ± 0.29	141.9 ± 2.38	782.68 ± 65.6	21.59 ± 1.8	35.69	10.9	16.68	19	0.25	1.14
200612A	Long		(1)	3	-4.55 ± 0.51	4.84 ± 0.25	141.49 ± 2.91	169.91 ± 7.55	7.33 ± 0.32	55.78	3.2	25.71	30.07	0.39	1.17
			(2)	3	-31.87 ± 6.1	2.34 ± 0.22	366.16 ± 4.11	76.55 ± 7.14	8.3 ± 0.64	148.47	3.84	17.47	131	0.41	7.5
200806A	Long		(1)	3	-5.27 ± 1.54	6.55 ± 1.33	248.18 ± 11.91	28.56 ± 3.54	1.72 ± 0.2	77.72	0.68	38.54	39.18	0.31	1.02
200917A	Long		(1)	3	-10.89 ± 5.96	1.91 ± 0.22	2226.93 ± 253.53	3.56 ± 1.22	3.47 ± 1.02	1317.02	14.29	252.2	1064.82	0.59	4.22
201026A	Long		(1)	3	-78.66 ± 17.86	6.63 ± 6.04	143.27 ± 1.31	430.89 ± 72.79	6.12 ± 0.62	19.19	3.81	2.74	16.45	0.13	6.01
			(2)	3	-37.31 ± 11.8	6.92 ± 1.58	162.72 ± 1.32	1062.2 ± 192.03	19.34 ± 2.72	24.18	13.66	5.55	18.64	0.15	3.36
			(3)	3	-8.51 ± 0.35	8.96 ± 0.17	227.08 ± 1	3316.8 ± 72.23	123.16 ± 2.65	48.01	111.78	23.15	24.87	0.21	1.07
201029A	Long		(1)	3	-20.03 ± 1.72	6.03 ± 0.65	308.52 ± 1.98	286.3 ± 13.35	13.09 ± 0.43	60.15	34.79	17.5	42.65	0.19	2.44
			(2)	3	-1428.78 ± 0	15.32 ± 7.59	417.17 ± 1.61	91.75 ± 16.55	1.33 ± 0.23	20.04	11.24	0.63	19.41	0.05	30.69
			(3)	3	-7.54 ± 1.09	12.52 ± 0.8	485.74 ± 4.85	188.26 ± 17.41	13.51 ± 1.14	92.83	23.22	51.79	41.04	0.19	0.79
			(4)	3	-14.11 ± 2.03	4.57 ± 0.49	1448.72 ± 20.54	53.56 ± 4.12	15.68 ± 0.93	385.54	11.8	113.56	271.99	0.27	2.4
201104B	Long	1.954	(1)	3	-22.08 ± 10.61	7.23 ± 1.74	203 ± 4.94	26.33 ± 5.42	0.68 ± 0.11	33.66	0.86	10.3	23.36	0.17	2.27
			(2)	3	-268.28 ± 0.02	8.16 ± 3.64	308.18 ± 3.1	10.93 ± 4.13	0.24 ± 0.09	29.84	0.43	2.1	27.75	0.1	13.23
201223A	Long		(1)	3	-13.51 ± 12.42	4.95 ± 3.59	760.28 ± 85.17	1.27 ± 0.59	0.19 ± 0.07	193.39	1.29	60.62	132.77	0.25	2.19
210112A	Long		(1)	3	-6.55 ± 1.58	18.1 ± 3.44	73.18 ± 1.32	3917.38 ± 477.69	39.44 ± 3.69	13.07	3.58	8.38	4.7	0.18	0.56
			(2)	3	-9.14 ± 2.45	14.49 ± 9	107.39 ± 2.93	908.37 ± 216.72	12.16 ± 2.51	17.32	1.63	9.6	7.72	0.16	0.8
			(3)	3	-9.56 ± 8.29	14.24 ± 3.8	132.37 ± 4.75	644.83 ± 114.61	10.48 ± 1.48	21.01	1.67	11.44	9.57	0.16	0.84
			(4)	3	-2.98 ± 0.3	44.82 ± 19.07	189.57 ± 3.19	116.77 ± 20.57	4.15 ± 0.62	47.22	0.56	40.38	6.84	0.25	0.17

Table 1. *Cont.*

GRB	Type ^a	z ^b	Flare (Index)	ω	α_1	α_2	t_p (s)	$F_{X,p,-11}$ ^c (erg/cm ² /s)	$S_{X,-8}$ ^c (erg/cm ²)	Δt (s)	$\Delta F/F$	t_r (s)	t_d (s)	$\Delta t/t$	t_d/t_r
210207B	Long		(1)	3	-14.2 ± 1.98	6.96 ± 0.38	104.53 ± 1.1	749.95 ± 45.49	11.9 ± 0.6	20.68	2.29	7.5	13.18	0.2	1.76
			(2)	3	-116.29 ± 28.45	14.93 ± 1.13	152.15 ± 0.42	370.78 ± 30.06	2.63 ± 0.16	9.48	2.69	1.81	7.66	0.06	4.22
210209A	Long		(1)	3	-13.76 ± 2.97	7.5 ± 1.02	333.85 ± 6.82	50.51 ± 6.62	2.47 ± 0.28	63.64	4.95	24.2	39.45	0.19	1.63
			(1)	3	-661.96 ± 66.2	21.51 ± 7.08	99.88 ± 0.46	151.88 ± 42.66	0.4 ± 0.11	3.59	0.61	0.27	3.32	0.04	12.18
210402A	Long		(2)	3	-192.01 ± 70.19	12.08 ± 0.82	115.26 ± 0.33	405.48 ± 35.08	2.39 ± 0.15	7.97	2.05	0.96	7.01	0.07	7.31
			(1)	3	-5.83 ± 1.74	10.82 ± 2.85	184.51 ± 5.35	1123 ± 115.32	37.57 ± 2.87	43.26	1.97	24.68	18.58	0.23	0.75
			(2)	3	-20 ± 8.06	17.17 ± 3.02	237.14 ± 3.5	660.52 ± 77.57	12.11 ± 1.33	23.73	1.23	10.99	12.75	0.1	1.16
			(3)	3	-36.19 ± 5.61	5.42 ± 0.88	729.12 ± 4.69	92.27 ± 7.14	9.21 ± 0.5	133.39	9.88	26.74	106.65	0.18	3.99
			(4)	3	-14.32 ± 4.21	10.75 ± 3.91	899.53 ± 18.01	51.26 ± 7.84	5.37 ± 0.74	135.76	7.43	59.07	76.69	0.15	1.3
			(5)	3	-107.19 ± 39.35	16.13 ± 6.6	1054.87 ± 5.37	44.95 ± 7.29	2.12 ± 0.23	62.74	7.86	13.21	49.52	0.06	3.75
			(6)	3	-8.81 ± 6.78	16.55 ± 3.61	1244.51 ± 33.43	26.75 ± 5.3	3.99 ± 0.6	193.3	5.61	112.57	80.73	0.16	0.72
210410A	Long		(1)	3	-179.29 ± 0	6.44 ± 3.07	138.02 ± 0.83	13.89 ± 5.57	0.18 ± 0.07	17.32	0.79	1.36	15.96	0.13	11.71
			(2)	3	-107.83 ± 0.05	7.49 ± 4.97	256.31 ± 2.96	10.79 ± 7.56	0.23 ± 0.16	29.41	1.12	3.72	25.7	0.11	6.91
			(3)	3	-15.74 ± 1.57	5.11 ± 4.16	505.14 ± 56.64	2.35 ± 1.64	0.21 ± 0.14	119.73	0.46	35.63	84.1	0.24	2.36
210411C	Long	2.826	(1)	3	-10.18 ± 2.07	4.54 ± 0.38	174.18 ± 3.61	76.88 ± 6.13	3.04 ± 0.19	51.83	6.03	17.5	34.33	0.3	1.96
210419A	Long		(1)	3	-17.68 ± 4.86	9.67 ± 1.13	382.09 ± 6.59	53.94 ± 7.86	2.34 ± 0.3	56.31	10.23	21.72	34.6	0.15	1.59
210420B	Long	1.4	(1)	3	-42.41 ± 39.15	3.72 ± 0.48	637.52 ± 16.8	13.8 ± 2.86	1.62 ± 0.23	158.7	1.81	22.24	136.46	0.25	6.14
210504A	Long		(1)	3	-22.3 ± 5.78	8.09 ± 0.6	448.62 ± 6.21	47.8 ± 6.05	2.5 ± 0.26	68.47	13.21	22.07	46.39	0.15	2.1

^a Types are mainly adopted from Refs. [23,49] & GCN network. ^b Redshifts are taken from https://www.mpe.mpg.de/~jcg/grbgen.html?tdsourcetag=s_pctim_aiomsg (accessed date: 1 May 2021). ^c The symbolic notation $Q_n = Q/10^n$ is adopted.

Table 2. The Derived Physical Quantities of Flares with Redshift.

GRB ^a	$t_{p,z}$ (s)	Δt_z (s)	$t_{r,z}$ (s)	$t_{d,z}$ (s)	$L_{X,p,45}$ ^b (erg/s)	$E_{X,iso,49}$ ^b (erg)
050502B(1)	116.22 ± 0.11	30.48	14.56	15.92	977,214.45 ± 10,336.78	2368.05 ± 23.94
050502B(2)	4822.28 ± 26.09	3015.34	584.67	2430.67	198.41 ± 45.32	44.29 ± 9.62
050502B(3)	12,281.1 ± 89.33	5870.76	3120.32	2750.44	300.56 ± 25.74	136.81 ± 10.7
050714B(1)	112.35 ± 2.28	22.29	10.6	11.69	8636.43 ± 807.73	14.88 ± 1.39
050724(1)	211.92 ± 1.22	35.72	14.55	21.17	113.33 ± 7.23	0.31 ± 0.02
050724(2)	45,122.25 ± 466.45	27,822.42	14,892.44	12,929.98	0.37 ± 0.03	0.79 ± 0.06
050730(1)	46.29 ± 0.42	2.58	0.91	1.67	110,288.31 ± 20,739.72	21.86 ± 3.25
050730(2)	87.04 ± 0.7	12.78	5.75	7.03	164,571.2 ± 7790.13	162.4 ± 7.24
050730(3)	137.23 ± 0.91	13.59	3.78	9.81	83,087.32 ± 9139.06	85.75 ± 7.02
050803(1)	170.28 ± 9.86	71.76	61.9	9.87	5262.34 ± 1334.27	28.65 ± 6.52
050803(2)	258.74 ± 28.02	78.91	27.2	51.71	3952.13 ± 1482.8	23.85 ± 6.75
050820A(1)	64.72 ± 0.15	21.77	1.63	20.15	469,902.43 ± 17,280.21	740.91 ± 22.13
050822(1)	97.09 ± 1.57	18.47	6.49	11.97	9066.42 ± 914.27	12.83 ± 1.05
050822(2)	182.49 ± 0.8	28	8.92	19.08	24,138.22 ± 947.68	51.6 ± 1.66
050904(1)	63.97 ± 0.4	13.12	9.08	4.05	434,001.14 ± 21,150.99	436.79 ± 16.5
050904(2)	924.78 ± 2.03	145.04	55.6	89.45	31,045.07 ± 2015.41	346.19 ± 19.82
050904(3)	1901.56 ± 18.53	516.52	130.1	386.42	15,268.48 ± 2181.04	594.66 ± 57.84
050904(4)	2943.31 ± 50.42	881.75	346.18	535.57	15,483.68 ± 2727.06	1049.8 ± 155.56
050908(1)	89.22 ± 0.2	10.26	1.02	9.23	20,676.98 ± 3015.96	15.58 ± 2.19
050915A(1)	29.95 ± 0.86	6.43	2.77	3.66	23,999.95 ± 2483.69	11.91 ± 1.1
050915A(2)	148.96 ± 2.97	8.23	2.65	5.57	1207.76 ± 470.84	0.76 ± 0.29
050922B(1)	67.84 ± 0.62	16.34	5	11.34	285,029.1 ± 13,614.93	354.53 ± 9.67
050922B(2)	90.59 ± 0.32	3.32	0.48	2.85	75,617.14 ± 15,719.1	18.69 ± 2.88
050922B(3)	149.11 ± 1.16	28.6	13.35	15.26	379,843.85 ± 16,906.59	839.79 ± 36.94
060111A(1)	30.13 ± 1.22	19.86	13.51	6.35	96,609.46 ± 9247.53	149.18 ± 9.09
060111A(2)	50.41 ± 1	11.06	5.29	5.77	55,464.95 ± 3008.21	47.44 ± 2.52
060111A(3)	85.46 ± 0.33	20.82	7.82	13	197,924.33 ± 3292.63	316.43 ± 4.46
060115(1)	90.39 ± 3.53	20.67	9.33	11.34	16,560.25 ± 2550.24	26.44 ± 3.93
060124(1)	111.99 ± 1.22	44.39	6.11	38.28	33,586.58 ± 3196.49	109.45 ± 8.56
060124(2)	174.11 ± 0.29	23.76	15.99	7.77	725,852.19 ± 14,976.72	1323.31 ± 22.44
060124(3)	212.5 ± 0.27	16.93	6.19	10.74	615,145.55 ± 12,883.37	799.63 ± 14.32
060124(4)	296.61 ± 0.88	82.19	2.12	80.07	28,275.82 ± 2103.98	166.53 ± 10.29
060202(1)	213.46 ± 3.32	46.69	11.02	35.66	1904.18 ± 253.8	6.69 ± 0.61
060202(2)	298.72 ± 9.25	53.2	20.35	32.86	1237.11 ± 280.24	5.06 ± 0.92
060202(3)	403.07 ± 6.99	120.27	65.8	54.48	2403.6 ± 217.92	22.38 ± 1.74
060204B(1)	95.34 ± 0.42	9.21	2.76	6.45	41,097.47 ± 2696.77	28.84 ± 1.42
060210(1)	21.6 ± 0.12	2.91	0.42	2.49	413,093.19 ± 32,936.38	89.14 ± 4.81
060210(2)	40.54 ± 0.23	7.26	3.22	4.03	476,705.59 ± 13,217.99	267.07 ± 6.95
060210(3)	75.72 ± 0.22	8.2	1.98	6.22	230,793.53 ± 10,862.45	142.87 ± 5.18
060223A(1)	279.03 ± 12.86	76.51	28.08	48.44	5265.21 ± 1098.6	30.9 ± 5.32
060319(1)	115.83 ± 1.27	19.67	3.08	16.58	1038.83 ± 340.45	1.52 ± 0.47
060418(1)	51.85 ± 0.12	5.9	1.32	4.58	295,485.05 ± 10,677.46	131.14 ± 3.97
060510B(1)	33.2 ± 0.45	3.22	1.76	1.46	328,797.48 ± 39,181.68	81.91 ± 8.67
060510B(2)	50.51 ± 0.26	3.78	1.87	1.92	645,999.56 ± 33,648.21	189.04 ± 9.78
060512(1)	64.96 ± 1.14	10.03	3	7.03	12,022.79 ± 2262.82	9.18 ± 1.37
060522(1)	26.81 ± 1.5	6.38	3.45	2.92	62,992.18 ± 12,186.79	31.09 ± 4.96
060526(1)	59.5 ± 0.11	4.9	1.34	3.57	1,427,083.06 ± 63,110.57	530.99 ± 18.41
060526(2)	73.54 ± 0.36	10.49	3.95	6.54	596,274.78 ± 29,830.77	480.78 ± 19.83
060604(1)	43.95 ± 0.34	10.7	4.2	6.5	129,527.25 ± 3798.15	106.57 ± 2.62
060604(2)	54.01 ± 0.15	3.42	0.65	2.77	95,875.87 ± 7329.24	24.58 ± 1.35
060607A(1)	20.22 ± 1.4	6.92	4.69	2.23	153,814.26 ± 41,301.64	81.98 ± 12.73
060607A(2)	23.68 ± 0.12	3.73	0.45	3.28	381,840.81 ± 44,141.24	104.88 ± 9.97
060607A(3)	43.84 ± 1.23	6.41	2.69	3.71	55,939.39 ± 7963.14	27.63 ± 3.29
060607A(4)	63.83 ± 0.39	12.54	5.22	7.32	300,370.77 ± 8266.99	290.44 ± 6.99
060707(1)	42.2 ± 0.14	5.47	0.22	5.25	22,979.31 ± 6255.54	9.1 ± 2.43
060714(1)	30.87 ± 0.47	3.76	3.04	0.72	154,037.95 ± 46,879.04	43.62 ± 9.6
060714(2)	37.36 ± 0.39	7.94	5.06	2.88	339,827.15 ± 19,136.1	207.96 ± 8.14
060714(3)	47.05 ± 0.17	4.56	1.67	2.89	256,018.34 ± 11,025.3	89.68 ± 3.06
060719(1)	81.54 ± 4.18	12.89	5.33	7.56	1662.66 ± 441.31	1.65 ± 0.38
060729(1)	115.1 ± 0.46	18.71	4.86	13.85	12,135.85 ± 469.5	17.18 ± 0.48
060814(1)	44.4 ± 0.4	13.3	1.55	11.74	153,647.6 ± 7934.95	149.65 ± 5.21
060904B(1)	91.17 ± 0.74	15.57	4.04	11.53	23,264.2 ± 4490.29	27.4 ± 4.89
060904B(2)	103.37 ± 1.38	18.63	5.26	13.37	31,454.82 ± 13,313.72	44.48 ± 16.07

Table 2. Cont.

GRB ^a	$t_{p,z}$ (s)	Δt_z (s)	$t_{r,z}$ (s)	$t_{d,z}$ (s)	$L_{X,p,45}$ ^b (erg/s)	$E_{X,iso,49}$ ^b (erg)
060926(1)	96.34 ± 50.97	37.5	4.46	33.04	2739.08 ± 340.92	7.51 ± 0.75
061121(1)	32.38 ± 0.2	2.02	1.16	0.86	630,151.94 ± 63,614.7	98.23 ± 8.65
061121(2)	51.2 ± 0.46	4.27	1.39	2.88	39,730.97 ± 5651.94	12.97 ± 1.42
061202(1)	43.1 ± 0.4	11.32	3.85	7.48	155,787.56 ± 6014.83	134.83 ± 3.8
061202(2)	73.57 ± 1.13	31.5	0.87	30.63	6452.98 ± 1050.13	14.49 ± 2.33
070103(1)	218.43 ± 53.43	170.85	69.35	101.5	524.45 ± 133.81	6.9 ± 1.76
070129(1)	63.07 ± 1.22	5.42	2.92	2.5	28,642.34 ± 4403.92	12 ± 1.54
070129(2)	71.41 ± 1.19	8.56	2.54	6.02	33,953.18 ± 8177.8	22.12 ± 3.55
070129(3)	92.1 ± 0.67	9.91	4.2	5.71	303,216.52 ± 20,545.65	231.73 ± 13.27
070129(4)	109.84 ± 0.48	10.31	6.52	3.79	459,046.99 ± 24,470.78	364.35 ± 14.07
070129(5)	133.12 ± 0.51	17.27	5.98	11.29	163,219.66 ± 5852.94	215.95 ± 5.74
070129(6)	164.91 ± 1.55	14.71	4.88	9.83	51,027.19 ± 7042.33	57.43 ± 5.68
070129(7)	173.4 ± 0.28	10.93	0.98	9.95	38,535.53 ± 6080.27	30.94 ± 4.45
070129(8)	198.97 ± 0.78	14.93	4.41	10.52	29,666.51 ± 3100.98	33.74 ± 2.61
070129(9)	270.16 ± 3.74	19.39	6.33	13.07	1605.06 ± 533.24	2.38 ± 0.72
070306(1)	72.59 ± 0.39	10.07	2.59	7.47	43,077.64 ± 2682.93	32.81 ± 1.48
070318(1)	154.93 ± 2.51	50.87	19.78	31.09	2592 ± 126.57	10.13 ± 0.44
070419B(1)	78.35 ± 0.68	21.28	7.3	13.98	131,563.65 ± 4768.09	214.06 ± 6.23
070721B(1)	57.54 ± 0.3	3.72	0.65	3.07	146,801.16 ± 60,869.25	40.8 ± 15.47
070721B(2)	67.08 ± 0.83	1.67	0.75	0.93	313,314.79 ± 159,657.41	40.49 ± 19.59
070721B(3)	74.86 ± 0.52	3.78	1.37	2.41	110,251.88 ± 18,075.56	31.99 ± 4.14
070724A(1)	74.73 ± 1.5	10.06	6.06	4	576.49 ± 92.99	0.45 ± 0.06
070724A(2)	152.26 ± 2.61	21.3	14.46	6.84	616.85 ± 262.42	1.01 ± 0.4
071021(1)	63.45 ± 0.81	7.3	3.68	3.63	83,096.89 ± 7759.09	46.93 ± 4.24
071021(2)	1800.17 ± 5.81	286.41	130.17	156.24	1390.95 ± 113.67	30.78 ± 2.42
071031(1)	39.49 ± 1.18	25.75	18.42	7.33	439,214.42 ± 31,955.1	878.28 ± 40.74
071031(2)	54.13 ± 0.46	9.13	2.13	7	147,959.78 ± 20,410.57	101.74 ± 10.68
071031(3)	70.05 ± 0.49	9.43	2.68	6.74	81,848.86 ± 9115.83	58.62 ± 4.85
071031(4)	121.87 ± 1.1	43.31	13.9	29.41	57,733.89 ± 1866.86	190.48 ± 4.64
071112C(1)	354.25 ± 16.86	117.83	36.48	81.35	498.35 ± 95.73	4.47 ± 0.67
071122(1)	189.42 ± 1.13	12.15	1.84	10.31	880.7 ± 540.88	0.8 ± 0.47
080210(1)	52.47 ± 0.55	5.95	2.35	3.61	97,359.69 ± 9954.34	44.61 ± 4.01
080310(1)	43.19 ± 0.29	13.92	1.85	12.06	120,211.65 ± 9575.23	122.92 ± 8.3
080310(2)	56.45 ± 0.92	9.39	2.34	7.05	121,941.25 ± 25,342.63	86.49 ± 12.19
080310(3)	67.56 ± 2.42	17.12	7.75	9.37	133,737.26 ± 38,825.19	176.89 ± 50.39
080310(4)	82.19 ± 0.67	4.48	1.05	3.44	67,199.74 ± 17,691.35	22.75 ± 4.09
080310(5)	105.74 ± 1.04	29.08	18.51	10.58	180,918.15 ± 8365.43	405.87 ± 12.67
080310(6)	148.4 ± 0.94	11.1	3.47	7.63	64,872.32 ± 6405.52	54.98 ± 3.39
080310(7)	164.95 ± 0.32	15.96	4.8	11.16	158,667.66 ± 11,340.77	192.96 ± 11.31
080325(1)	60.08 ± 1.37	11.33	7.5	3.83	75,641.27 ± 15,406.69	65.86 ± 9.51
080325(2)	78.59 ± 1.35	27.07	10.09	16.98	91,205.09 ± 3293.81	189.38 ± 4.49
080325(3)	106.72 ± 1.6	18.44	3.12	15.32	13,788.16 ± 3204.79	18.92 ± 3.29
080325(4)	123.81 ± 1.58	9.01	3.9	5.11	13,566.68 ± 1927.93	9.43 ± 1.16
080607(1)	29.85 ± 0.09	3.86	0.26	3.6	1,329,946.91 ± 111,727.84	374.04 ± 26.91
080607(2)	34.85 ± 0.45	5.44	2.61	2.83	821,102.49 ± 69,333.45	345.33 ± 29.09
080805(1)	47.62 ± 0.67	18.7	6.29	12.41	45,119.9 ± 1801.41	64.41 ± 2.01
080810(1)	24.1 ± 0.21	5.22	2.58	2.64	644,219.6 ± 24,305.55	260.19 ± 9.47
080810(2)	47.9 ± 0.33	7.17	1.92	5.24	147,713.46 ± 11,318.69	80.2 ± 4.76
080906(1)	56.32 ± 0.56	11.52	3.1	8.42	34,950.93 ± 2671.88	30.49 ± 1.74
080906(2)	190.45 ± 5.51	92.33	16.97	75.37	3840.12 ± 458.94	26.26 ± 2.23
080928(1)	77.46 ± 0.47	17.95	7.9	10.04	264,195.73 ± 6375.59	366.01 ± 8.33
080928(2)	132.41 ± 0.5	11.43	4.96	6.47	44,604.48 ± 1796.27	39.35 ± 1.43
081008(1)	100.22 ± 0.25	10.4	2.48	7.92	68,378.96 ± 2779.56	53.68 ± 1.69
081210(1)	45.11 ± 0.41	4.8	2.03	2.78	85,255.11 ± 6462.06	31.6 ± 2.02
081210(2)	53.74 ± 2.45	9.8	5.85	3.96	19,539.68 ± 10,178.05	14.79 ± 6.52
081210(3)	69.38 ± 4.37	23.29	12.76	10.53	20,940.74 ± 2699.7	37.76 ± 3.24
081210(4)	102.07 ± 2.21	42.79	8.78	34	11,169.06 ± 1901.38	35.6 ± 4.74
081210(5)	128.31 ± 2.68	11.73	6.19	5.54	6926.38 ± 1208.81	6.28 ± 0.99
090407(1)	56.87 ± 0.49	11.03	5.56	5.47	36,460.4 ± 1300.86	31.11 ± 1.04
090407(2)	102.96 ± 2.1	40.46	28.38	12.09	15,971.22 ± 1408.06	49.76 ± 2.3
090407(3)	122.72 ± 1.07	19.94	4.47	15.47	10,253.32 ± 2944	15.37 ± 3.7

Table 2. *Cont.*

GRB ^a	$t_{p,z}$ (s)	Δt_z (s)	$t_{r,z}$ (s)	$t_{d,z}$ (s)	$L_{X,p,45}^{\text{b}}$ (erg/s)	$E_{X,iso,49}^{\text{b}}$ (erg)
090417B(1)	382.15 ± 10.87	289.02	180.11	108.91	738.02 ± 38.23	16.64 ± 0.58
090417B(2)	1032.27 ± 5.06	221.98	42.89	179.09	619.64 ± 31.3	10.27 ± 0.37
090417B(3)	1144.3 ± 6.84	93.67	25.51	68.16	648.93 ± 78.74	4.61 ± 0.36
090417B(4)	1248.38 ± 8.32	91.33	37.47	53.86	534.33 ± 96.11	3.76 ± 0.6
090423(1)	17.84 ± 0.41	4.01	1.41	2.6	397,595.48 ± 51,892.69	122.2 ± 14.33
090715B(1)	19.29 ± 0.22	3.06	1.67	1.39	827,516.24 ± 53,538.22	195.67 ± 11.31
090715B(2)	27 ± 0.5	5.04	1.29	3.75	141,085.74 ± 20,191.47	53.72 ± 4.62
090715B(3)	39.51 ± 0.24	1.82	0.65	1.17	208,683.78 ± 32,684.77	29.11 ± 3.49
090715B(4)	45.06 ± 0.32	1.26	0.75	0.5	153,177.21 ± 36,903.84	14.83 ± 2.84
090715B(5)	48.45 ± 0.62	11.37	7.91	3.46	294,391.68 ± 25,527.61	256.71 ± 14.78
090715B(6)	62.45 ± 0.27	3.03	0.67	2.37	608,008.78 ± 106,894.63	139.03 ± 18.72
090715B(7)	71.36 ± 0.41	10.58	6.53	4.05	897,448.16 ± 76,319.51	732.31 ± 57.33
090809(1)	1294.93 ± 4.86	354.26	143.43	210.83	2132.35 ± 135.95	58.16 ± 3.41
090809(2)	5315.29 ± 134.93	1680.48	785.79	894.7	149.86 ± 69.23	19.47 ± 8.93
090812(1)	38.78 ± 0.4	13.35	4.57	8.78	173,326.99 ± 5880.38	176.85 ± 4.86
090812(2)	75.4 ± 0.38	12.19	3.31	8.88	88,082.53 ± 4528.78	81.4 ± 3.09
091029(1)	82.82 ± 3.39	18.49	6.33	12.16	5655.95 ± 1426.33	8 ± 1.63
100117A(1)	72.55 ± 2.29	2.64	1.37	1.27	1830.28 ± 187.44	0.37 ± 0.04
100117A(2)	96.23 ± 1.38	6.55	4.63	1.92	1757.72 ± 737.66	0.88 ± 0.27
100117A(3)	118.11 ± 4.7	15.49	10.13	5.35	1090.7 ± 414.92	1.3 ± 0.34
100302A(1)	23.19 ± 0.69	6.96	4.47	2.49	435,752.35 ± 55,803.44	234.08 ± 20.85
100302A(2)	32.18 ± 0.73	5.51	2.38	3.13	174,428.95 ± 17,096.07	74.1 ± 6.23
100302A(3)	43.48 ± 0.14	3.83	1.07	2.76	574,184.29 ± 33,143.62	167.29 ± 7.07
100302A(4)	53.86 ± 0.25	9.47	1.3	8.17	243,733.36 ± 13,524.9	170.49 ± 6.92
100728A(1)	28.1 ± 0.5	1.55	0.53	1.02	99,459.51 ± 37,670.26	11.81 ± 3.75
100728A(2)	35.43 ± 1.24	12.41	8.07	4.34	191,277.62 ± 27,003.48	183.19 ± 16.42
100728A(3)	47.89 ± 0.53	8.86	3.33	5.53	255,008.7 ± 18,845.11	173.5 ± 10.17
100728A(4)	86.99 ± 1.41	17.53	8.94	8.59	93,774.99 ± 3841.93	127.18 ± 4.41
100728A(5)	104.12 ± 1	7.2	3.03	4.17	55,608 ± 7876.35	30.88 ± 3.7
100728A(6)	123.71 ± 0.36	10.8	4.05	6.75	172,605.12 ± 6682.1	143.28 ± 4.5
100728A(7)	151.4 ± 0.13	4.7	0.94	3.76	156,271.63 ± 8318.06	55.12 ± 2.24
100728A(8)	180.15 ± 0.78	7.43	3.22	4.2	36,587.23 ± 3278.52	20.98 ± 1.66
100728A(9)	222.28 ± 0.4	17.15	8.04	9.11	163,478.41 ± 3277.17	216.73 ± 4.18
100728A(10)	272.52 ± 0.73	24.96	5.77	19.19	38,917.29 ± 1975.49	73.23 ± 2.73
100816A(1)	76.13 ± 2.2	20.73	5.82	14.91	1270.79 ± 211.71	2 ± 0.26
100816A(2)	155.48 ± 15.99	27.85	2.87	24.98	155.81 ± 20.33	0.32 ± 0.03
100901A(1)	89.23 ± 1.72	30.36	16.83	13.53	10,686.73 ± 1000.49	25.12 ± 1.71
100901A(2)	103.8 ± 0.55	14.35	1.51	12.84	7000.77 ± 1304.13	7.38 ± 1.27
100901A(3)	129.42 ± 0.98	27.08	5.19	21.89	7250.48 ± 978.77	14.66 ± 1.78
100901A(4)	164.69 ± 0.69	33.93	9.46	24.47	26,056.94 ± 995.23	67.04 ± 2.02
100901A(5)	11,063.02 ± 96.5	8862.33	3312.41	5549.92	103.59 ± 5.69	70.38 ± 3.7
100905A(1)	35.52 ± 0.4	5.09	2	3.09	411,894.64 ± 32,443.6	161.2 ± 10.75
100905A(2)	44.79 ± 0.34	3.77	0.97	2.8	346,419.93 ± 57,498.8	98.85 ± 12.69
100906A(1)	43.76 ± 0.17	7.31	3.78	3.53	1,938,564.05 ± 52,220.83	1096.6 ± 28.52
101219B(1)	229.84 ± 7.43	75.08	31.78	43.3	314.98 ± 26.36	1.82 ± 0.14
110205A(1)	146.2 ± 0.98	9.06	1.49	7.57	18,904.03 ± 3885.95	12.78 ± 1.9
110205A(2)	189.45 ± 0.42	10.57	2.55	8.02	50,514.51 ± 3415.86	40.36 ± 2.05
110731A(1)	19.61 ± 0.52	5.62	3.9	1.72	143,146.09 ± 21,578.78	61.75 ± 7.15
110801A(1)	74.41 ± 0.94	16.58	7.43	9.15	27,545.09 ± 1310.75	35.28 ± 1.6
110801A(2)	125.36 ± 0.16	16.19	4.17	12.01	405,808.94 ± 7172.21	497.1 ± 7.58
111107A(1)	83.25 ± 4.75	24.64	13.37	11.27	6432.94 ± 1405.14	12.27 ± 2.4
111123A(1)	67.78 ± 0.76	16.97	4.93	12.04	124,133.39 ± 10,121.55	159.93 ± 9.65
111123A(2)	108.16 ± 1.13	10.77	1.81	8.96	43,645.69 ± 9552.46	35.03 ± 5.06
111123A(3)	124.9 ± 2.9	46.68	32.05	14.63	71,098.42 ± 14,380.07	255.68 ± 43.14
111129A(1)	126.9 ± 14.48	11.77	6.64	5.13	507.74 ± 54.54	0.46 ± 0.05
111129A(2)	200.11 ± 19.75	36.94	16.52	20.42	236.46 ± 105.88	0.67 ± 0.29
111215A(1)	212.6 ± 2.25	29.99	13.55	16.44	22,337.32 ± 1345.36	51.76 ± 2.92
111215A(2)	318.54 ± 1.05	86.44	14.2	72.24	51,187.66 ± 1307.58	327.88 ± 6.2
111225A(1)	180.69 ± 2.95	60.16	15.68	44.48	156.82 ± 12.45	0.71 ± 0.04
120805A(1)	45.41 ± 2.84	12.9	4.17	8.74	30,734.02 ± 7933.88	30.24 ± 5.59
120922A(1)	77.8 ± 0.36	6.69	1.73	4.96	154,002.83 ± 13,317.48	78.06 ± 4.87
120922A(2)	90.77 ± 0.87	5.17	1.14	4.03	59,988.57 ± 18,437.79	23.37 ± 4.57
120922A(3)	100.72 ± 1.1	8.85	4.06	4.79	86,598.12 ± 18,628.81	59.25 ± 12.11

Table 2. Cont.

GRB ^a	$t_{p,z}$ (s)	Δt_z (s)	$t_{r,z}$ (s)	$t_{d,z}$ (s)	$L_{X,p,45}$ ^b (erg/s)	$E_{X,iso,49}$ ^b (erg)
121024A(1)	62.87 ± 0.99	9.09	3.56	5.53	25,860.2 ± 2720.66	18.09 ± 1.6
121024A(2)	81.78 ± 0.83	8.28	2.31	5.97	15,971.53 ± 2752.89	10.05 ± 1.27
121027A(1)	91.45 ± 0.68	22	5.73	16.27	31,522.79 ± 1601.62	52.41 ± 2.03
121128A(1)	30.16 ± 0.52	4.59	1.88	2.71	49,420.44 ± 5217.02	17.47 ± 1.6
121211A(1)	46.8 ± 1.65	16.33	9.56	6.77	23,531.46 ± 2616.79	29.75 ± 2.5
121211A(2)	81.87 ± 0.61	29.69	9.96	19.73	69,045.39 ± 1655.62	156.49 ± 3.05
130427B(1)	34.49 ± 0.57	4.74	2.33	2.4	55,179 ± 5421.06	20.21 ± 1.95
130514A(1)	23.96 ± 0.36	8.91	3.61	5.29	19,178,206 ± 70,387.24	1314.63 ± 43.59
130514A(2)	51.94 ± 0.76	20.08	12.84	7.23	109,451,773 ± 53,090.34	1698.11 ± 54.65
130514A(3)	81.51 ± 0.84	13.46	7.9	5.57	412,058.8 ± 25,706.52	428.53 ± 21.19
130606A(1)	12.63 ± 0.2	5.21	0.72	4.49	799,929.16 ± 98,731.16	305.53 ± 31.13
130606A(2)	23.67 ± 0.18	3.83	3.04	0.79	902,769.52 ± 82,882.71	261.59 ± 17.75
130606A(3)	31.98 ± 0.19	2.59	1.1	1.49	107,572,613 ± 71,056.31	215.3 ± 12.37
130606A(4)	37.29 ± 0.13	4.72	0.91	3.82	144,956,712 ± 77,984.74	512.38 ± 19.78
130606A(5)	59.25 ± 0.41	6.94	3.62	3.32	622,291.35 ± 28,266.09	333.95 ± 13.87
131004A(1)	276.88 ± 12.6	124.51	33.6	90.91	243.25 ± 39.2	2.29 ± 0.28
131004A(2)	449.28 ± 59.54	48.3	8.54	39.76	239.44 ± 23.94	0.86 ± 0.84
131030A(1)	49.97 ± 0.61	31.96	20.82	11.14	659,402.87 ± 24,288.01	1638.47 ± 49.28
131103A(1)	52.72 ± 1.44	16.97	10.49	6.48	2455.59 ± 279.44	3.22 ± 0.29
131103A(2)	254.77 ± 1.71	21.76	2.99	18.76	304.97 ± 115.15	0.49 ± 0.18
131103A(3)	426.55 ± 0.48	52.93	5.82	47.11	7053.71 ± 227.79	27.47 ± 0.75
131117A(1)	18.86 ± 0.18	2.46	0.88	1.58	196,335.71 ± 16,650.12	37.03 ± 2.61
140114A(1)	47.88 ± 0.47	30.36	19.96	10.4	112,184,608 ± 27,320.1	2646.78 ± 49.28
140114A(2)	79.93 ± 0.15	10.23	1.96	8.27	424,062.76 ± 10,863.04	324.43 ± 6.19
140206A(1)	16.02 ± 0.12	3.36	1.15	2.21	33,152,218 ± 152,933.04	852.99 ± 34.51
140206A(2)	59.5 ± 0.2	11.36	4.36	7	798,705.37 ± 16,879.07	697.45 ± 13.37
140301A(1)	35.56 ± 0.33	10.24	2.62	7.62	29,636.73 ± 1695.91	22.89 ± 0.94
140301A(2)	237.71 ± 1.69	33.37	8.3	25.06	3194.89 ± 264.71	8.05 ± 0.52
140304A(1)	54.17 ± 3.56	32.2	12.8	19.4	115,373.81 ± 10,963.25	285.68 ± 25.45
140304A(2)	129.72 ± 3.61	47.15	10.74	36.41	50,919.59 ± 7709.05	179.92 ± 19.85
140419A(1)	39.64 ± 0.33	5.62	1.61	4.01	213,145.22 ± 19,101.2	91 ± 6.1
140430A(1)	59.54 ± 0.51	4.63	1.35	3.28	93,627.52 ± 16,070	33.01 ± 4.11
140430A(2)	66 ± 0.19	4.41	1.11	3.3	210,076.1 ± 19,013.97	70.19 ± 4.74
140430A(3)	83.58 ± 0.18	7.69	2.15	5.54	150,392 ± 5856.68	87.86 ± 2.74
140506A(1)	63.8 ± 0.27	12.46	5.21	7.25	220,599.69 ± 5610.26	211.84 ± 5.12
140506A(2)	126.46 ± 0.76	26.78	8.14	18.63	23,937.46 ± 918.11	48.79 ± 1.36
140506A(3)	183.05 ± 0.72	27.09	10.61	16.49	54,301.71 ± 1955.46	113.21 ± 3.61
140512A(1)	74.59 ± 0.51	14.71	7.29	7.42	51,480.87 ± 1838.04	58.56 ± 2.04
140512A(2)	132.75 ± 1.67	8.64	2.48	6.16	1859.06 ± 554.25	1.22 ± 0.27
140515A(1)	406.36 ± 2.8	356.23	104.06	252.17	10,405.25 ± 1144.98	279.92 ± 28.68
140710A(1)	246.24 ± 6.68	55.12	18.13	37	207.87 ± 39.84	0.88 ± 0.14
140907A(1)	81.12 ± 4.58	28.57	6.38	22.18	1376.22 ± 443.61	2.94 ± 0.69
141109A(1)	77.66 ± 0.14	6.96	0.87	6.09	308,864.49 ± 13,011.13	158.94 ± 5.03
141109A(2)	113.97 ± 0.02	3.68	0.04	3.64	37,231.75 ± 7837.18	9.91 ± 2.07
141221A(1)	138.96 ± 6.71	53.36	24.5	28.86	6865.38 ± 762.6	28.31 ± 3.11
150206A(1)	754.59 ± 3.43	159.11	94.87	64.24	188,505.23 ± 4482.6	2316.72 ± 43.79
150821A(1)	348.31 ± 6.16	102.33	45.81	56.52	1840.12 ± 75.37	14.54 ± 0.57
150821A(2)	640.93 ± 13.62	513.45	445.35	68.1	674.48 ± 52.55	27.13 ± 1.7
150821A(3)	882.6 ± 8.78	84.99	18.12	66.88	204.38 ± 51.82	1.31 ± 0.3
150910A(1)	140.72 ± 4.49	34.76	11.13	23.63	2567.46 ± 418.15	6.8 ± 0.85
151027A(1)	69.52 ± 0.48	17.81	9.02	8.79	114,870.69 ± 3828.25	158.33 ± 5.08
151027A(2)	172.07 ± 2.99	63.68	33.29	30.4	3639.76 ± 143.26	17.95 ± 0.6
151111A(1)	29.47 ± 0.93	11.08	4.83	6.25	107,364.33 ± 7472.88	91.83 ± 6.16
160227A(1)	59.75 ± 0.11	8.44	1.95	6.49	487,334.8 ± 13,581.88	309.78 ± 7.24
160227A(2)	116.41 ± 0.3	29.04	3.01	26.02	98,725.47 ± 2306.97	209.7 ± 3.8
160410A(1)	114.84 ± 7.13	17.54	9	8.54	1649.07 ± 512.13	2.24 ± 0.65
160425A(1)	144.22 ± 1.29	10.18	7.93	2.25	756.37 ± 181.95	0.58 ± 0.1
160425A(2)	174.7 ± 0.38	11.39	3.21	8.18	52,182.02 ± 2937.89	45.18 ± 1.98
160425A(3)	200.37 ± 0.66	27.81	13.51	14.3	39,972.67 ± 2216.08	85.96 ± 4.76
160804A(1)	243.15 ± 0.97	21.8	6.05	15.74	4370.84 ± 306.58	7.24 ± 0.38
161017A(1)	29.63 ± 0.51	1.75	0.85	0.9	35,469.83 ± 7593.64	4.81 ± 1.01
161017A(2)	49.28 ± 2.35	21.65	6.39	15.26	82,312.5 ± 20,079.74	135.09 ± 26.02
161017A(3)	64.96 ± 1.12	7.09	1.72	5.37	107,520.52 ± 31,871.11	57.59 ± 11.52
161017A(4)	78.43 ± 2.11	24.86	14.46	10.4	221,510.95 ± 52,910.03	426.19 ± 92.89
161017A(5)	108.37 ± 0.8	23.89	1.56	22.33	47,793.46 ± 7791.94	82.85 ± 11.36
161017A(6)	129.54 ± 2.29	15.64	7.44	8.2	71,668.35 ± 12,130.22	86.66 ± 14.37
161017A(7)	152.5 ± 2.57	21.43	12.71	8.72	60,699.25 ± 9809.11	100.41 ± 12.71

Table 2. Cont.

GRB ^a	$t_{p,z}$ (s)	Δt_z (s)	$t_{r,z}$ (s)	$t_{d,z}$ (s)	$L_{X,p,45}$ ^b (erg/s)	$E_{X,iso,49}$ ^b (erg)
161108A(1)	52.7 ± 0.81	9.05	5.09	3.95	36,403.28 ± 3149.86	25.46 ± 1.9
161117A(1)	45.89 ± 0.22	9.86	4.36	5.49	833,412.5 ± 20,550.52	634.12 ± 15.13
161219B(1)	333.94 ± 2.57	86.26	24.33	61.93	57.12 ± 2.51	0.37 ± 0.01
170113A(1)	31.57 ± 0.25	8.37	4.32	4.05	229,171.18 ± 8351.26	148.43 ± 5.12
170405A(1)	35.77 ± 0.23	5.46	1.89	3.57	684,969.1 ± 36,462.91	286.47 ± 12.28
170519A(1)	106.37 ± 0.13	12.47	1.94	10.53	94,785.55 ± 2143.52	87.86 ± 1.72
170531B(1)	48.57 ± 0.16	9.87	3.31	6.57	247,449.75 ± 5143.07	186.77 ± 3.29
170531B(2)	169.99 ± 0.36	17.06	6.65	10.41	94,216.45 ± 2373.82	123.69 ± 2.74
170604A(1)	115.37 ± 2.11	5.64	2.78	2.85	6848.48 ± 1759.39	2.99 ± 0.77
170604A(2)	145.59 ± 1.4	31.16	8.39	22.77	66,832.17 ± 4681.59	157.63 ± 7.46
170604A(3)	158.17 ± 0.69	9.33	1.37	7.97	44,679.62 ± 6256.23	30.99 ± 2.84
170705A(1)	65.65 ± 0.28	21.56	8.37	13.18	225,601.65 ± 3843.82	373.72 ± 5.87
180205A(1)	72.81 ± 0.8	11.27	3.01	8.26	13,686.39 ± 1720.59	11.68 ± 1.14
180325A(1)	24.89 ± 0.22	4.08	1.01	3.07	737,040.61 ± 46,943.87	227.02 ± 11.87
180329B(1)	50.07 ± 0.35	11.52	2.84	8.68	215,785.7 ± 16,426.58	190.62 ± 8.59
180329B(2)	67.33 ± 1.93	13.56	5.62	7.94	54,055.88 ± 7024.33	56.49 ± 6.3
180329B(3)	74.45 ± 0.44	6.53	1.99	4.55	70,839.94 ± 8498.52	35.29 ± 2.99
180620B(1)	48.02 ± 0.55	8.88	1.64	7.24	51,970.79 ± 5611.13	34.41 ± 2.62
180624A(1)	46.72 ± 0.1	8.14	2.1	6.04	768,402.87 ± 20,393.94	472.78 ± 10.68
180624A(2)	87.93 ± 0.27	22.11	4.71	17.41	340,470.51 ± 8895.32	563.81 ± 11.9
180624A(3)	97.28 ± 0.32	6.65	1.62	5.03	321,624.68 ± 27,806.05	161.75 ± 10.76
180624A(4)	119.76 ± 0.48	6.38	2.41	3.97	120,398.49 ± 9456.67	59.12 ± 3.66
181020A(1)	63.45 ± 0.34	13.29	7.44	5.84	885,659.22 ± 21,632.58	910.07 ± 18.95
181020A(2)	94.2 ± 0.69	18.02	9.93	8.1	262,452.43 ± 7884.61	365.85 ± 8.89
190106A(1)	27.09 ± 0.46	1.63	0.93	0.69	225,575.64 ± 50,296.91	28.32 ± 5.06
190106A(2)	34.48 ± 0.16	1.32	0.33	0.99	232,164.81 ± 46,257.34	23.16 ± 3.4
191221B(1)	447.2 ± 11.49	224.02	73.92	150.1	2332.59 ± 122.58	39.82 ± 1.61
201104B(1)	68.72 ± 1.67	11.39	3.49	7.91	7364.04 ± 1517.07	6.39 ± 1.00
201104B(2)	104.33 ± 1.05	10.1	0.71	9.39	3057.13 ± 1155.7	2.26 ± 0.82
210411C(1)	45.52 ± 0.94	13.55	4.58	8.97	53,157.07 ± 4238.71	55.02 ± 3.48
210420B(1)	265.63 ± 7	66.12	9.27	56.86	1685.25 ± 349.52	8.22 ± 1.18

^a The number in parentheses is the index of the flare. ^b The symbolic notation $Q_n = Q/10^n$ is adopted.

3. Statistical Properties of the X-ray Flares

3.1. Distributions of Flare Parameters

The distributions of the observed X-ray flare parameters (i.e., t_p , Δt , t_r , t_d , α_1 , α_2 , $F_{X,p}$ and S_X) from the fitting and the other derived quantities (i.e., $\Delta t/t$, $\Delta F/F$, t_d/t_r , $L_{X,p}$ and $E_{X,iso}$) are demonstrated in Figure 2. For the LGRB flares, it is found that all distributions of the flare parameters are lognormal or logarithmic bimodal. We use a single or double Gaussian function to fit the distributions. The distributions of α_1 , α_2 , $F_{X,p}$, Δt , t_r , t_d , $\Delta t/t$, t_p , S_X and t_d/t_r can be fitted by a single Gaussian function. The median values and the standard deviations of these parameters are $\alpha_1 \sim 19.50$ ($\sigma \sim 0.46$), $\alpha_2 \sim 8.71$ ($\sigma \sim 0.29$), $F_{X,p} \sim 1.38 \times 10^{-9}$ erg cm⁻² s⁻¹ ($\sigma \sim 0.75$), $\Delta t \sim 43.65$ s ($\sigma \sim 0.42$), $t_r \sim 13.80$ s ($\sigma \sim 0.46$), $t_d \sim 26.30$ s ($\sigma \sim 0.44$), $\Delta t/t \sim 0.16$ ($\sigma \sim 0.28$), $t_p \sim 269.15$ s ($\sigma \sim 0.33$), $S_X \sim 4.57 \times 10^{-8}$ erg cm⁻² ($\sigma \sim 0.63$) and $t_d/t_r \sim 1.82$ ($\sigma \sim 0.32$), respectively. In addition, the distributions of the t_p , Δt , t_r , t_d and $F_{X,p}$ slightly deviate from lognormal distribution, we still use the Gaussian function to fit these quantities. Apart from $F_{X,p}$, the other quantities all extend to the larger value. We also find that $\Delta F/F$, $L_{X,p}$ and $E_{X,iso}$ deviate from the lognormal distributions significantly and show the obvious bimodal distributions. Thus, a double Gaussian function is adopted to the fitting. We obtain the median values and the standard deviations are $\Delta F/F \sim 3.39$ ($\sigma \sim 0.50$), $L_{X,p} \sim 1.26 \times 10^{50}$ erg s⁻¹ ($\sigma \sim 0.57$) and $E_{X,iso} \sim 6.92 \times 10^{50}$ erg ($\sigma \sim 0.69$) for the high peak, and $\Delta F/F \sim 63.10$ ($\sigma \sim 0.56$), $L_{X,p} \sim 2.29 \times 10^{48}$ erg s⁻¹ ($\sigma \sim 0.78$) and $E_{X,iso} \sim 5.25 \times 10^{48}$ erg ($\sigma \sim 0.34$) for the low peak. The distribution results are listed in Table 3.

For the SGRB flares, α_1 , α_2 , $F_{X,p}$, Δt , t_r , t_d and $\Delta t/t$ are basically lognormal. However, t_p , S_X and t_d/t_r for the SGRB flares obviously deviate from the lognormal distribution. The median values and the standard deviations of α_1 , α_2 , $F_{X,p}$, Δt , t_r , t_d and $\Delta t/t$ for the

SGRB flares are $\alpha_1 \sim 13.80$ ($\sigma \sim 0.69$), $\alpha_2 \sim 5.50$ ($\sigma \sim 0.16$), $F_{X,p} \sim 4.79 \times 10^{-10}$ erg cm $^{-2}$ s $^{-1}$ ($\sigma \sim 0.58$), $\Delta t \sim 30.20$ s ($\sigma \sim 0.30$), $t_r \sim 11.22$ s ($\sigma \sim 0.32$), $t_d \sim 24.55$ s ($\sigma \sim 0.53$) and $\Delta t/t \sim 0.20$ ($\sigma \sim 0.43$), respectively. Similarity, t_p , Δt , t_r , t_d and $F_{X,p}$ are slightly span to the larger value. Unfortunately, we can not give the statistical results of $\Delta F/F$, $L_{X,p}$ and $E_{X,iso}$ for the SGRB flares due to the small numbers. We find that $\Delta F/F$, $L_{X,p}$ and $E_{X,iso}$ are all located at the weak region. Noteworthily, $\Delta F/F$ in SGRB sample is the only quantity located at the high peak defined by the LGRB flares, which is in agreement with the $\Delta F/F$ distribution shown by [23].

Table 3. Best-fit Parameters of X-ray Flare Distributions.

Distr.	LGRB Flares			SGRB Flares		
	A	μ	σ	A	μ	σ
α_1	87.80 ± 3.45	1.30 ± 0.02	0.46 ± 0.01	6.49 ± 2.02	1.14 ± 0.24	0.69 ± 0.28
α_2	48.55 ± 1.91	0.94 ± 0.01	0.29 ± 0.01	2.25 ± 0.63	0.74 ± 0.05	0.16 ± 0.04
$F_{X,p}$	127.73 ± 5.06	-8.86 ± 0.03	0.75 ± 0.03	6.49 ± 5.14	-9.32 ± 0.56	0.58 ± 0.40
Δt	99.99 ± 3.96	1.64 ± 0.02	0.42 ± 0.01	5.56 ± 1.34	1.48 ± 0.07	0.30 ± 0.06
t_r	125.61 ± 4.99	1.14 ± 0.02	0.46 ± 0.01	6.00 ± 1.49	1.05 ± 0.08	0.32 ± 0.07
t_d	101.10 ± 4.02	1.42 ± 0.02	0.44 ± 0.01	5.81 ± 1.56	1.39 ± 0.16	0.53 ± 0.16
$\Delta t/t$	44.60 ± 1.77	-0.79 ± 0.01	0.28 ± 0.01	2.23 ± 0.93	-0.70 ± 0.18	0.43 ± 0.24
t_p	72.28 ± 2.92	2.43 ± 0.01	0.33 ± 0.01			
S_X	132.23 ± 5.19	-7.34 ± 0.02	0.63 ± 0.02			
t_d/t_r	65.98 ± 2.60	0.26 ± 0.01	0.32 ± 0.01			
$\Delta F/F$	62.76 ± 9.89	0.53 ± 0.09	0.50 ± 0.06			
	29.67 ± 9.37	1.80 ± 0.21	0.56 ± 0.10			
$L_{X,p}$	13.02 ± 5.61	48.36 ± 0.42	0.78 ± 0.28			
	39.87 ± 5.95	50.10 ± 0.09	0.57 ± 0.06			
$E_{X,iso}$	2.19 ± 2.98	48.72 ± 0.50	0.34 ± 0.45			
	33.58 ± 2.28	50.84 ± 0.05	0.69 ± 0.05			

The single or double Gaussian function are chosen to the fitting. A, μ , σ are the corresponding fitting parameters. For the LGRB flares, a double Gaussian function is the best-fit for $\Delta F/F$, $L_{X,p}$ and $E_{X,iso}$.

As shown in Figure 2, the distributions of the temporal parameters for the SGRB flares (α_1 , α_2 , Δt , t_r , t_d , $\Delta t/t$, t_d/t_r and t_p) are similar to those of the long ones. It is a self-similar behavior in the flare profile through flare emission [45], whether different types of GRBs or different time sequences. Then, the values of $F_{X,p}$, S_X , $\Delta F/F$, $L_{X,p}$ and $E_{X,iso}$ of the SGRB flares are weaker or smaller than those of the long ones. It is known that the isotropic energy and luminosity during the prompt emission phase of SGRBs are different from those of the long ones, and the flare is tightly related to the prompt emission phase. The morphology of t_p distribution obtained from the previous studies [25,36,50] is similar to our results. The mean value of t_d/t_r derived by [36] is 24.64. Our result is smaller than their result. It is more likely that the duration time is defined in a different way compared to [36]. We consider the significant part of a flare, which shows how strict the definition of the duration time in describing the burst or the flare [25]. $\Delta F/F$ in the LGRB sample obtained from [16] by the double Gaussian function fitting are 0.50 ($\sigma = 0.52$) and 2.10 ($\sigma = 0.36$), which is consistent with our result for the LGRB sample. In addition, there are no cases of the SGRB flare with $\Delta t/t$ exceeding 2, which is consistent with [16]. It can generally exclude the origin of external shock [25]. Ref. [45] obtained a similar result of $\Delta t/t$ as well. The median values for the late flares and the early flares are 0.28 and 0.23, respectively. But the late flares have a larger standard deviation ($\sigma = 0.33$ compared with $\sigma = 0.14$), which is not dependent with redshift. Again, the smaller value of $\Delta t/t$ in this paper may be due to a different definition of the duration. The distribution of the peak luminosity $L_{X,p}$, which span from 10^{46} erg/s to 10^{51} erg/s, is wider than that of [36].

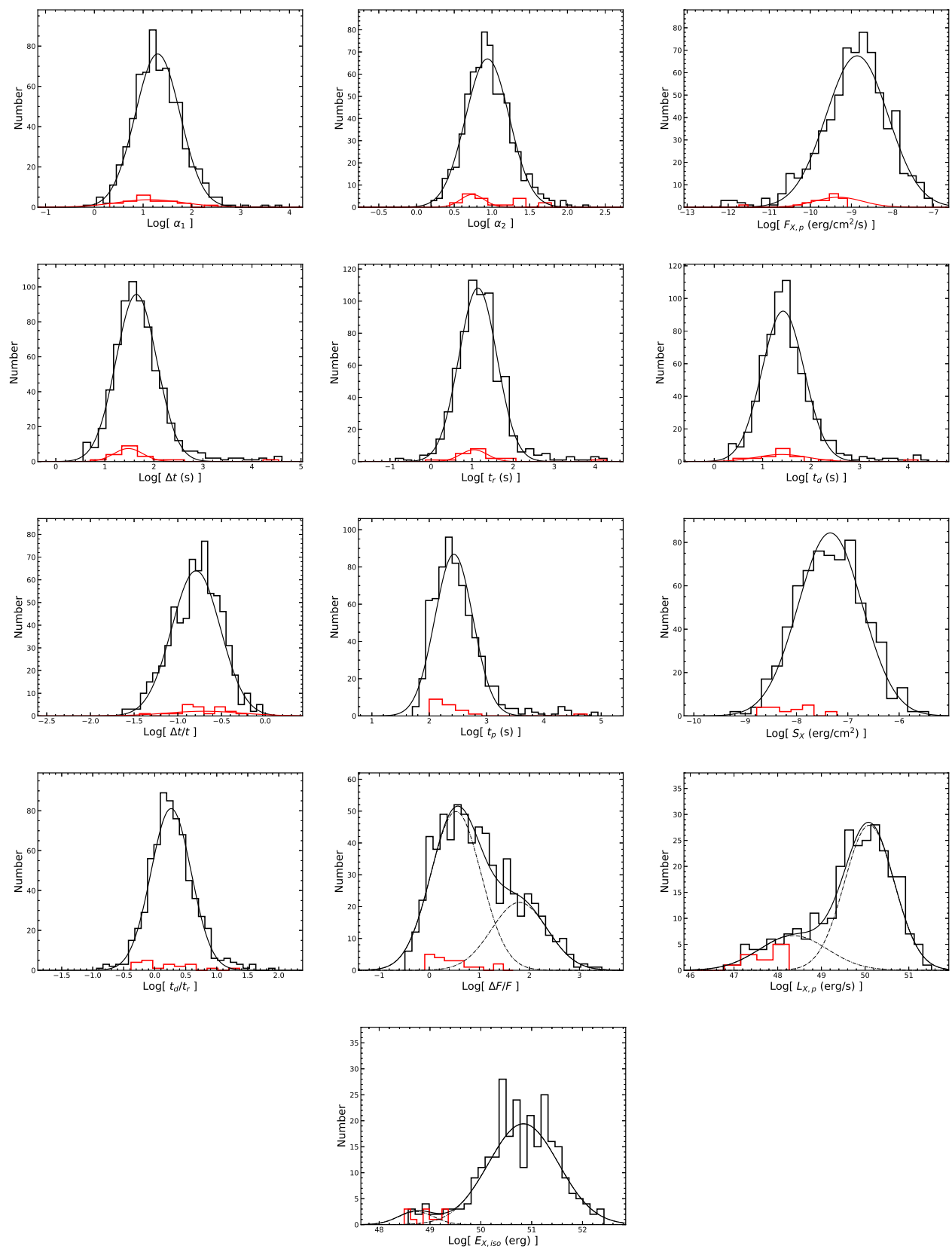


Figure 2. The distributions of the parameters for the X-ray flares. The black (red) solid lines represent the best fitting results for the LGRB (SGRB) flares with single or double Gaussian functions.

3.2. Two-Parameter Correlations of Early Flares and Late Flares

We first study the relationships among the observed temporal quantities. Δt , t_r and t_d of the flares as a function of t_p are shown in Figure 3. We find that Δt is correlated with t_p both for the early and late flares. We perform the regression analysis for the total sample, i.e., $\Delta t \propto t_p^{1.05^{+0.02}_{-0.02}}$ with a Pearson correlation coefficient $r = 0.86$ and a chance probability $p < 10^{-4}$. This result is similar to the $\Delta t-t_p$ correlation found in [26,36,45]. Similarly, t_r and t_d are also correlated with t_p . Besides, there is a strong correlation between the rise time and the decay time, i.e., $t_d \propto t_r^{0.75^{+0.02}_{-0.02}}$ for the total flares, with $r = 0.80$ and $p < 10^{-4}$. It is known that the ratio t_d/t_r can reflect the asymmetry of the flares and we find that the early flares are more asymmetric with a larger t_d/t_r . As shown in the last panel of Figure 3, the value of t_d/t_r gradually tend to $t_d/t_r = 1$ at later time. The results of the correlations are shown in Table 4.

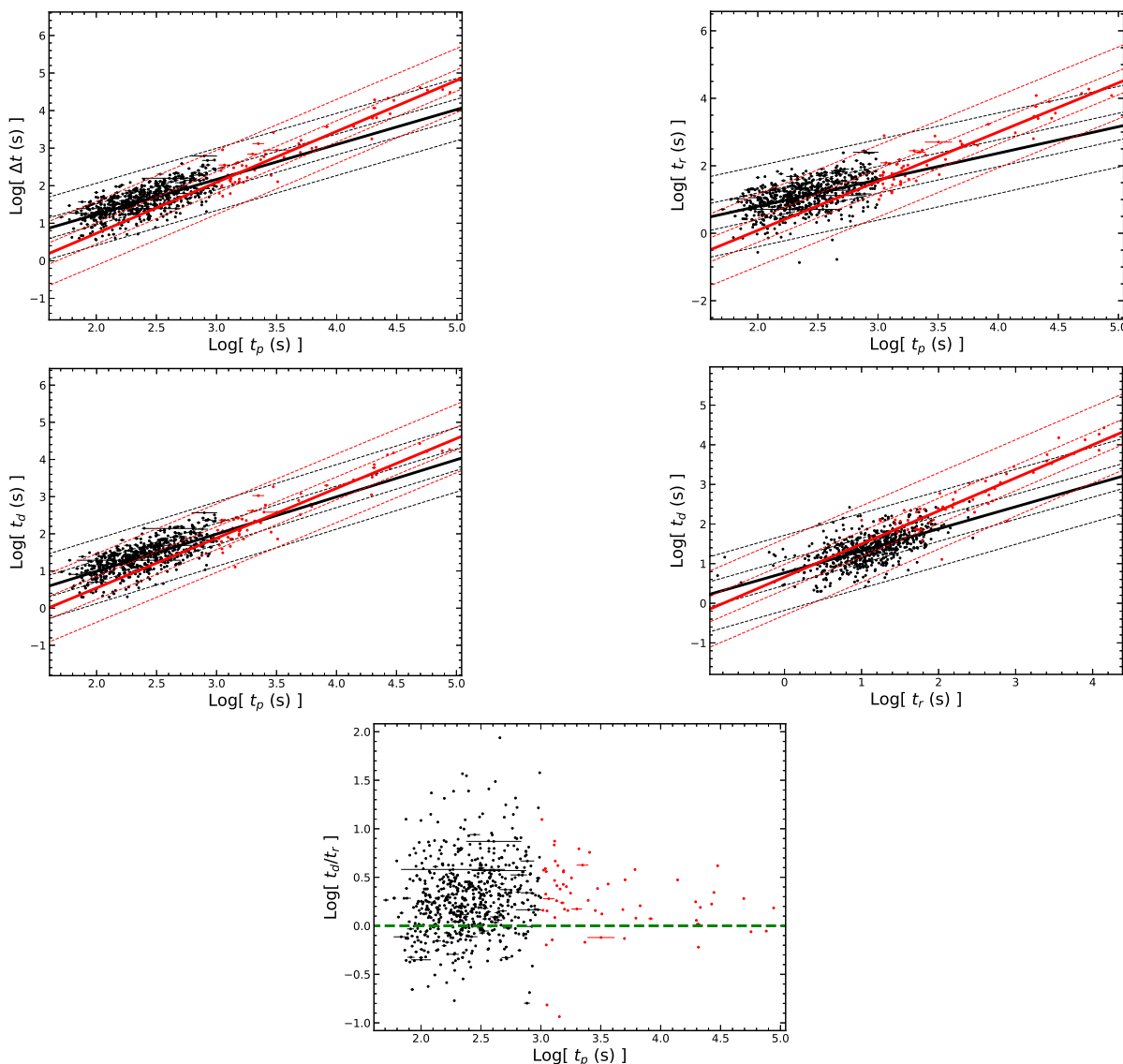


Figure 3. The correlations among the temporal parameters of flares. The black (red) dots represent the early (late) flares. The black (red) solid lines represent the best fits for the early (late) flares. The dashed lines represent the 1σ and 3σ confidence regions. The green dashed line in the last graph represents the axis of $t_d/t_r = 1$. The regression results with a correlation coefficient less than 0.3 are not shown on the figure.

Table 4. The correlations of early and late flares.

Correlations	Types	Expressions	σ_{int}	δ	r	p
$\Delta t(t_p)$	Early	$\log \Delta t = -0.63^{+0.09}_{-0.09} + 0.93^{+0.04}_{-0.04} \times \log t_p$	0.28	0.28	0.69	$<10^{-4}$
	Late	$\log \Delta t = -1.99^{+0.24}_{-0.24} + 1.36^{+0.07}_{-0.07} \times \log t_p$	0.29	0.28	0.93	$<10^{-4}$
	Total	$\log \Delta t = -0.92^{+0.06}_{-0.06} + 1.05^{+0.02}_{-0.02} \times \log t_p$	0.28	0.28	0.86	$<10^{-4}$
$t_r(t_p)$	Early	$\log t_r = -0.78^{+0.13}_{-0.13} + 0.79^{+0.06}_{-0.06} \times \log t_p$	0.40	0.40	0.49	$<10^{-4}$
	Late	$\log t_r = -2.83^{+0.31}_{-0.30} + 1.46^{+0.08}_{-0.09} \times \log t_p$	0.36	0.36	0.91	$<10^{-4}$
	Total	$\log t_r = -1.32^{+0.09}_{-0.09} + 1.02^{+0.03}_{-0.03} \times \log t_p$	0.41	0.41	0.75	$<10^{-4}$
$t_d(t_p)$	Early	$\log t_d = -1.01^{+0.10}_{-0.10} + 1.00^{+0.04}_{-0.04} \times \log t_p$	0.29	0.29	0.70	$<10^{-4}$
	Late	$\log t_d = -2.14^{+0.27}_{-0.26} + 1.34^{+0.07}_{-0.07} \times \log t_p$	0.32	0.31	0.92	$<10^{-4}$
	Total	$\log t_d = -1.19^{+0.06}_{-0.06} + 1.08^{+0.02}_{-0.02} \times \log t_p$	0.29	0.29	0.86	$<10^{-4}$
$t_d(t_r)$	Early	$\log t_d = 0.77^{+0.03}_{-0.03} + 0.56^{+0.03}_{-0.03} \times \log t_r$	0.32	0.32	0.63	$<10^{-4}$
	Late	$\log t_d = 0.66^{+0.12}_{-0.12} + 0.83^{+0.05}_{-0.05} \times \log t_r$	0.33	0.32	0.92	$<10^{-4}$
	Total	$\log t_d = 0.58^{+0.03}_{-0.03} + 0.75^{+0.02}_{-0.02} \times \log t_r$	0.34	0.34	0.80	$<10^{-4}$
$t_d/t_r(t_p)$	Early	$\log t_d/t_r = -0.23^{+0.12}_{-0.12} + 0.21^{+0.05}_{-0.05} \times \log t_p$	0.37	0.37	0.16	$<10^{-4}$
	Late	$\log t_d/t_r = 0.69^{+0.30}_{-0.30} - 0.12^{+0.08}_{-0.08} \times \log t_p$	0.36	0.35	-0.18	0.1622
	Total	$\log t_d/t_r = 0.13^{+0.08}_{-0.08} + 0.06^{+0.03}_{-0.03} \times \log t_p$	0.37	0.37	0.07	0.0558
$F_{X,p}(t_p)$	Early	$\log F_{X,p} = -6.07^{+0.22}_{-0.22} - 1.16^{+0.09}_{-0.09} \times \log t_p$	0.64	0.65	-0.45	$<10^{-4}$
	Late	$\log F_{X,p} = -4.53^{+0.55}_{-0.55} - 1.54^{+0.15}_{-0.15} \times \log t_p$	0.66	0.66	-0.79	$<10^{-4}$
	Total	$\log F_{X,p} = -6.12^{+0.14}_{-0.14} - 1.13^{+0.05}_{-0.05} \times \log t_p$	0.64	0.65	-0.62	$<10^{-4}$
$F_{X,p}(\Delta t)$	Early	$\log F_{X,p} = -7.50^{+0.11}_{-0.11} - 0.84^{+0.07}_{-0.07} \times \log \Delta t$	0.64	0.65	-0.44	$<10^{-4}$
	Late	$\log F_{X,p} = -6.92^{+0.30}_{-0.30} - 1.09^{+0.10}_{-0.10} \times \log \Delta t$	0.63	0.63	-0.81	$<10^{-4}$
	Total	$\log F_{X,p} = -7.36^{+0.08}_{-0.08} - 0.92^{+0.04}_{-0.04} \times \log \Delta t$	0.64	0.65	-0.62	$<10^{-4}$
$F_{X,p}(t_r)$	Early	$\log F_{X,p} = -8.36^{+0.07}_{-0.07} - 0.43^{+0.06}_{-0.06} \times \log t_r$	0.69	0.70	-0.27	$<10^{-4}$
	Late	$\log F_{X,p} = -7.73^{+0.24}_{-0.24} - 0.97^{+0.10}_{-0.10} \times \log t_r$	0.66	0.65	-0.79	$<10^{-4}$
	Total	$\log F_{X,p} = -8.10^{+0.06}_{-0.06} - 0.69^{+0.04}_{-0.04} \times \log t_r$	0.71	0.71	-0.51	$<10^{-4}$
$F_{X,p}(t_d)$	Early	$\log F_{X,p} = -7.71^{+0.09}_{-0.09} - 0.82^{+0.06}_{-0.06} \times \log t_d$	0.64	0.64	-0.46	$<10^{-4}$
	Late	$\log F_{X,p} = -7.22^{+0.29}_{-0.29} - 1.06^{+0.11}_{-0.11} \times \log t_d$	0.66	0.66	-0.79	$<10^{-4}$
	Total	$\log F_{X,p} = -7.59^{+0.07}_{-0.07} - 0.91^{+0.04}_{-0.04} \times \log t_d$	0.64	0.65	-0.62	$<10^{-4}$
$S_X(t_p)$	Early	$\log S_X = -6.82^{+0.22}_{-0.22} - 0.22^{+0.09}_{-0.09} \times \log t_p$	0.65	0.65	-0.10	0.0125
	Late	$\log S_X = -6.65^{+0.53}_{-0.52} - 0.18^{+0.15}_{-0.15} \times \log t_p$	0.63	0.62	-0.16	0.2273
	Total	$\log S_X = -7.17^{+0.14}_{-0.14} - 0.07^{+0.05}_{-0.05} \times \log t_p$	0.65	0.65	-0.05	0.1678
$S_X(\Delta t)$	Early	$\log S_X = -7.62^{+0.11}_{-0.11} + 0.16^{+0.07}_{-0.07} \times \log \Delta t$	0.65	0.65	0.09	0.0176
	Late	$\log S_X = -7.05^{+0.30}_{-0.30} - 0.09^{+0.10}_{-0.10} \times \log \Delta t$	0.63	0.63	-0.11	0.4072
	Total	$\log S_X = -7.48^{+0.08}_{-0.08} + 0.08^{+0.04}_{-0.04} \times \log \Delta t$	0.64	0.65	0.06	0.0937
$S_X(t_r)$	Early	$\log S_X = -7.65^{+0.07}_{-0.07} + 0.27^{+0.06}_{-0.06} \times \log t_r$	0.64	0.64	0.19	$<10^{-4}$
	Late	$\log S_X = -7.10^{+0.23}_{-0.23} - 0.08^{+0.09}_{-0.09} \times \log t_r$	0.63	0.63	-0.11	0.3990
	Total	$\log S_X = -7.52^{+0.05}_{-0.05} + 0.14^{+0.04}_{-0.04} \times \log t_r$	0.64	0.65	0.13	0.0005
$S_X(t_d)$	Early	$\log S_X = -7.46^{+0.09}_{-0.09} + 0.07^{+0.06}_{-0.06} \times \log t_r$	0.65	0.65	0.04	0.2833
	Late	$\log S_X = -7.08^{+0.28}_{-0.28} - 0.08^{+0.10}_{-0.10} \times \log t_d$	0.63	0.63	-0.10	0.4384
	Total	$\log S_X = -7.41^{+0.07}_{-0.07} + 0.04^{+0.04}_{-0.04} \times \log t_d$	0.65	0.65	0.03	0.3868

Table 4. Cont.

Correlations	Types	Expressions	σ_{int}	δ	r	p
$F_{X,p}(S_X)$	Early	$\log F_{X,p} = -1.93^{+0.17}_{-0.17} + 0.94^{+0.02}_{-0.02} \times \log S_X$	0.37	0.38	0.85	$<10^{-4}$
	Late	$\log F_{X,p} = -1.70^{+1.24}_{-1.22} + 1.14^{+0.17}_{-0.17} \times \log S_X$	0.82	0.80	0.67	$<10^{-4}$
	Total	$\log F_{X,p} = -2.02^{+0.24}_{-0.24} + 0.94^{+0.03}_{-0.03} \times \log S_X$	0.54	0.56	0.74	$<10^{-4}$
$L_{X,p}(t_{p,z})$	Early	$\log L_{X,p} = 53.44^{+0.28}_{-0.29} - 1.97^{+0.15}_{-0.15} \times \log t_{p,z}$	0.74	0.74	-0.63	$<10^{-4}$
	Late	$\log L_{X,p} = 52.82^{+1.27}_{-1.27} - 1.47^{+0.39}_{-0.39} \times \log t_{p,z}$	0.95	0.85	-0.70	0.0008
	Total	$\log L_{X,p} = 52.66^{+0.20}_{-0.20} - 1.55^{+0.10}_{-0.10} \times \log t_{p,z}$	0.77	0.77	-0.69	$<10^{-4}$
$L_{X,p}(\Delta t_z)$	Early	$\log L_{X,p} = 51.08^{+0.14}_{-0.14} - 1.26^{+0.12}_{-0.12} \times \log \Delta t_z$	0.80	0.81	-0.54	$<10^{-4}$
	Late	$\log L_{X,p} = 50.83^{+0.88}_{-0.89} - 1.03^{+0.32}_{-0.32} \times \log \Delta t_z$	1.02	0.92	-0.64	0.0032
	Total	$\log L_{X,p} = 50.95^{+0.11}_{-0.11} - 1.13^{+0.08}_{-0.08} \times \log \Delta t_z$	0.82	0.82	-0.63	$<10^{-4}$
$L_{X,p}(t_{r,z})$	Early	$\log L_{X,p} = 50.18^{+0.09}_{-0.09} - 0.81^{+0.11}_{-0.11} \times \log t_{r,z}$	0.87	0.87	-0.41	$<10^{-4}$
	Late	$\log L_{X,p} = 50.09^{+0.74}_{-0.74} - 0.90^{+0.31}_{-0.31} \times \log t_{r,z}$	1.06	0.95	-0.60	0.0065
	Total	$\log L_{X,p} = 50.22^{+0.08}_{-0.08} - 0.89^{+0.08}_{-0.08} \times \log t_{r,z}$	0.88	0.88	-0.55	$<10^{-4}$
$L_{X,p}(t_{d,z})$	Early	$\log L_{X,p} = 50.74^{+0.11}_{-0.11} - 1.20^{+0.11}_{-0.11} \times \log t_{d,z}$	0.81	0.81	-0.54	$<10^{-4}$
	Late	$\log L_{X,p} = 50.57^{+0.83}_{-0.83} - 1.03^{+0.33}_{-0.33} \times \log t_{d,z}$	1.03	0.92	-0.63	0.0037
	Total	$\log L_{X,p} = 50.68^{+0.09}_{-0.09} - 1.12^{+0.08}_{-0.08} \times \log t_{d,z}$	0.82	0.82	-0.63	$<10^{-4}$
$E_{X,iso}(t_{p,z})$	Early	$\log E_{X,iso} = 52.59^{+0.29}_{-0.29} - 1.01^{+0.15}_{-0.15} \times \log t_{p,z}$	0.75	0.75	-0.38	$<10^{-4}$
	Late	$\log E_{X,iso} = 51.55^{+1.34}_{-1.34} - 0.28^{+0.41}_{-0.41} \times \log t_{p,z}$	1.00	0.90	-0.17	0.4753
	Total	$\log E_{X,iso} = 51.55^{+0.20}_{-0.20} - 0.44^{+0.10}_{-0.10} \times \log t_{p,z}$	0.79	0.79	-0.26	$<10^{-4}$
$E_{X,iso}(\Delta t_z)$	Early	$\log E_{X,iso} = 50.96^{+0.14}_{-0.14} - 0.26^{+0.12}_{-0.12} \times \log \Delta t_z$	0.80	0.81	-0.13	0.0293
	Late	$\log E_{X,iso} = 50.70^{+0.88}_{-0.89} - 0.03^{+0.32}_{-0.31} \times \log \Delta t_z$	1.02	0.92	-0.02	0.9258
	Total	$\log E_{X,iso} = 50.83^{+0.11}_{-0.11} - 0.13^{+0.08}_{-0.08} \times \log \Delta t_z$	0.82	0.82	-0.10	0.1061
$E_{X,iso}(t_{r,z})$	Early	$\log E_{X,iso} = 50.73^{+0.08}_{-0.08} - 0.09^{+0.10}_{-0.10} \times \log t_{r,z}$	0.81	0.81	-0.05	0.3853
	Late	$\log E_{X,iso} = 50.61^{+0.71}_{-0.71} + 0.01^{+0.30}_{-0.30} \times \log t_{r,z}$	1.02	0.92	0.01	0.9655
	Total	$\log E_{X,iso} = 50.71^{+0.07}_{-0.07} - 0.05^{+0.07}_{-0.07} \times \log t_{r,z}$	0.82	0.82	-0.04	0.4674
$E_{X,iso}(t_{d,z})$	Early	$\log E_{X,iso} = 50.93^{+0.11}_{-0.11} - 0.29^{+0.11}_{-0.11} \times \log t_{d,z}$	0.80	0.80	-0.16	0.0098
	Late	$\log E_{X,iso} = 50.74^{+0.82}_{-0.83} - 0.05^{+0.33}_{-0.32} \times \log t_{d,z}$	1.02	0.92	-0.04	0.8844
	Total	$\log E_{X,iso} = 50.82^{+0.09}_{-0.09} - 0.16^{+0.08}_{-0.08} \times \log t_{d,z}$	0.81	0.82	-0.12	0.0502
$L_{X,p}(E_{X,iso})$	Early	$\log L_{X,p} = -4.35^{+1.59}_{-1.58} + 1.07^{+0.03}_{-0.03} \times \log E_{X,iso}$	0.40	0.41	0.91	$<10^{-4}$
	Late	$\log L_{X,p} = -3.63^{+10.55}_{-10.48} + 1.02^{+0.21}_{-0.21} \times \log E_{X,iso}$	0.82	0.74	0.78	$<10^{-4}$
	Total	$\log L_{X,p} = -4.64^{+2.17}_{-2.18} + 1.07^{+0.04}_{-0.04} \times \log E_{X,iso}$	0.58	0.59	0.83	$<10^{-4}$

The correlations are derived from early and late flares. r is the Pearson correlation coefficient, p is the chance probability, δ is the dispersion of correlation and σ_{int} is the intrinsic scatter.

The relationships between the peak flux ($F_{X,p}$) and the temporal quantities of the flares are demonstrated in Figure 4. We find that there is an anti-correlation between $F_{X,p}$ and t_p for all the sample, i.e., $F_{X,p} \propto t_p^{-1.13^{+0.05}}$ with $r = -0.62$ and $p < 10^{-4}$. Obviously, the $F_{X,p}$ - t_p correlation for the late flares is tighter than the early flares. As shown in Figure 5, we find that the fluence of the flares (S_X) is independent of the temporal quantities of the flares. Figure 6 (upper left) shows the relationship between $F_{X,p}$ and S_X . For the early flares, $F_{X,p} \propto S_X^{0.94^{+0.02}}$ with $r = 0.85$ and $p < 10^{-4}$. For the late flares, $F_{X,p} \propto S_X^{1.14^{+0.17}}$ with $r = 0.67$ and $p < 10^{-4}$.

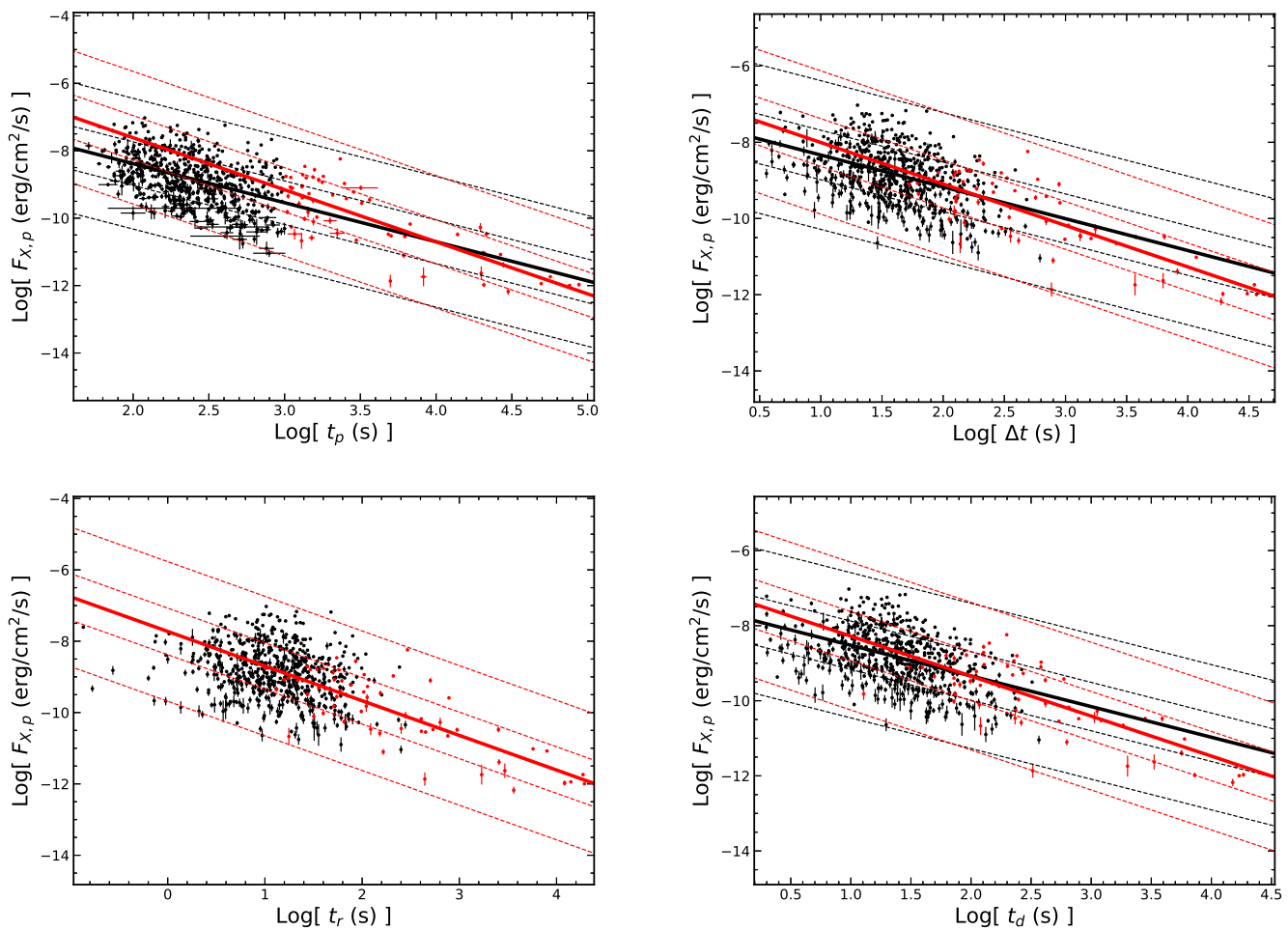


Figure 4. The correlations between the peak flux of flares and the temporal quantities in the observer frame. All symbols and descriptions are the same as in Figure 3.

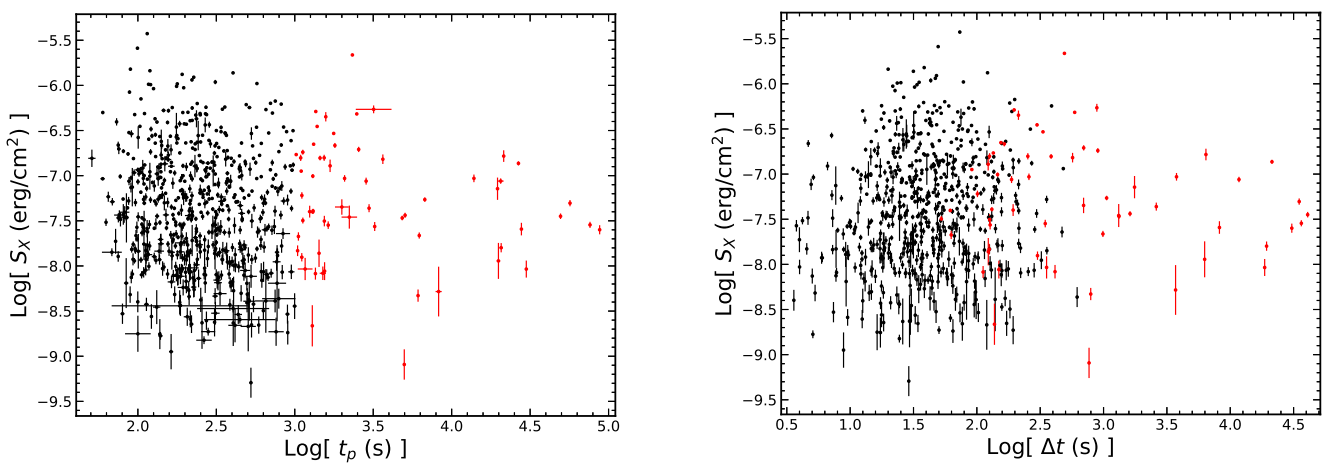


Figure 5. Cont.

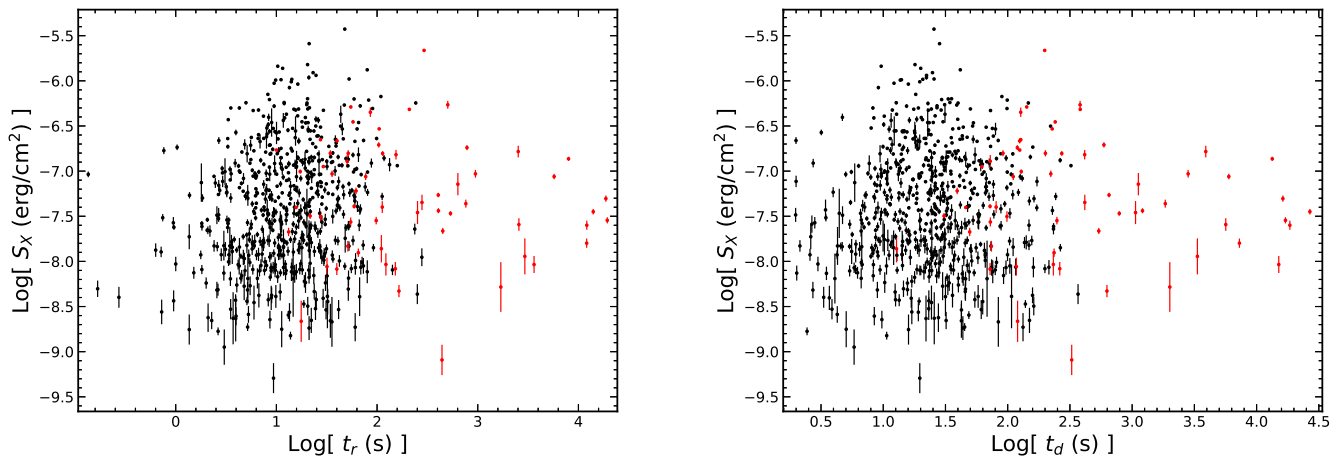


Figure 5. Relationships between the flare fluence and the temporal quantities in the observer frame. All symbols and descriptions are the same as in Figure 3.

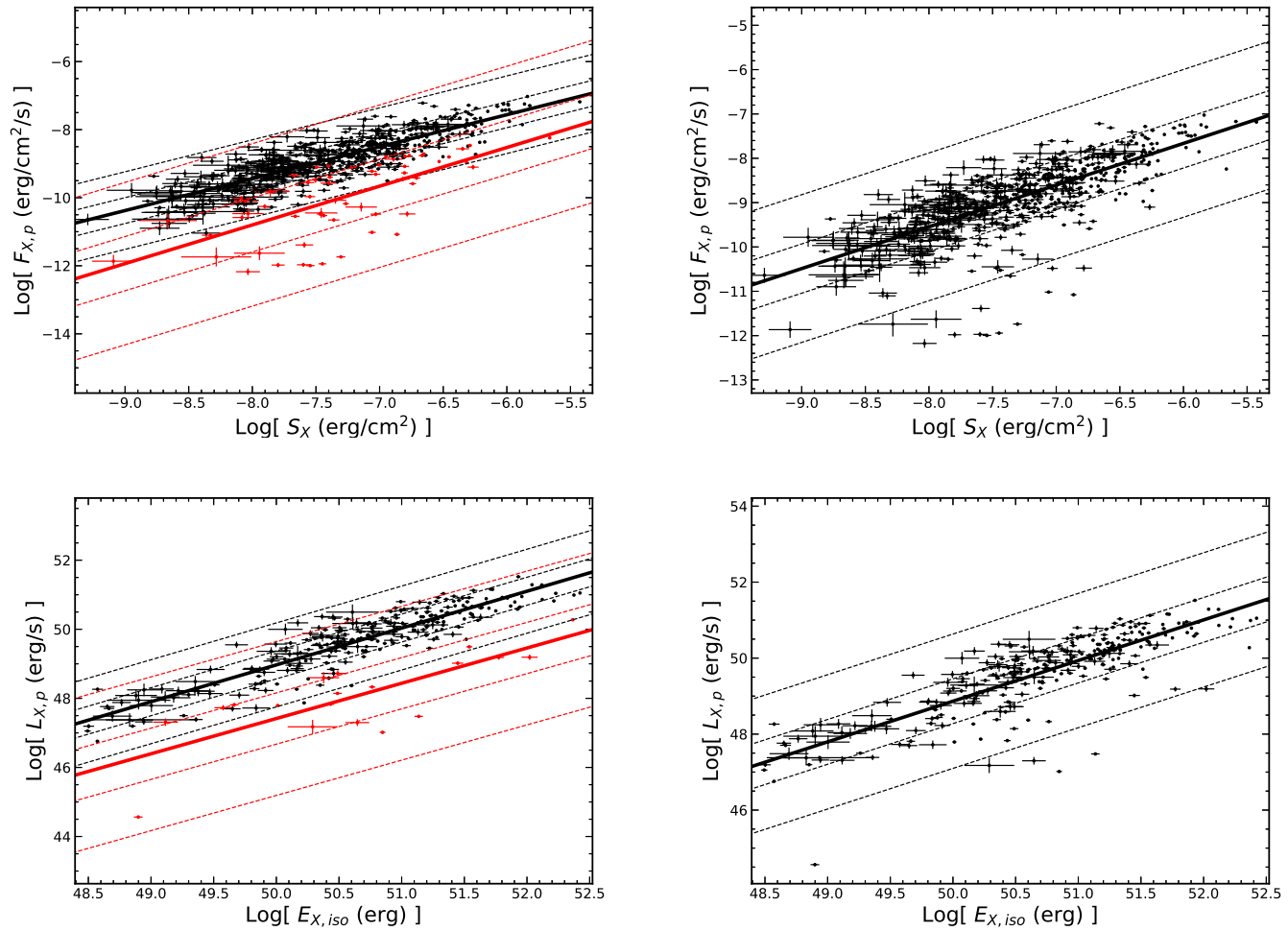


Figure 6. The $F_{X,p}$ - S_X correlation and the $L_{X,p}$ - $E_{X,iso}$ correlation are shown at top and bottom panel, respectively. The left panel are derived from the early and late flares, while the right panel are derived from the total flares. All symbols and descriptions are the same as in Figure 3.

It is known that the rest frame relationships can reflect the physical nature of the flares. We investigate the relations among the rest frame quantities of the flares and find that the peak luminosity ($L_{X,p}$) is correlated with the temporal parameters of the flares as shown in Figure 7. For all flares, $L_{X,p} \propto t_{p,z}^{-1.55^{+0.10}}$ with $r = -0.69$ and $p < 10^{-4}$, which is consistent with the total sample of [36,45]. This result indicate that the dimmer X-ray flares are more likely to appear at the later time and have a longer duration. Besides, the flare energy ($E_{X,iso}$) is independent of the temporal parameters as shown in Figure 8. From the Figure 6 (bottom panel), a more tight correlation between $L_{X,p}$ and $E_{X,iso}$ in the rest frame is found. For the early flares, $L_{X,p} \propto E_{X,iso}^{1.07^{+0.03}}$ with $r = 0.91$ and $p < 10^{-4}$. For the late flares, $L_{X,p} \propto E_{X,iso}^{1.02^{+0.21}}$ with $r = 0.78$ and $p < 10^{-4}$. Ref. [36] obtained a similar result, i.e., $L_{X,p} \propto E_{X,iso}^{1.04^{+0.07}}$.

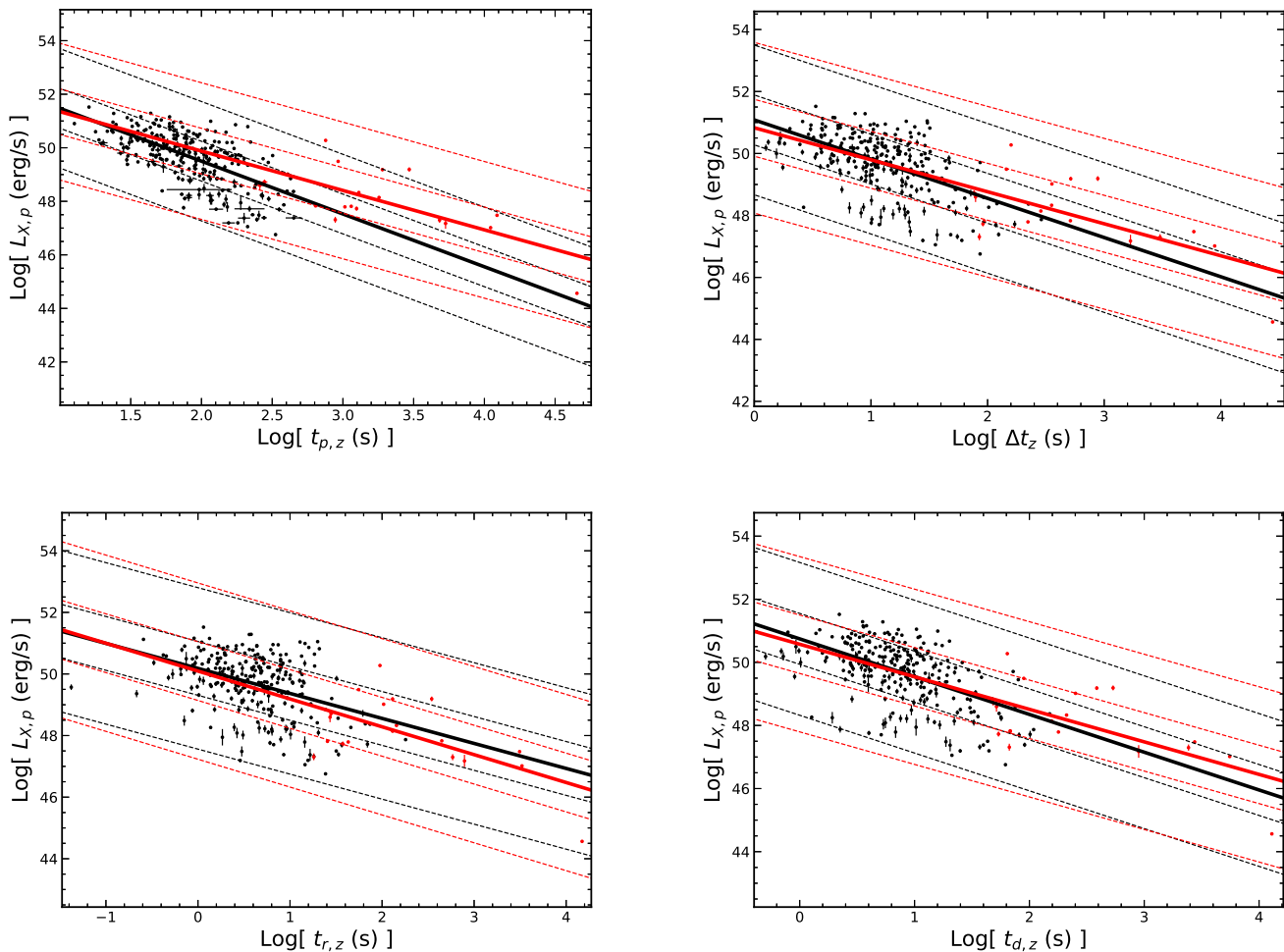


Figure 7. The peak luminosity ($L_{X,p}$) of flares is correlated with the temporal parameters in the rest frame. All symbols and descriptions are the same as in Figure 3.

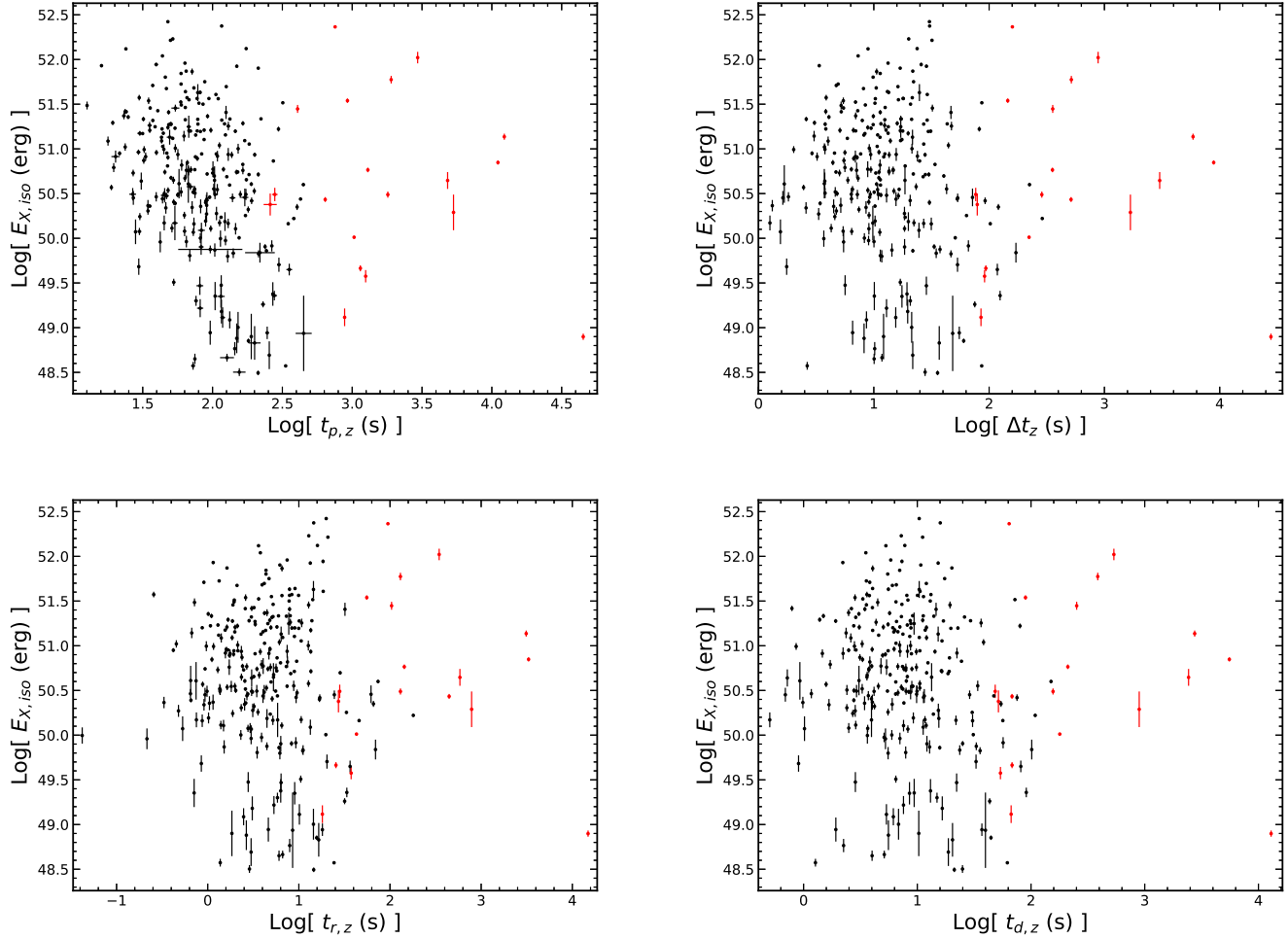


Figure 8. No correlations are found between the $E_{X,\text{iso}}$ and the temporal quantities in the rest frame. All symbols and descriptions are the same as in Figure 3.

3.3. Two-Parameter Correlations of LGRB Flares and SGRB Flares

We further analyze the correlations for the LGRB flares and SGRB flares and find that the correlations among the temporal parameters of the LGRB flares are similar to that of the short ones as shown in Figure 9. We also find that the relationships between $F_{X,p}$ and the temporal quantities/fluence are different for the LGRB flares and SGRB flares (see Figures 10 and 11). For the LGRB flares, $F_{X,p} \propto t_p^{-1.20^{+0.09}}$ with $r = -0.48$ and $p < 10^{-4}$, and $F_{X,p} \propto S_X^{0.95^{+0.02}}$ with $r = 0.85$ and $p < 10^{-4}$. For the SGRB flares, $F_{X,p} \propto t_p^{-0.58^{+0.34}}$ with $r = -0.39$ and $p = 0.0983$, and $F_{X,p} \propto S_X^{0.46^{+0.17}}$ with $r = 0.59$ and $p = 0.0079$. The integrated fluence of the flare S_X is independent of the temporal quantities for both the LGRB flares and SGRB flares as well (Figure 12). The results of correlations are shown in Table 5.

Similarly, we analyze the rest frame correlations for the LGRB flares and SGRB flares. As shown in Figure 13, For the LGRB flares, $L_{X,p} \propto t_{p,z}^{-1.45^{+0.10}_{-0.10}}$ ($r = -0.67$ and $p < 10^{-4}$). For the SGRB flares, $L_{X,p} \propto t_{p,z}^{-1.27^{+0.13}_{-0.13}}$ ($r = -0.96$ and $p < 10^{-4}$). The $L_{X,p}$ - $t_{p,z}$ correlation in our SGRB flares quantitatively confirms the conclusion of [23] that there is a factor of approximately 0.01 smaller than the long ones. $L_{X,p}$ is also correlated with the other temporal quantities (Δt , $t_{r,z}$ and $t_{d,z}$) for the LGRB flares and SGRB flares. In addition, we do not find the significant dependence of the X-ray flare total energy ($E_{X,iso}$) with the temporal quantities in the rest frame for either the LGRB flares or SGRB flares as shown in Figure 14. We also analyze the relationship between the peak luminosity and the total energy for the LGRB flares and SGRB flares and find that these two quantities are correlated, and the correlation of the SGRB flares may not be as tight as that of the long ones (see the right panel of Figure 11). For the LGRB flares, $L_{X,p} \propto E_{X,iso}^{1.04^{+0.05}_{-0.05}}$ with $r = 0.81$ and $p < 10^{-4}$. For the SGRB flares, $L_{X,p} \propto E_{X,iso}^{0.59^{+0.96}_{-0.87}}$ with $r = 0.19$ and $p = 0.5532$.

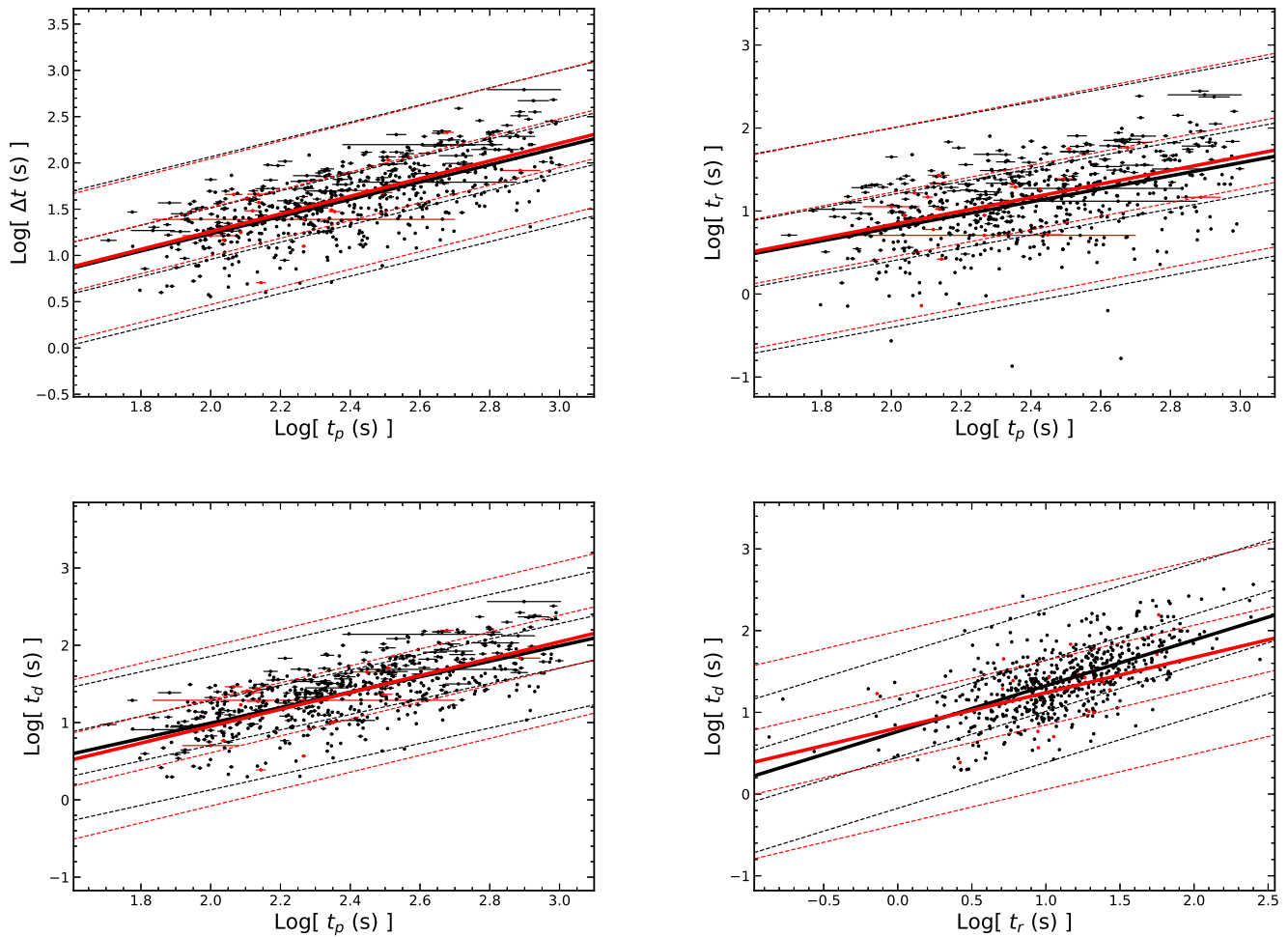


Figure 9. The correlations between LGRB and SGRB flares about the temporal parameters are similar. The black (red) dot represents LGRB (SGRB) flares. The dashed lines represent the 1σ and 3σ confidence regions. The regression results with a correlation coefficient less than 0.3 are not shown on the figure.

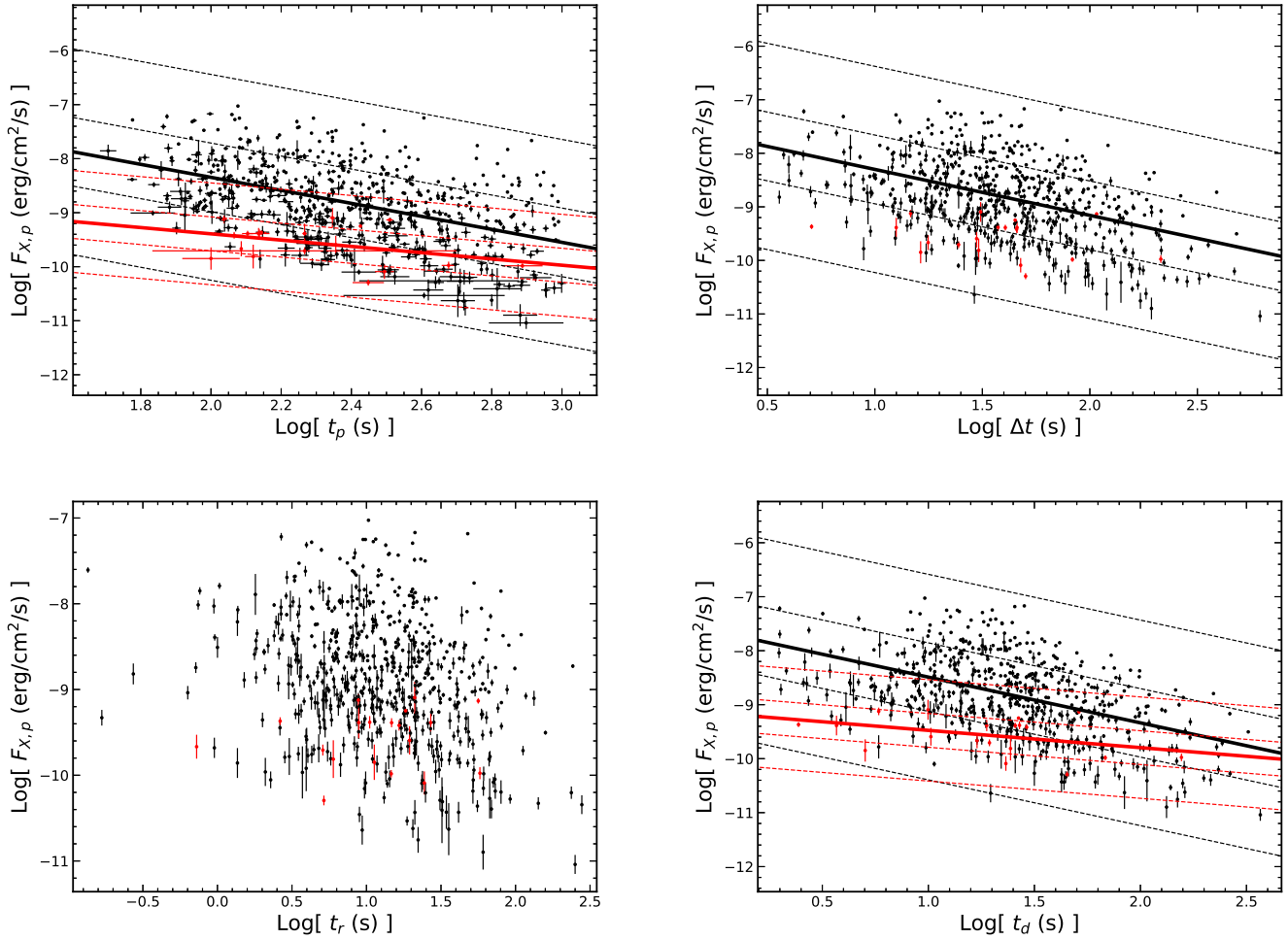


Figure 10. The correlations between the peak flux of flares and the temporal quantities in the observer frame. All symbols and descriptions are the same as in Figure 9.

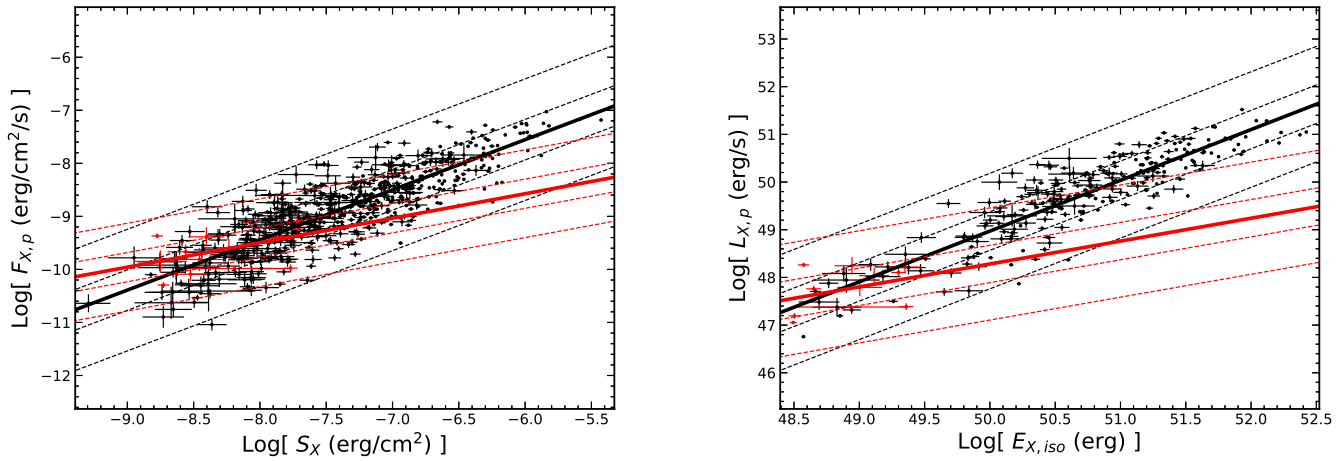


Figure 11. The $F_{X,p}$ - S_X correlation and the $L_{X,p}$ - $E_{X,iso}$ correlation are shown at left and right panel of the figure, respectively. All symbols and descriptions are the same as in Figure 9.

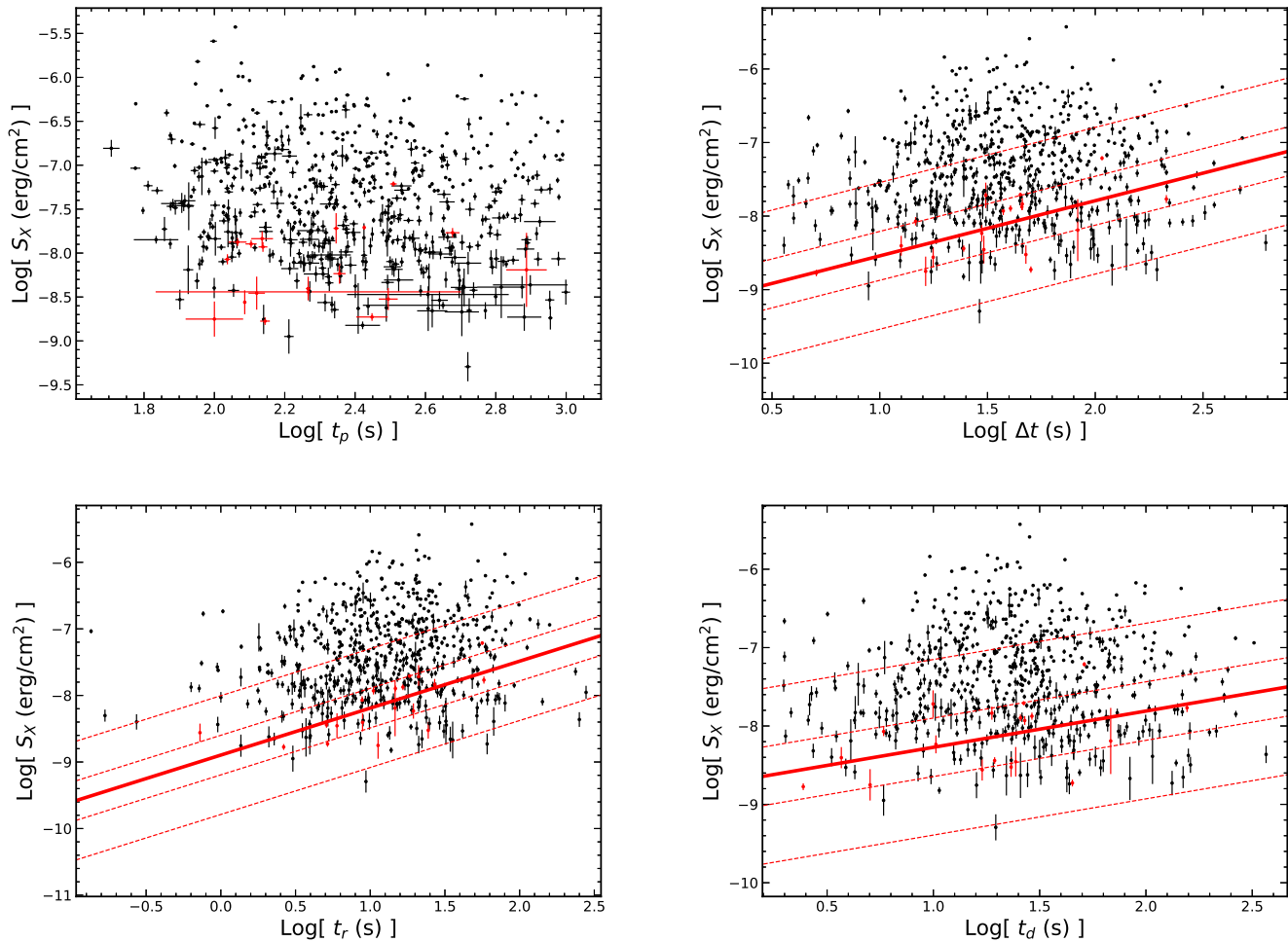


Figure 12. The correlations between the flare fluence and the temporal quantities are shown in the observer frame. All symbols and descriptions are the same as in Figure 9.

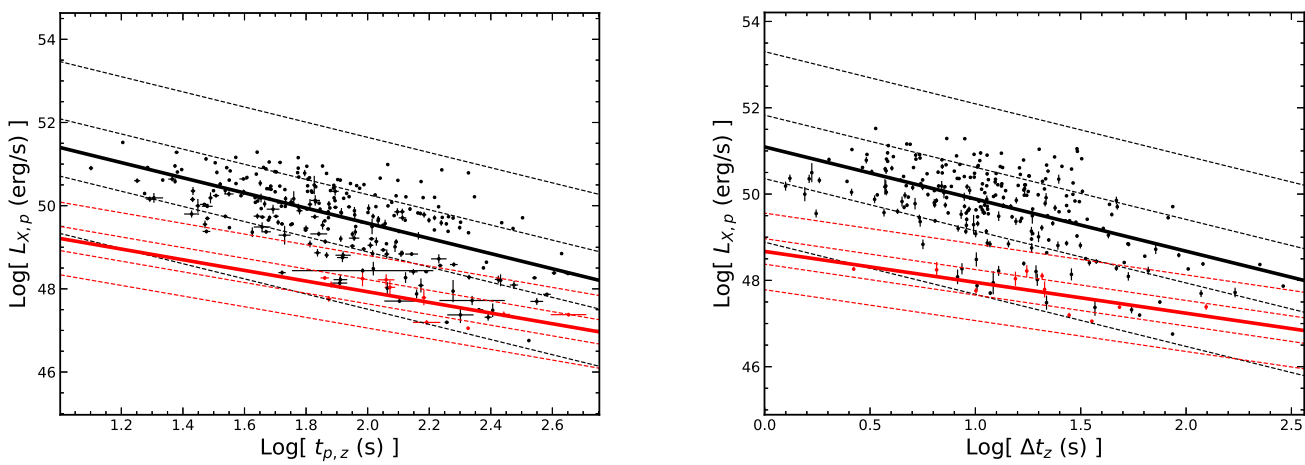


Figure 13. Cont.

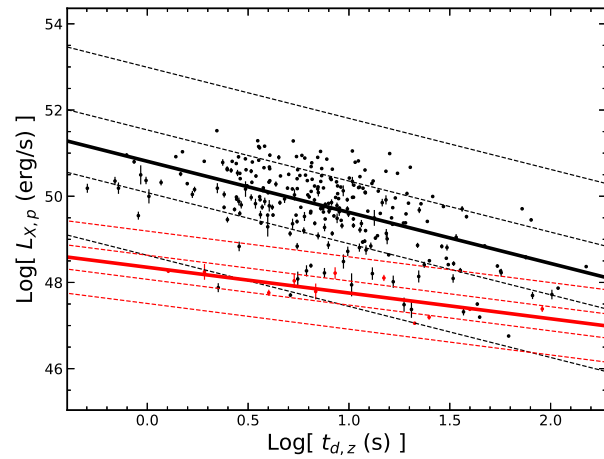
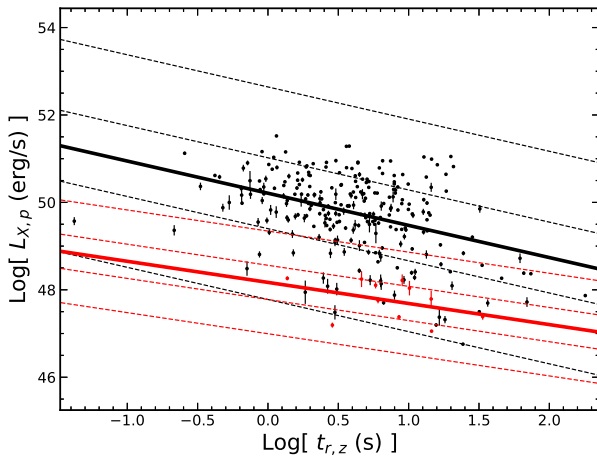


Figure 13. The peak luminosity ($L_{X,p}$) of flares is correlated with the temporal parameters of flares in the rest frame. All symbols and descriptions are the same as in Figure 9.

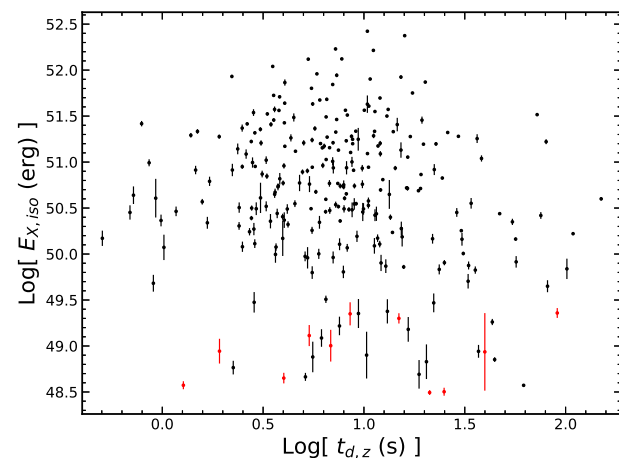
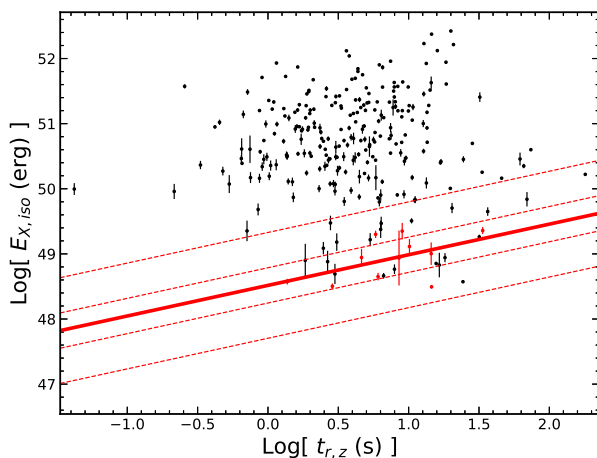
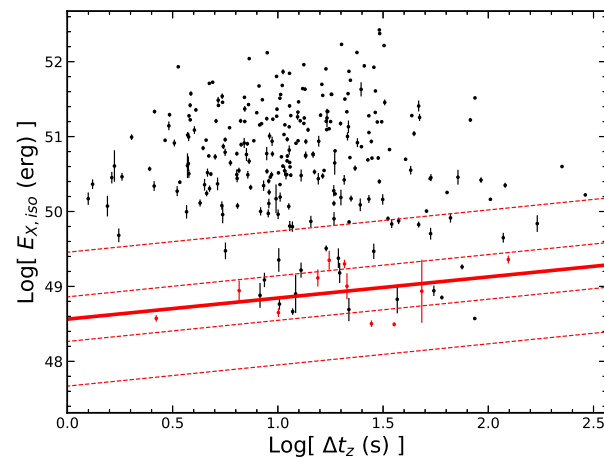
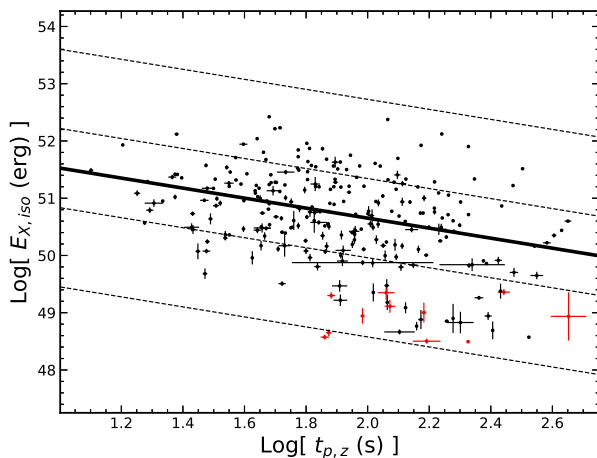


Figure 14. No correlations are found between the $E_{X,iso}$ and the temporal quantities in the rest frame. All symbols and descriptions are the same as in Figure 9.

Table 5. The correlations of LGRB flares and SGRB flares.

Correlations	Types	Expressions	σ_{int}	δ	r	p
$\Delta t(t_p)$	Total Long	$\log \Delta t = -0.91^{+0.06}_{-0.06} + 1.05^{+0.02}_{-0.02} \times \log t_p$	0.28	0.28	0.86	$<10^{-4}$
	Total Short	$\log \Delta t = -1.17^{+0.29}_{-0.28} + 1.18^{+0.11}_{-0.11} \times \log t_p$	0.29	0.26	0.94	$<10^{-4}$
	Early Long	$\log \Delta t = -0.63^{+0.09}_{-0.09} + 0.93^{+0.04}_{-0.04} \times \log t_p$	0.28	0.28	0.69	$<10^{-4}$
	Early Short	$\log \Delta t = -0.65^{+0.69}_{-0.69} + 0.96^{+0.30}_{-0.30} \times \log t_p$	0.30	0.26	0.67	0.0018
$t_r(t_p)$	Total Long	$\log t_r = -1.30^{+0.09}_{-0.09} + 1.01^{+0.03}_{-0.03} \times \log t_p$	0.41	0.41	0.74	$<10^{-4}$
	Total Short	$\log t_r = -1.72^{+0.41}_{-0.41} + 1.22^{+0.17}_{-0.17} \times \log t_p$	0.43	0.39	0.88	$<10^{-4}$
	Early Long	$\log t_r = -0.77^{+0.14}_{-0.14} + 0.78^{+0.06}_{-0.06} \times \log t_p$	0.40	0.40	0.49	$<10^{-4}$
	Early Short	$\log t_r = -0.80^{+0.97}_{-0.98} + 0.82^{+0.43}_{-0.42} \times \log t_p$	0.43	0.39	0.46	0.0498
$t_d(t_p)$	Total Long	$\log t_d = -1.18^{+0.06}_{-0.06} + 1.07^{+0.02}_{-0.03} \times \log t_p$	0.29	0.29	0.85	$<10^{-4}$
	Total Short	$\log t_d = -1.43^{+0.36}_{-0.36} + 1.18^{+0.14}_{-0.15} \times \log t_p$	0.38	0.33	0.90	$<10^{-4}$
	Early Long	$\log t_d = -1.01^{+0.10}_{-0.10} + 1.00^{+0.04}_{-0.04} \times \log t_p$	0.29	0.29	0.70	$<10^{-4}$
	Early Short	$\log t_d = -1.23^{+0.90}_{-0.89} + 1.09^{+0.39}_{-0.39} \times \log t_p$	0.39	0.34	0.62	0.0047
$t_d(t_r)$	Total Long	$\log t_d = 0.59^{+0.03}_{-0.03} + 0.75^{+0.02}_{-0.02} \times \log t_r$	0.34	0.34	0.80	$<10^{-4}$
	Total Short	$\log t_d = 0.45^{+0.19}_{-0.19} + 0.79^{+0.13}_{-0.13} \times \log t_r$	0.47	0.42	0.84	$<10^{-4}$
	Early Long	$\log t_d = 0.77^{+0.03}_{-0.03} + 0.56^{+0.03}_{-0.03} \times \log t_r$	0.31	0.31	0.63	$<10^{-4}$
	Early Short	$\log t_d = 0.81^{+0.27}_{-0.27} + 0.43^{+0.23}_{-0.23} \times \log t_r$	0.44	0.39	0.43	0.0651
$t_d/t_r(t_p)$	Total Long	$\log t_d/t_r = 0.12^{+0.08}_{-0.08} + 0.07^{+0.03}_{-0.03} \times \log t_p$	0.37	0.37	0.08	0.0386
	Total Short	$\log t_d/t_r = 0.30^{+0.48}_{-0.49} - 0.04^{+0.20}_{-0.19} \times \log t_p$	0.51	0.46	-0.06	0.8088
	Early Long	$\log t_d/t_r = -0.24^{+0.13}_{-0.13} + 0.22^{+0.05}_{-0.05} \times \log t_p$	0.37	0.37	0.17	$<10^{-4}$
	Early Short	$\log t_d/t_r = -0.45^{+1.13}_{-1.14} + 0.29^{+0.49}_{-0.49} \times \log t_p$	0.51	0.46	0.15	0.5304
$F_{X,p}(t_p)$	Total Long	$\log F_{X,p} = -6.05^{+0.14}_{-0.14} - 1.15^{+0.05}_{-0.05} \times \log t_p$	0.63	0.64	-0.63	$<10^{-4}$
	Total Short	$\log F_{X,p} = -7.63^{+0.32}_{-0.33} - 0.84^{+0.13}_{-0.13} \times \log t_p$	0.32	0.31	-0.84	$<10^{-4}$
	Early Long	$\log F_{X,p} = -5.94^{+0.22}_{-0.21} - 1.20^{+0.09}_{-0.09} \times \log t_p$	0.63	0.64	-0.48	$<10^{-4}$
	Early Short	$\log F_{X,p} = -8.23^{+0.78}_{-0.79} - 0.58^{+0.34}_{-0.34} \times \log t_p$	0.33	0.31	-0.39	0.0983
$F_{X,p}(\Delta t)$	Total Long	$\log F_{X,p} = -7.32^{+0.08}_{-0.08} - 0.94^{+0.04}_{-0.04} \times \log \Delta t$	0.63	0.64	-0.63	$<10^{-4}$
	Total Short	$\log F_{X,p} = -8.62^{+0.22}_{-0.22} - 0.63^{+0.12}_{-0.12} \times \log \Delta t$	0.37	0.35	-0.80	$<10^{-4}$
	Early Long	$\log F_{X,p} = -7.44^{+0.11}_{-0.11} - 0.86^{+0.07}_{-0.07} \times \log \Delta t$	0.63	0.64	-0.46	$<10^{-4}$
	Early Short	$\log F_{X,p} = -9.14^{+0.38}_{-0.38} - 0.28^{+0.24}_{-0.24} \times \log \Delta t$	0.35	0.33	-0.28	0.2450
$F_{X,p}(t_r)$	Total Long	$\log F_{X,p} = -8.07^{+0.06}_{-0.06} - 0.70^{+0.04}_{-0.04} \times \log t_r$	0.70	0.71	-0.52	$<10^{-4}$
	Total Short	$\log F_{X,p} = -9.10^{+0.20}_{-0.20} - 0.47^{+0.13}_{-0.13} \times \log t_r$	0.47	0.43	-0.66	0.0016
	Early Long	$\log F_{X,p} = -8.32^{+0.07}_{-0.07} - 0.45^{+0.06}_{-0.06} \times \log t_r$	0.69	0.69	-0.28	$<10^{-4}$
	Early Short	$\log F_{X,p} = -9.68^{+0.23}_{-0.23} + 0.10^{+0.20}_{-0.20} \times \log t_r$	0.37	0.34	0.13	0.5864
$F_{X,p}(t_d)$	Total Long	$\log F_{X,p} = -7.54^{+0.07}_{-0.07} - 0.92^{+0.04}_{-0.04} \times \log t_d$	0.63	0.64	-0.63	$<10^{-4}$
	Total Short	$\log F_{X,p} = -8.79^{+0.18}_{-0.18} - 0.62^{+0.11}_{-0.11} \times \log t_d$	0.36	0.34	-0.81	$<10^{-4}$
	Early Long	$\log F_{X,p} = -7.64^{+0.09}_{-0.09} - 0.85^{+0.06}_{-0.06} \times \log t_d$	0.63	0.63	-0.48	$<10^{-4}$
	Early Short	$\log F_{X,p} = -9.16^{+0.25}_{-0.25} - 0.32^{+0.18}_{-0.18} \times \log t_d$	0.33	0.31	-0.40	0.0906
$S_X(t_p)$	Total Long	$\log S_X = -7.08^{+0.14}_{-0.14} - 0.10^{+0.05}_{-0.05} \times \log t_p$	0.64	0.64	-0.07	0.0576
	Total Short	$\log S_X = -8.96^{+0.42}_{-0.42} + 0.36^{+0.17}_{-0.17} \times \log t_p$	0.43	0.40	0.47	0.0375
	Early Long	$\log S_X = -6.68^{+0.22}_{-0.22} - 0.27^{+0.09}_{-0.09} \times \log t_p$	0.64	0.64	-0.12	0.0024
	Early Short	$\log S_X = -9.20^{+1.09}_{-1.09} + 0.46^{+0.48}_{-0.48} \times \log t_p$	0.45	0.41	0.24	0.3232
$S_X(\Delta t)$	Total Long	$\log S_X = -7.44^{+0.08}_{-0.08} + 0.06^{+0.04}_{-0.04} \times \log \Delta t$	0.64	0.64	0.05	0.1912
	Total Short	$\log S_X = -8.74^{+0.22}_{-0.22} + 0.37^{+0.12}_{-0.12} \times \log \Delta t$	0.38	0.35	0.63	0.0032
	Early Long	$\log S_X = -7.56^{+0.11}_{-0.11} + 0.14^{+0.07}_{-0.07} \times \log \Delta t$	0.64	0.64	0.08	0.0423
	Early Short	$\log S_X = -9.29^{+0.38}_{-0.38} + 0.75^{+0.24}_{-0.24} \times \log \Delta t$	0.35	0.33	0.61	0.0056

Table 5. Cont.

Correlations	Types	Expressions	σ_{int}	δ	r	p
$S_X(t_r)$	Total Long	$\log S_X = -7.49^{+0.05}_{-0.05} + 0.13^{+0.04}_{-0.04} \times \log t_r$	0.63	0.64	0.12	0.0018
	Total Short	$\log S_X = -8.57^{+0.15}_{-0.15} + 0.38^{+0.10}_{-0.10} \times \log t_r$	0.35	0.33	0.69	0.0008
	Early Long	$\log S_X = -7.62^{+0.07}_{-0.07} + 0.25^{+0.06}_{-0.06} \times \log t_r$	0.63	0.64	0.18	$<10^{-4}$
	Early Short	$\log S_X = -8.90^{+0.20}_{-0.20} + 0.71^{+0.17}_{-0.17} \times \log t_r$	0.30	0.30	0.71	0.0007
$S_X(t_d)$	Total Long	$\log S_X = -7.36^{+0.07}_{-0.07} + 0.02^{+0.04}_{-0.04} \times \log t_d$	0.64	0.64	0.02	0.6654
	Total Short	$\log S_X = -8.58^{+0.19}_{-0.19} + 0.34^{+0.12}_{-0.12} \times \log t_d$	0.40	0.37	0.58	0.0079
	Early Long	$\log S_X = -7.40^{+0.09}_{-0.09} + 0.05^{+0.06}_{-0.06} \times \log t_d$	0.64	0.65	0.03	0.5106
	Early Short	$\log S_X = -8.73^{+0.30}_{-0.30} + 0.46^{+0.22}_{-0.23} \times \log t_d$	0.40	0.37	0.46	0.0498
$F_{X,p}(S_X)$	Total Long	$\log F_{X,p} = -1.94^{+0.24}_{-0.24} + 0.95^{+0.03}_{-0.03} \times \log S_X$	0.54	0.55	0.75	$<10^{-4}$
	Total Short	$\log F_{X,p} = -10.08^{+2.56}_{-2.57} - 0.05^{+0.32}_{-0.32} \times \log S_X$	0.64	0.58	-0.03	0.8967
	Early Long	$\log F_{X,p} = -1.88^{+0.18}_{-0.18} + 0.95^{+0.02}_{-0.02} \times \log S_X$	0.37	0.38	0.85	$<10^{-4}$
	Early Short	$\log F_{X,p} = -5.80^{+1.36}_{-1.40} + 0.46^{+0.17}_{-0.17} \times \log S_X$	0.29	0.28	0.59	0.0079
$L_{X,p}(t_{p,z})$	Total Long	$\log L_{X,p} = 52.54^{+0.20}_{-0.20} - 1.45^{+0.10}_{-0.10} \times \log t_{p,z}$	0.71	0.71	-0.67	$<10^{-4}$
	Total Short	$\log L_{X,p} = 50.46^{+0.33}_{-0.32} - 1.27^{+0.13}_{-0.13} \times \log t_{p,z}$	0.24	0.28	-0.96	$<10^{-4}$
	Early Long	$\log L_{X,p} = 53.22^{+0.27}_{-0.27} - 1.82^{+0.14}_{-0.14} \times \log t_{p,z}$	0.69	0.69	-0.63	$<10^{-4}$
	Early Short	$\log L_{X,p} = 50.50^{+1.00}_{-0.99} - 1.28^{+0.46}_{-0.47} \times \log t_{p,z}$	0.27	0.29	-0.73	0.0107
$L_{X,p}(\Delta t_z)$	Total Long	$\log L_{X,p} = 50.95^{+0.11}_{-0.11} - 1.07^{+0.08}_{-0.08} \times \log \Delta t_z$	0.74	0.75	-0.63	$<10^{-4}$
	Total Short	$\log L_{X,p} = 48.97^{+0.21}_{-0.20} - 0.96^{+0.11}_{-0.11} \times \log \Delta t_z$	0.29	0.30	-0.95	$<10^{-4}$
	Early Long	$\log L_{X,p} = 51.09^{+0.13}_{-0.13} - 1.21^{+0.11}_{-0.11} \times \log \Delta t_z$	0.73	0.74	-0.56	$<10^{-4}$
	Early Short	$\log L_{X,p} = 48.67^{+0.36}_{-0.36} - 0.72^{+0.27}_{-0.27} \times \log \Delta t_z$	0.26	0.30	-0.72	0.0125
$L_{X,p}(t_{r,z})$	Total Long	$\log L_{X,p} = 50.23^{+0.07}_{-0.07} - 0.81^{+0.08}_{-0.08} \times \log t_{r,z}$	0.82	0.82	-0.53	$<10^{-4}$
	Total Short	$\log L_{X,p} = 48.52^{+0.22}_{-0.22} - 0.91^{+0.14}_{-0.14} \times \log t_{r,z}$	0.40	0.41	-0.91	$<10^{-4}$
	Early Long	$\log L_{X,p} = 50.21^{+0.08}_{-0.08} - 0.74^{+0.10}_{-0.11} \times \log t_{r,z}$	0.81	0.81	-0.40	$<10^{-4}$
	Early Short	$\log L_{X,p} = 48.17^{+0.39}_{-0.38} - 0.48^{+0.41}_{-0.41} \times \log t_{r,z}$	0.37	0.39	-0.40	0.2290
$L_{X,p}(t_{d,z})$	Total Long	$\log L_{X,p} = 50.72^{+0.09}_{-0.09} - 1.08^{+0.08}_{-0.08} \times \log t_{d,z}$	0.74	0.74	-0.64	$<10^{-4}$
	Total Short	$\log L_{X,p} = 48.65^{+0.19}_{-0.19} - 0.92^{+0.12}_{-0.12} \times \log t_{d,z}$	0.31	0.33	-0.94	$<10^{-4}$
	Early Long	$\log L_{X,p} = 50.81^{+0.10}_{-0.10} - 1.18^{+0.11}_{-0.11} \times \log t_{d,z}$	0.72	0.73	-0.57	$<10^{-4}$
	Early Short	$\log L_{X,p} = 48.35^{+0.23}_{-0.23} - 0.60^{+0.20}_{-0.20} \times \log t_{d,z}$	0.24	0.28	-0.75	0.0074
$E_{X,iso}(t_{p,z})$	Total Long	$\log E_{X,iso} = 51.48^{+0.20}_{-0.20} - 0.37^{+0.10}_{-0.10} \times \log t_{p,z}$	0.73	0.73	-0.22	0.0002
	Total Short	$\log E_{X,iso} = 48.91^{+0.38}_{-0.37} + 0.00^{+0.15}_{-0.15} \times \log t_{p,z}$	0.32	0.30	-0.00	0.9915
	Early Long	$\log E_{X,iso} = 52.40^{+0.27}_{-0.27} - 0.87^{+0.14}_{-0.14} \times \log t_{p,z}$	0.69	0.69	-0.36	$<10^{-4}$
	Early Short	$\log E_{X,iso} = 48.65^{+1.23}_{-1.22} + 0.13^{+0.57}_{-0.58} \times \log t_{p,z}$	0.29	0.32	0.07	0.8284
$E_{X,iso}(\Delta t_z)$	Total Long	$\log E_{X,iso} = 50.83^{+0.11}_{-0.11} - 0.07^{+0.08}_{-0.08} \times \log \Delta t_z$	0.75	0.75	-0.06	0.3640
	Total Short	$\log E_{X,iso} = 48.85^{+0.21}_{-0.21} + 0.04^{+0.11}_{-0.11} \times \log \Delta t_z$	0.30	0.30	0.12	0.7028
	Early Long	$\log E_{X,iso} = 50.97^{+0.13}_{-0.13} - 0.21^{+0.11}_{-0.11} \times \log \Delta t_z$	0.74	0.74	-0.11	0.0691
	Early Short	$\log E_{X,iso} = 48.56^{+0.38}_{-0.37} + 0.28^{+0.28}_{-0.28} \times \log \Delta t_z$	0.29	0.30	0.35	0.2849
$E_{X,iso}(t_{r,z})$	Total Long	$\log E_{X,iso} = 50.73^{+0.07}_{-0.07} + 0.02^{+0.07}_{-0.07} \times \log t_{r,z}$	0.75	0.75	0.02	0.7911
	Total Short	$\log E_{X,iso} = 48.86^{+0.17}_{-0.17} + 0.05^{+0.11}_{-0.11} \times \log t_{r,z}$	0.31	0.30	0.16	0.6254
	Early Long	$\log E_{X,iso} = 50.76^{+0.07}_{-0.07} - 0.02^{+0.10}_{-0.10} \times \log t_{r,z}$	0.74	0.74	-0.01	0.8558
	Early Short	$\log E_{X,iso} = 48.52^{+0.28}_{-0.28} + 0.47^{+0.30}_{-0.30} \times \log t_{r,z}$	0.28	0.27	0.53	0.0967
$E_{X,iso}(t_{d,z})$	Total Long	$\log E_{X,iso} = 50.86^{+0.09}_{-0.09} - 0.12^{+0.08}_{-0.08} \times \log t_{d,z}$	0.74	0.75	-0.09	0.1254
	Total Short	$\log E_{X,iso} = 48.87^{+0.18}_{-0.18} + 0.04^{+0.11}_{-0.11} \times \log t_{d,z}$	0.30	0.30	0.11	0.7310
	Early Long	$\log E_{X,iso} = 50.99^{+0.11}_{-0.10} - 0.28^{+0.11}_{-0.11} \times \log t_{d,z}$	0.73	0.73	-0.16	0.0097
	Early Short	$\log E_{X,iso} = 48.76^{+0.26}_{-0.25} + 0.17^{+0.23}_{-0.23} \times \log t_{d,z}$	0.28	0.31	0.27	0.4306
$L_{X,p}(E_{X,iso})$	Total Long	$\log L_{X,p} = -3.29^{+2.34}_{-2.33} + 1.04^{+0.05}_{-0.05} \times \log E_{X,iso}$	0.56	0.56	0.81	$<10^{-4}$
	Total Short	$\log L_{X,p} = 18.72^{+42.71}_{-46.78} + 0.59^{+0.96}_{-0.87} \times \log E_{X,iso}$	1.00	0.96	0.19	0.5532
	Early Long	$\log L_{X,p} = -4.24^{+1.75}_{-1.77} + 1.06^{+0.03}_{-0.03} \times \log E_{X,iso}$	0.39	0.40	0.89	$<10^{-4}$
	Early Short	$\log L_{X,p} = 24.29^{+21.82}_{-21.65} + 0.48^{+0.44}_{-0.45} \times \log E_{X,iso}$	0.36	0.39	0.39	0.2311

The correlations are derived from LGRB flares and SGRB flares. r is the Pearson correlation coefficient, p is the chance probability, δ is the dispersion of correlation and σ_{int} is the intrinsic scatter.

3.4. Three-Parameter Correlations of Flares

We extend the $F_{X,p}$ - S_X correlation and the $L_{X,p}$ - $E_{X,iso}$ correlation by adding a third parameter (the peak time of the flare) and find that the $F_{X,p}$ - t_p - S_X correlation and the $L_{X,p}$ -

$t_{p,z}$ - $E_{X,iso}$ correlation become much tighter. For the early flares, $F_{X,p} \propto t_p^{-0.94^{+0.04}_{-0.04}} S_X^{0.90^{+0.02}_{-0.02}}$ with $r = 0.93$ and $p < 10^{-4}$, and $L_{X,p} \propto t_{p,z}^{-1.03^{+0.06}_{-0.06}} E_{X,iso}^{0.92^{+0.02}_{-0.02}}$ ($r = 0.96$, $p < 10^{-4}$). As shown in the Figure 15, all late events almost fall into the 3σ confidence region of the three-parameter correlations defined by the early flares. The results of the regression analysis are listed in Table 6.

We also analyze the above three-parameters for the LGRB flares and SGRB flares and obtain $F_{X,p} \propto t_p^{-0.94^{+0.04}_{-0.04}} S_X^{0.90^{+0.02}_{-0.02}}$ ($r = 0.93$ and $p < 10^{-4}$) and $L_{X,p} \propto t_{p,z}^{-1.01^{+0.06}_{-0.06}} E_{X,iso}^{0.92^{+0.03}_{-0.03}}$ ($r = 0.95$ and $p < 10^{-4}$) for LGRB flares, while $F_{X,p} \propto t_p^{-0.85^{+0.29}_{-0.28}} S_X^{0.54^{+0.14}_{-0.14}}$ ($r = 0.80$ and $p < 10^{-4}$) and $L_{X,p} \propto t_{p,z}^{-1.50^{+0.42}_{-0.40}} E_{X,iso}^{0.60^{+0.26}_{-0.26}}$ ($r = 0.86$ and $p = 0.0008$) for SGRB flares. The results are presented in the Figure 16 and Table 6. It can be seen from the fitting results that the slope index of $E_{X,iso}$ varies significantly, while the slope index of the peak time is consistent within the error range.

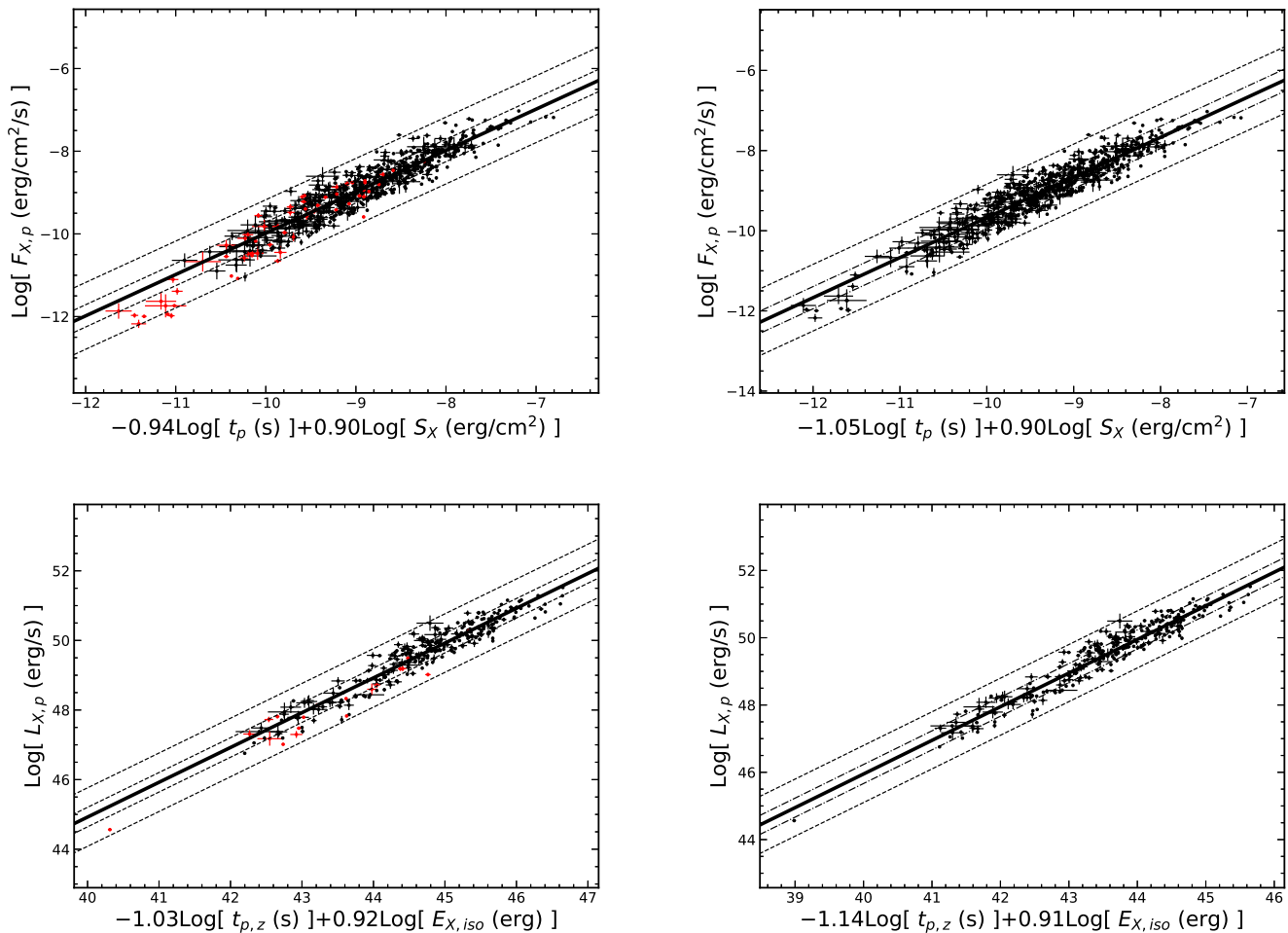


Figure 15. The $F_{X,p}$ - t_p - S_X correlation and $L_{X,p}$ - $t_{p,z}$ - $E_{X,iso}$ of flares. The black (red) dot represent the early (late) flares. The left panel is derived from early and late flares, while the right panel is derived from total flares. All symbols and descriptions are the same as in Figure 3.

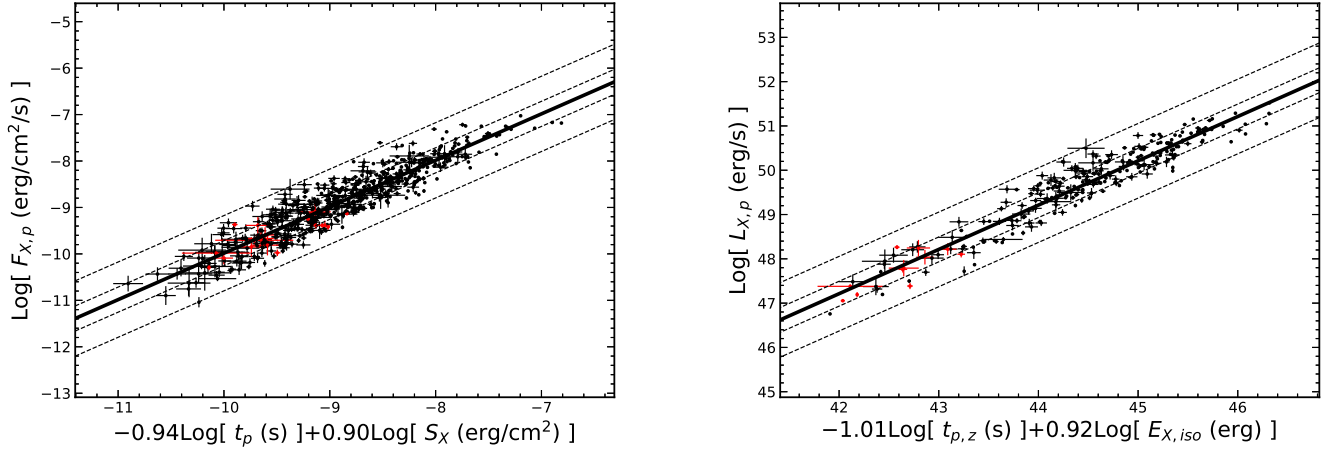


Figure 16. The $F_{X,p}$ - t_p - S_X and $L_{X,p}$ - $t_{p,z}$ - $E_{X,iso}$ correlation of LGRB and SGRB flares are shown at left and right panel, respectively. All symbols and descriptions are the same as in Figure 9.

Table 6. The three-parameter correlations of flares.

Correlations	Types	Expressions	σ_{int}	δ	r	p
$F_{X,p}(t_p, S_X)$	Early	$\log F_{X,p} = 0.02^{+0.15}_{-0.15} - 0.94^{+0.04}_{-0.04} \times \log t_p + 0.90^{+0.02}_{-0.02} \times \log S_X$	0.25	0.27	0.93	$<10^{-4}$
	Late	$\log F_{X,p} = 1.71^{+0.48}_{-0.48} - 1.38^{+0.07}_{-0.07} \times \log t_p + 0.93^{+0.06}_{-0.06} \times \log S_X$	0.28	0.28	0.96	$<10^{-4}$
	Total	$\log F_{X,p} = 0.32^{+0.13}_{-0.13} - 1.05^{+0.02}_{-0.02} \times \log t_p + 0.90^{+0.02}_{-0.02} \times \log S_X$	0.26	0.28	0.94	$<10^{-4}$
	Total Long	$\log F_{X,p} = 0.28^{+0.13}_{-0.14} - 1.05^{+0.02}_{-0.02} \times \log t_p + 0.90^{+0.02}_{-0.02} \times \log S_X$	0.26	0.28	0.94	$<10^{-4}$
	Total Short	$\log F_{X,p} = -2.69^{+1.23}_{-1.22} - 1.05^{+0.10}_{-0.10} \times \log t_p + 0.55^{+0.14}_{-0.13} \times \log S_X$	0.21	0.21	0.93	$<10^{-4}$
	Early Long	$\log F_{X,p} = 0.00^{+0.15}_{-0.15} - 0.94^{+0.04}_{-0.04} \times \log t_p + 0.90^{+0.02}_{-0.02} \times \log S_X$	0.26	0.27	0.93	$<10^{-4}$
	Early Short	$\log F_{X,p} = -3.22^{+1.45}_{-1.43} - 0.85^{+0.29}_{-0.28} \times \log t_p + 0.54^{+0.14}_{-0.14} \times \log S_X$	0.22	0.20	0.80	$<10^{-4}$
$L_{X,p}(t_{p,z}, E_{X,iso})$	Early	$\log L_{X,p} = 4.92^{+1.24}_{-1.22} - 1.03^{+0.06}_{-0.06} \times \log t_{p,z} + 0.92^{+0.02}_{-0.02} \times \log E_{X,iso}$	0.27	0.28	0.96	$<10^{-4}$
	Late	$\log L_{X,p} = 7.05^{+4.45}_{-4.46} - 1.23^{+0.14}_{-0.14} \times \log t_{p,z} + 0.89^{+0.09}_{-0.09} \times \log E_{X,iso}$	0.32	0.28	0.97	$<10^{-4}$
	Total	$\log L_{X,p} = 5.91^{+1.12}_{-1.12} - 1.14^{+0.04}_{-0.04} \times \log t_{p,z} + 0.91^{+0.02}_{-0.02} \times \log E_{X,iso}$	0.27	0.28	0.96	$<10^{-4}$
	Total Long	$\log L_{X,p} = 6.35^{+1.25}_{-1.24} - 1.11^{+0.04}_{-0.04} \times \log t_{p,z} + 0.90^{+0.02}_{-0.02} \times \log E_{X,iso}$	0.27	0.28	0.96	$<10^{-4}$
	Total Short	$\log L_{X,p} = 23.64^{+12.23}_{-12.19} - 1.27^{+0.10}_{-0.11} \times \log t_{p,z} + 0.55^{+0.25}_{-0.25} \times \log E_{X,iso}$	0.26	0.21	0.98	$<10^{-4}$
	Early Long	$\log L_{X,p} = 5.20^{+1.37}_{-1.35} - 1.01^{+0.06}_{-0.06} \times \log t_{p,z} + 0.92^{+0.03}_{-0.03} \times \log E_{X,iso}$	0.27	0.28	0.95	$<10^{-4}$
	Early Short	$\log L_{X,p} = 21.70^{+12.71}_{-12.41} - 1.50^{+0.42}_{-0.40} \times \log t_{p,z} + 0.60^{+0.26}_{-0.26} \times \log E_{X,iso}$	0.26	0.22	0.86	0.0008

The correlations are derived from different sample types. r is the Pearson correlation coefficient, p is the chance probability, δ is the dispersion of correlation and σ_{int} is the intrinsic scatter.

4. Origin of the Flares

The kinematic arguments proposed by [32] can give limits on the flux variability $\Delta F/F$ and timescale variability $\Delta t/t$. In Figure 17, all the X-ray flares in our sample are demonstrated in the $\Delta F/F$ - $\Delta t/t$ plane, where the fraction of cooling energy $f_c \sim 1/2$ and $F/\nu F_\nu \sim 1$ are adopted referring to [32]. We find an apparent discrepancy existing between our sample and that of [23]. The $\Delta t/t$ of the second flare in GRB 050724 is 0.62 in our sample, while [33] obtained the value of 1.46. Additionally, the $\Delta t/t$ of GRB 050724 in our sample is close to that derived by [21]. It is shown that this analysis is significantly affected by the fitting model and the goodness of fitting. All flares in our sample are located on the left side of the axis $\Delta t/t = 1$, confirming that flares cannot be responsible for the scheme of patchy shells [25]. The flare with $\Delta t/t \geq 1$ may occur at an extremely late-time, but our samples prefer that a majority of flares can be explained by internal shocks. Contrarily, regardless of the LGRB flares or SGRB flares, more flares prefer the constraint of refreshed shock and off-axis density fluctuations. These results are in agreement with [21,23,25,26].

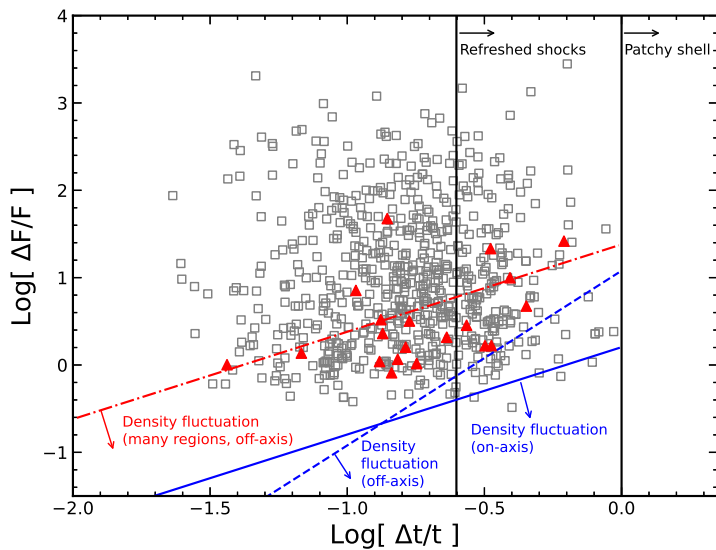


Figure 17. The relative variability of flux $\Delta F/F$ and relative temporal variability $\Delta t/t$ plotted on the constraint plane of the kinematic parameters [32]. Besides, the LGRB flares (grey squares) and the SGRB flares (red triangles) are demonstrated, respectively. The black solid lines shown are the case of patchy shells ($\Delta t/t \geq 1$) and refreshed shocks ($\Delta t/t \geq 0.25$). Off-axis density fluctuation of single variable regions ($\Delta F/F \leq 12(\Delta t/t)^2$) and of many variable regions ($\Delta F/F \leq 24\Delta t/t$) are demonstrated by blue dash line and red dot dash line, respectively. The case of on-axis density fluctuations ($\Delta F/F \leq 1.6\Delta t/t$) is plotted by blue solid line. The fraction of cooling energy $f_c \sim 1/2$ and $F/\nu F_\nu \sim 1$ are adopted here. More detailed description can refer to Ref. [32].

Compared to the LGRB flares, none of the SGRB flares in our sample conform to on-axis density fluctuations and off-axis density fluctuations of single variable regions. 4/20 SGRB flares can only be interpreted as internal shocks. Although the promising explanation for flares is the internal shock origin, the SGRB flares may have a discrepancy compared to the long ones. Ref. [45] studied the late flares and showed that quite a few late flares satisfy the scheme of on-axis fluctuations. Thus, we speculate that the scarcity of the late SGRB flares is the main reason accounting for this phenomenon. Whether it is due to the scarcity of the late SGRB flares or the observational selection effect is worth exploring in the future.

5. Conclusions

In this work, 697 bright X-ray flares of GRBs detected by Swift/XRT are extensively analyzed up to 2021 April, including 677 LGRB flares and 20 SGRB flares. Among this sample, there are 636 early flares ($t_p < 10^3$ s) and 61 late flares ($t_p > 10^3$ s). We apply the smooth broken power-law function to fit all the X-ray flares, and obtain their physical parameters.

Obvious features are found after analyzing the morphological structures of X-ray flares in the time domain: The peak times of the flares span from 10^2 s to 10^5 s, and there is clustering around 10^3 s. In addition, the flare durations are mainly distributed between 10^2 and 10^3 s. The early flares appear with higher frequency, shorter duration, and more asymmetry. Especially, the morphological features of the SGRB flares are similar to those of the LGRB flares. This implies that the flares with different origins may have similar radiative mechanisms. The 0.3–10 keV isotropic energy (peak luminosity) of the flares is mainly distributed from 10^{50} to 10^{52} erg (10^{46} to 10^{51} erg/s). It is noted that the isotropic energy and peak luminosity of the SGRB flares is about two or three orders of magnitude less than that of the LGRB flares. The distributions of $L_{X,p}$ and $E_{X,iso}$ for the LGRB flares are mainly bimodal. Although the SGRB flares are not statistically significant due to their

limited number, they are concentrated at the weak end of the LGRB flares. The SGRB flares are less energetic on average than the LGRB flares, which is similar to the prompt emission.

We also analyze the relationships between the parameters of the X-ray flares, and find some tight correlations. There is an anti-correlation between the peak luminosity and the peak time of the flares, i.e., $L_{X,p} \propto t_{p,z}^{-1.55}$, which indicates that the later flares are usually dimmer. Furthermore, $\Delta t - t_p$ correlation ($\Delta t \propto t_p^{1.05}$) and the distribution of t_d/t_r show that the later flares have a broader duration and a more symmetric structure. We also find that the peak luminosities of the flares are tightly correlated with their total energy, i.e., $L_{X,p} \propto E_{X,iso}^{1.07}$. By adding the third parameter (the peak time of the flare), we obtain

a more tighter three-parameter correlation $L_{X,p} \propto t_{p,z}^{-1.14^{+0.04}_{-0.04}} E_{X,iso}^{0.91^{+0.02}_{-0.02}}$ ($r = 0.96$). There is no significant time evolution of the correlations between the early flares and late flares. In addition, we do the first quantitative analysis on the $L_{X,p} - t_{p,z}$ correlation of SGRB flares, confirming the conclusion that this correlation of the SGRB flares differ from the long ones by a factor of 0.01 [23].

From the point of kinematic arguments, the SGRB flares and LGRB flares have a similar appearance in the $\Delta F/F - \Delta t/t$ plane, irrespective of the possible observational selection effect of the SGRB flares. Almost all flares support a common scheme of internal origin as shown in Figure 17. From the different viewpoint, some studies also concluded that the LGRB flares and SGRB flares may have a common origin [20,23]. Our results confirm this scheme. To sum up, we conclude that the flare emission of LGRBs and SGRBs have similar physical mechanisms, but the energy budgets of these two types are different.

Author Contributions: Y.-R.S. and F.-W.Z. led the data analysis and wrote the manuscript. X.-K.D., S.-Y.Z. and W.-P.S. helped with the data analysis. All authors have read and agreed to the published version of the manuscript.

Funding: This research was funded in part by NSFC under grants 11763003, and by the Guangxi Natural Science Foundation (No. 2022GXNSFDA035083).

Data Availability Statement: The data are available at the UK Swift Science Data Centre at the University of Leicester <http://www.swift.ac.uk/xrtcurves/>.

Acknowledgments: We thank the anonymous reviewer for important suggestions that helped us to improve the presentation of our results.

Conflicts of Interest: The authors declare no conflict of interest.

References

- Kouveliotou, C.; Meegan, C.A.; Fishman, G.J.; Bhat, N.P.; Briggs, M.S.; Koshut, T.M.; Paciesas, W.S.; Pendleton, G.N. Identification of Two Classes of Gamma-Ray Bursts. *Astrophys. J.* **1993**, *413*, L101. [[CrossRef](#)]
- Zhang, Z.-B.; Choi, C.-S. An Analysis of the Durations of Swift Gamma-Ray Bursts. *Astron. Astrophys.* **2008**, *484*, 293. [[CrossRef](#)]
- MacFadyen, A.I.; Woosley, S.E. Collapsars: Gamma-Ray Bursts and Explosions in “Failed Supernovae”. *Astrophys. J.* **1998**, *524*, 262. [[CrossRef](#)]
- Xu, D.; de Ugarte Postigo, A.; Leloudas, G.; Krühler, T.; Cano, Z.; Hjorth, J.; Malesani, D.; Fynbo, J.P.U.; Thöne, C.C.; Sánchez-Ramírez, R.; et al. Discovery of the Broad-lined Type Ic SN 2013cq Associated with the Very Energetic GRB 130427A. *Astrophys. J.* **2013**, *776*, 98. [[CrossRef](#)]
- Berger, E. The Environments of Short-duration Gamma-Ray Bursts and Implications for Their Progenitors. *New Astron. Rev.* **2011**, *55*, 1. [[CrossRef](#)]
- Gehrels, N.; Ramirez-Ruiz, E.; Fox, D.B. Gamma-Ray Bursts in the Swift Era. *Annu. Rev. Astron. Astrophys.* **2009**, *47*, 567. [[CrossRef](#)]
- Nakar, E. Short-hard Gamma-Ray Bursts. *Phys. Rep.* **2007**, *442*, 166. [[CrossRef](#)]
- Burrows, D.N.; Romano, P.; Falcone, A.; Kobayashi, S.; Zhang, B.; Moretti, A.; O’Brien, P.T.; Goad, M.R.; Campana, S.; Page, K.L.; et al. Bright X-ray Flares in Gamma-Ray Burst Afterglows. *Science* **2005**, *309*, 1833. [[CrossRef](#)]
- Butler, N.R.; Kocevski, D.; Bloom, J.S.; Curtis, J.L. A Complete Catalog of Swift Gamma-Ray Burst Spectra and Durations: Demise of a Physical Origin for Pre-Swift High-Energy Correlations. *Astrophys. J.* **2007**, *671*, 656. [[CrossRef](#)]
- Evans, P.A.; Beardmore, A.P.; Page, K.L.; Osborne, J.P.; O’Brien, P.T.; Willingale, R.; Starling, R.L.C.; Burrows, D.N.; Godet, O.; Vetere, L.; et al. Methods and Results of an Automatic Analysis of a Complete Sample of Swift-XRT Observations of GRBs. *Mon. Not. R. Astron. Soc.* **2009**, *397*, 1177. [[CrossRef](#)]

11. Falcone, A.D.; Burrows, D.N.; Lazzati, D.; Campana, S.; Kobayashi, S.; Zhang, B.; Mészáros, P.; Page, K.L.; Kennea, J.A.; Romano, P.; et al. The Giant X-Ray Flare of GRB 050502B: Evidence for Late-Time Internal Engine Activity. *Astrophys. J.* **2006**, *641*, 1010. [[CrossRef](#)]
12. Falcone, A.D.; Morris, D.; Racusin, J.; Chincarini, G.; Moretti, A.; Romano, P.; Burrows, D.N.; Pagani, C.; Stroh, M.; Grupe, D.; et al. The First Survey of X-Ray Flares from Gamma-Ray Bursts Observed by Swift: Spectral Properties and Energetics. *Astrophys. J.* **2007**, *671*, 1921. [[CrossRef](#)]
13. O'Brien, P.T.; Willingale, R.; Osborne, J.; Goad, M.R.; Page, K.L.; Vaughan, S.; Rol, E.; Beardmore, A.; Godet, O.; Hurkett, C.P.; et al. The Early X-Ray Emission from GRBs. *Astrophys. J.* **2006**, *647*, 1213. [[CrossRef](#)]
14. D'Avanzo, P. Short Gamma-Ray Bursts: A Review. *J. High Energy Astrophys.* **2015**, *7*, 73. [[CrossRef](#)]
15. Li, L.; Liang, E.-W.; Tang, Q.-W.; Chen, J.-M.; Xi, S.-Q.; Lü, H.-J.; Gao, H.; Zhang, B.; Zhang, J.; Yi, S.-X.; et al. A Comprehensive Study of Gamma-Ray Burst Optical Emission. I. Flares and Early Shallow-decay Component. *Astrophys. J.* **2012**, *758*, 27. [[CrossRef](#)]
16. Margutti, R.; Bernardini, G.; Barniol Duran, R.; Guidorzi, C.; Shen, R.F.; Chincarini, G. On the Average Gamma-Ray Burst X-ray Flaring Activity. *Mon. Not. R. Astron. Soc.* **2011**, *410*, 1064. [[CrossRef](#)]
17. Nousek, J.A.; Kouveliotou, C.; Grupe, D.; Page, K.L.; Granot, J.; Ramirez-Ruiz, E.; Patel, S.K.; Burrows D.N.; Mangano, V.; Barthelmy, S.; et al. Evidence for a Canonical Gamma-Ray Burst Afterglow Light Curve in the Swift XRT Data. *Astrophys. J.* **2006**, *642*, 389. [[CrossRef](#)]
18. Ruffini, R.; Wang, Y.; Aimurato, Y.; Barres de Almeida, U.; Becerra, L.; Bianco, C.L.; Chen, Y.C.; Karlica, M.; Kovacevic, M.; Li, L.; et al. Early X-Ray Flares in GRBs. *Astrophys. J.* **2018**, *852*, 53. [[CrossRef](#)]
19. Zhang, B.; Fan, Y.Z.; Dyks, J.; Kobayashi, S.; Mészáros, P.; Burrows, D.N.; Nousek, J.A.; Gehrels, N. Physical Processes Shaping Gamma-Ray Burst X-Ray Afterglow Light Curves: Theoretical Implications from the Swift X-Ray Telescope Observations. *Astrophys. J.* **2006**, *642*, 354. [[CrossRef](#)]
20. Wang, F.Y.; Dai, Z.G. Self-organized Criticality in X-ray Flares of Gamma-Ray-Burst Afterglows. *Nat. Phys.* **2013**, *9*, 465. [[CrossRef](#)]
21. Curran, P.A.; Starling, R.L.C.; O'Brien, P.T.; Godet, O.; van der Horst, A.J.; Wijers, R.A.M.J. On the nature of late X-ray flares in Swift gamma-ray bursts. *Astron. Astrophys.* **2008**, *487*, 533. [[CrossRef](#)]
22. Campana, S.; Tagliaferri, G.; Lazzati, D.; Chincarini, G.; Covino, S.; Page, K.; Romano, P.; Moretti, A.; Cusumano, G.; Mangano, V.; et al. The X-ray Afterglow of the Short Gamma Ray Burst 050724. *Astron. Astrophys.* **2006**, *454*, 113. [[CrossRef](#)]
23. Margutti, R.; Chincarini, G.; Granot, J.; Guidorzi, C.; Berger, E.; Bernardini, M.G.; Gehrels, N.; Soderberg, A.M.; Stamatikos, M.; Zaninoni, E. X-ray Flare Candidates in Short Gamma-Ray Bursts. *Mon. Not. R. Astron. Soc.* **2011**, *417*, 2144. [[CrossRef](#)]
24. Wang, Y.; Aimurato, Y.; Moradi, R.; Peresano, M.; Ruffini, R.; Shakeri, S. Revisiting the Statistics of X-ray Flares in Gamma-Ray Bursts. *Mem. Soc. Astron. Ital.* **2018**, *89*, 293. [[CrossRef](#)]
25. Chincarini, G.; Moretti, A.; Romano, P.; Falcone, A.D.; Morris, D.; Racusin, J.; Campana, S.; Covino, S.; Guidorzi, C.; Tagliaferri, G.; et al. The First Survey of X-Ray Flares from Gamma-Ray Bursts Observed by Swift: Temporal Properties and Morphology. *Astrophys. J.* **2007**, *671*, 1903. [[CrossRef](#)]
26. Chincarini, G.; Mao, J.; Margutti, R.; Bernardini, M.G.; Guidorzi, C.; Pasotti, F.; Giannios, D.; Della Valle, M.; Moretti, A.; Romano, P.; et al. Unveiling the Origin of X-ray Flares in Gamma-Ray Bursts. *Mon. Not. R. Astron. Soc.* **2010**, *406*, 2113. [[CrossRef](#)]
27. Liang, E.W.; Zhang, B.; O'Brien, P.T.; Willingale, R.; Angelini, L.; Burrows, D.N.; Campana, S.; Chincarini, G.; Falcone, A.; Gehrels, N.; et al. Testing the Curvature Effect and Internal Origin of Gamma-Ray Burst Prompt Emissions and X-Ray Flares with Swift Data. *Astrophys. J.* **2006**, *646*, 351. [[CrossRef](#)]
28. Liu, C.; Mao, J. GRB X-Ray Flare Properties among Different GRB Subclasses. *Astrophys. J.* **2019**, *884*, 59. [[CrossRef](#)]
29. Yi, S.-X.; Du, M.; Liu, T. Statistical Analyses of the Energies of X-Ray Plateaus and Flares in Gamma-Ray Bursts. *Astrophys. J.* **2022**, *924*, 69. [[CrossRef](#)]
30. Chang, X.Z.; Peng, Z.Y.; Chen, J.M.; Yin, Y.; Wang, D.Z.; Wu, H. A Comprehensive Study of Multiflare GRB Spectral Lag. *Astrophys. J.* **2021**, *922*, 34. [[CrossRef](#)]
31. Yi, S.-X.; Xie, W.; Ma, S.-B.; Lei, W.-H.; Du, M. Constraining Properties of GRB Central Engines with X-ray Flares. *Mon. Not. R. Astron. Soc.* **2021**, *507*, 1047. [[CrossRef](#)]
32. Ioka, K.; Kobayashi, S.; Zhang, B. Variabilities of Gamma-Ray Burst Afterglows: Long-acting Engine, Anisotropic Jet, or Many Fluctuating Regions? *Astrophys. J.* **2005**, *631*, 429. [[CrossRef](#)]
33. Mu, H.-J.; Gu, W.; Hou, S.-J.; Liu, T.; Lin, D.-B.; Yi, T.; Liang, E.-W.; Lu, J.-F. Central Engine of Late-time X-Ray Flares with Internal Origin. *Astrophys. J.* **2016**, *832*, 161. [[CrossRef](#)]
34. King, A.; O'Brien, P.T.; Goad, M.R.; Osborne, J.; Olsson, E.; Page, K. Gamma-Ray Bursts: Restarting the Engine. *Astrophys. J.* **2005**, *630*, L113. [[CrossRef](#)]
35. Perna, R.; Armitage, P.J.; Zhang, B. Flares in Long and Short Gamma-Ray Bursts: A Common Origin in a Hyperaccreting Accretion Disk. *Astrophys. J.* **2006**, *636*, L29. [[CrossRef](#)]
36. Yi, S.-X.; Xi, S.-Q.; Yu, H.; Wang, F.Y.; Mu, H.-J.; Lü, L.Z.; Liang, E.-W. Comprehensive Study of the X-ray Flares from Gamma-Ray Bursts Observed by Swift. *Astrophys. J. Suppl. Ser.* **2016**, *224*, 20. [[CrossRef](#)]
37. Duque, R.; Beniamini, P.; Daigne, F.; Mochkovitch, R. Flares in Gamma-Ray Burst X-ray Afterglows as Prompt Emission from Slightly Misaligned Structured Jets. *Mon. Not. R. Astron. Soc.* **2022**, *513*, 951. [[CrossRef](#)]
38. Fan, Y.Z.; Wei, D.M. Late Internal-shock Model for Bright X-ray Flares in Gamma-Ray Burst Afterglows and GRB 011121. *Mon. Not. R. Astron. Soc. Lett.* **2005**, *364*, L42. [[CrossRef](#)]

39. Romano, P.; Moretti, A.; Banat, P.L.; Burrows, D.N.; Campana, S.; Chincarini, G.; Covino, S.; Malesani, D.; Tagliaferri, G.; Kobayashi, S.; et al. X-ray Flare in XRF 050406: Evidence for Prolonged Engine Activity. *Astron. Astrophys.* **2006**, *836*, 570. [[CrossRef](#)]
40. Zhao, L.; Gao, H.; Lei, W.; Lan, L.; Liu, L. Giant X-Ray and Optical Bump in GRBs: Evidence for Fallback Accretion Model. *Astrophys. J.* **2021**, *906*, 60. [[CrossRef](#)]
41. Zheng, T.-C.; Li, L.; Zou, L.; Wang X.-G. X-ray Flares Raising upon Magnetar Plateau as an Implication of a Surrounding Disk of Newborn Magnetized Neutron Star. *Res. Astron. Astrophys.* **2021**, *21*, 300. [[CrossRef](#)]
42. Evans, P.A.; Beardmore, A.P.; Page, K.L.; Tyler, L.G.; Osborne, J.P.; Goad, M.R.; O'Brien, P.T.; Vetere, L.; Racusin, J.; Morris, D.; et al. An online repository of Swift/XRT light curves of γ -ray bursts. *Astron. Astrophys.* **2007**, *469*, 379. [[CrossRef](#)]
43. Liang, E.-W.; Zhang, B.-B.; Zhang, B. A Comprehensive Analysis of Swift XRT Data. II. Diverse Physical Origins of the Shallow Decay Segment. *Astrophys. J.* **2007**, *670*, 565. [[CrossRef](#)]
44. Wang, X.G.; Zhang, B.; Liang, E.W.; Lu, R.J.; Lin, D.B.; Li, J.; Li, L. Gamma-ray burst jet breaks revisited *Astrophys. J.* **2018**, *859*, 160. [[CrossRef](#)]
45. Bernardini, M.G.; Margutti, R.; Chincarini, G.; Guidorzi, C.; Mao, J. Gamma-Ray Burst Long Lasting X-ray Flaring Activity. *Astron. Astrophys.* **2011**, *526*, A27. [[CrossRef](#)]
46. Liang, E.; Zhang, B. Model-independent Multivariable Gamma-Ray Burst Luminosity Indicator and Its Possible Cosmological Implications. *Astrophys. J.* **2005**, *633*, 611. [[CrossRef](#)]
47. Dainotti, M.G.; Del Vecchio, R.; Tarnopolski, M. Gamma-Ray Burst Prompt Correlations. *Adv. Astron.* **2018**, *2018*, 4969503. [[CrossRef](#)]
48. Schaefer, B.E. The Hubble Diagram to Redshift >6 from 69 Gamma-Ray Bursts. *Astrophys. J.* **2007**, *660*, 16. [[CrossRef](#)]
49. Zhang, Z.B.; Zhang, C.T.; Zhao, Y.X.; Luo, J.J.; Jiang, L.Y.; Wang, X.L.; Han, X.L.; Terheide, R.K. Spectrum-energy Correlations in GRBs: Update, Reliability, and the Long/Short Dichotomy. *Publ. Astron. Soc. Pac.* **2018**, *130*, 054202. [[CrossRef](#)]
50. Swenson, C.A.; Roming, P.W.A. Gamma-Ray Burst Flares: X-ray Flaring. II. *Astrophys. J.* **2014**, *788*, 30. [[CrossRef](#)]